Nonequilibrium Entropic Filters for Lattice Boltzmann Methods and Shock Tube Case Studies

A thesis submitted for the degree of
Doctor of Philosophy
at the University of Leicester

by

Jianxia Zhang

Department of Mathematics,
University of Leicester,
United Kingdom.

September 2011

To All the Enlightened Ones above

and

My Root Master Lama Khemsar Rinpoche

and

my parents, sister and brothers.

Acknowledgements

My deepest love to the real compassion and the real truth of the universe, including all the enlightened Buddhas, all the enlightened Lamas, and my root Matster **Lama Keymsar Rinpoche**. I also would like to pay all my deepest respect and love to all the righteous religions in the universe. All the praises and devotion dedicate to the enlightened Bhuddhas, who are the holders of all the knowledge, compassion, and wisdom, and guidance of my whole life, from past, present and future. Every step of my life, happiness and pain, without their compassionate guidance, esp. my root Master, i would not be not able to make any step of my life.

I would like to express my heartily gratitude to my supervisor, **Prof. Alexandra Gorban** for his constant guidance, academic and emotional supports, encouragement and valuable suggestions which are the most inspirations for me to start, continue and finish my Phd studies. This thesis would be not able to finish without his insight and enthusiasm. I would like to give my deepest appreciation for his extremely kindness and supports he gave me when i encountered the most difficult time during my Phd. He is like a real academic father for me, to lead me to walk every step in the research. His enthusiasm for research and the attitudes for life, are real inspirations for me, not only for the time of being a Phd student, but certainly they will last for the rest of my life.

I would like to give my sincere gratitude to **Prof. Jeremy Levesley**, head of Deparment of Mathematics, for his constant encouragements and valuable suggestions about my research. His great kindness and emotional supports helped me to overcome a lot of difficult times. I also would like to pay my great gratitude to **Dr. Sergei Petrovskii** for his precious advice for me.

Many people have helped me throughout my Phd time, especially, Rob Brownlee, whom provided me in programming, and David Packwood whom gave me valuable advice. I also would like to say thanks to Tahir, whom gave me his valuable emotional supports.

There are no words to express my sincere gratitude for my kindhearted parents, sister, brothers and other family members for their ever lasting love, emotional supports and financial supports over all these years. I would like to say thanks to all my dear friends, especially Cesar. Finally I would like to give my appreciations to everyone in the department of mathematics.

Contents

Abstract

The Lattice Boltzmann Method (LBM) is a discrete velocity method which involves a single particle distribution function with two repeating procedures propagation and collision. When the Bhatnagar-Gross-Krook operator is applied as the collision operator for LBM, this is called lattice Bhatnagar-Gross-Krook method (LBGK). In comparison with the traditional computation methods, LBM appears as an efficient alternative computational approach for simulating complex fluid systems. However, LBM suffers numerical stability deficiencies when applied in low-viscosity fluid flow, such as local blow-ups and spurious oscillations where sharp gradients appear. The development of LBM has taken a further step to resolve the stability problem with applying a discrete entropy $H-$theorem. However, the stability and accuracy problems are not completely dealt with by the entropic lattice Boltzmann method. One of the remedies for the stability deficiencies is to construct nonequilibrium entropy limiters for LBM. The original concepts with the construction of nonequilibrium entropy limiters are based on flux filters (also called flux-corrected transport) by Boris and Book. The principal idea of the nonequilibrium entropy limiters is to control a scalar quantity, the nonequilibrium entropy. In this thesis, there are 6 limiters are developed and tested in 1D athermal shock tubes in uniformed discretized space lattice sites. Among these limiters, two new nonequilibrium limiters are constructed. All the median entropy limiters are tested with different stencils, which also have an effect on removing spurious oscillations. Apart from the test on a three-velocity set, we use five-velocity sets for the applications of nonequilibrium entropy limiters of LBM. The five-velocity sets are $\{-3,-1,0,1,3\}$, $\{-5,-2,0,2,5\}$ and $\{-7,-3,0,3,7\}$. The performance

of LBGK without limiters provides a frame of reference for comparison with the performance of LBGK which uses the nonequilibrium entropy limiters. The computations of the LBGK on different velocity sets have shown that the nonequilibrium entropy limiters are able to efficiently remove spurious oscillations for both post-shock and shock regions for high Reynolds number. Among the suggested limiters, we recommend the median nonequilibrium entropy limiter.

Chapter 1

Introduction

1.1 Brief History of Lattice Boltzmann Methods

Lattice Boltzmann Method (LBM) is a discrete velocity method which has been well developed in the last decade as an alternative approach to simulate hydrodynamic systems ([26], [29], [44], [47]). For each velocity v_i, a single-particle distribution function f_i is involved. Lattice Boltzmann methods include two repeating procedures propagation and collision. There are two well known approaches to obtaining lattice Boltzmann methods. One approach to derive this method comes originally from Lattice Gas Automata (LGA), and another approach is from the over-relaxation discretization of Boltzmann's kinetic transport equation.

Lattice gas automata ([24], [25]) appear as an alternative approach for studying complex physical systems. Lattice Boltzmann methods can be derived from lattice gas automata. The concept of continuum is not used in LGA and LBM, and the phase-space and time are discretized. The number of velocities are finite and usually take small numbers for a velocity set. Instead of using the macroscopic approach for some of the traditional numerical methods, LGA and LBM

use kinetic concepts to deal with physical systems.

The essence of kinetic theory is to make a connection between the microscopic and macroscopic dynamics, but does not treat macroscopic dynamics directly. This means the macroscopic equations are derived from microscopic equations, but at the same time ignoring many fine details of the true microscopic dynamics physics. The hydrodynamic equations can be obtained from the distribution functions.

In LBM, the advection (also called propagation, or free flight) equation is always the same, but the collision operator can have many different forms. Among these collision operators, the Bhatnager-Gross-Krook (BGK) operator [31] is a simplified operator, where collisions are interpreted as a single time relaxation to local equilibria. When the Bhatnager-Gross-Krook operator is applied in LBM, we obtain the well known LBGK method. LBGK is linear in the advection procedure, and is locally non-linear in the collision procedure.

1.2 The Stability Problem and the Construction of Schemes

LBGK encounters the classical stability and accuracy problems. When LBGK is applied in high Reynolds numbers, even with a sufficiently small relaxation time, it suffers numerical instabilities and lack of accuracy.

The explicit manifestations of these instabilities are spurious oscillations and local blow ups. There are a variety of reasons for the causes of instabilities. Positivity loss and large deviations are two of the reasons [42]. Positivity loss happens when the condition of positive populations or probabilities is not fulfilled. Large derivations happen when the distribution f is far from local equilibrium. When

hydrodynamic gradients not small and low, linear stability analysis is satisfactory, but when hydrodynamic gradients are sharp and high, the nonlinear stability analysis is needed. For other related lattice Boltzmann methods research approaches, please see ([53], [59], [60], [61], [66], [69], [71], [72], [73]).

The concept of bringing entropy to LBM has improved the stability and accuracy of LBGK. The lattice entropic Bhatnager-Gross-Krook Boltzmann equation is called ELBM, which uses the H-theorem ([43], [47]). However ELBM can not erase the instabilities entirely.

In the 1970s, Boris and Book (see [32], [33], [34]) introduced flux-corrected transport (FCT), which is also called flux limiter, to improve the quality of numerical convection algorithms. There are a lot of modern monotonicity-preserving and non-oscillatory fluid transport schemes which can originally trace back to Boris and Book's contributions.

The construction of nonequilibrium entropy limiters [44] is partially based on the concepts of flux limiter. The performance of nonequilibrium entropy limiters for lattice Boltzmann methods has similar effects as flux limiters do for finite difference, finite volumes and finite elements. The essence of the construction of nonequilibrium entropy limiters is to control a scalar quantity, the nonequilibrium entropy. The nonequilibrium entropy limiters are Ehrenfests' regularization, smooth limiter 1, smooth limiter 2, median and mean entropy limiters. The maximum median entropy limiter and the general median entropy limiter are newly constructed, but the general median entropy limiter does not have effective performance for front shock regions. All the median entropy limiters can have different effectively performance according to the the choices of stencils. These limiters are tested on $1D$ athermal shock tube, with three-velocity and five-velocity sets.

1.3 Thesis Structure

Chapter one briefly discusses the history of lattice Boltzmann methods, the instability problem that we face for LBM, and the concepts for the construction of nonequilibrium entropy limiters.

Chapter two gives the fundamental concepts and background of fluid dynamics and some important parameters which are closely associated with lattice Boltzmann method. Euler equations and Navier-stokes equations in one dimension, Mach number, Reynolds number and Knudsen number are given here.

Chapter three discusses the history and derivations of lattice Boltzmann method. The simplified collision operator we will use for lattice Boltzmann method is the Bhatnagar-Gross-Krook collision operator.

In Chapter four, the background and history of entropy is elaborated in detail. The interpretations of entropy both in a thermodynamics approach and in a statistical approach are stated. The two well known entropy H-functions, Boltzmann-Gibbs-Shannon entropy H-function, and the Kullback and Leibler entropy function are introduced here. The Kullback entropy is applied here in the lattice Boltzmann method.

In Chapter five, the history of flux-corrected transport is displayed, and the history of median filter, mean filter and conservative filter in image processing are given.

In Chapter six, the basic concepts for the construction of nonequilibrium entropy limiters are explained in details. The Positivity rule provides a way to keep the distribution positive. Ehrenfests' regularization offers a local-wise correction for LBGK methods. The smooth limiters and median entropy limiters are ensemble dependent limiters which are based on filtering the nonequilibrium entropy. The three-velocity set of LBGK is tested on shock tube with the comparison of

LBGK without limiters.

Chapter seven illustrates the numerical computations and performance which the nonequilibrium entropy limiters provide for LBGK methods, and the performance of LBGK without limiters as the frame of reference. In this chapter, 3 five-velocity sets are tested on shock tube. The calculations for the local equilibria for these velocity sets are non-entropic with the application of Kullback entropy.

Chapter eight concludes the analysis of nonequilibrium entropy limiters for lattice Boltzmann methods. Some future work about the nonequilibrium entropy limiters and their applications will be discussed.

Chapter 2

Equations of Fluid and Gas Automata

2.1 Some Basic Concepts

2.1.1 The Macroscopic and Microscopic Approaches

There are two different approaches for solving the problems involved in fluids, which are the continuum (macroscopic) approach and the molecular (microscopic) approach [15]. For the microscopic approach, fluids are defined in the form of particles, i.e. molecules or atoms. A fluid is described as a collection of discrete particles being in random motion and elastic collisions between particles and with the walls of its container. The conservation of mass, momentum and energy are employed for each particle.

In the macroscopic approach, instead of using particles, an infinitely divisible substance, the continuum, is used. The macroscopic approach in thermodynamics, is also known as classic thermodynamics. In the macroscopic approach, the concept of continuum has to be assumed, on the other hand, in the microscopic

approach, the concept of continuum is not valid. The detailed molecular and atomic nature of matter is taken into account in microscopic thermodynamics, on the other hand, the detailed molecular and atomic structures of the substance are neglected in macroscopic thermodynamics.

The equation of continuity describes the conservation of mass, the equation of motion (the momentum equation) describes the conservation of momentum, the equation of energy which is the first law of thermodynamics describes the conservation of energy in the fluid.

2.1.2 Kinetic Theory

Kinetic theory, also called dynamic theory, states that the laws of mechanics can be implemented to the individual molecules of a system [14]. Further more it sates that from these laws which are possible to derive other related properties of the equation of state, such as expressions for the pressure of a gas, its internal energy and its specific heat capacity. In other words, microscopic thermodynamics analysis can be done through the analysis of the behavior of gas molecules which is based on classical mechanics. The laws of mechanics are accepted as axiomatic in this analysis. From the detailed microscopic analysis, certain special macroscopic thermodynamic phenomena can be derived. As previously mentioned, the equation of state of a system describes the relationship between its measurable macroscopic properties. An ideal gas has the simplest equation of state, and to understand how a molecular model can be used to derive the equation of state of an ideal gas by using kinetic theory, the following assumptions (see [12], [13]) are necessary:

1. There is a very large number of molecules for any macroscopic volume of a gas. For example, at standard conditions, there are around 3×10^{25} molecules

in a cubic meter.

2. The second assumption is that molecules are in continuous motion, and the distances between molecules are much larger than the length of their own diameters.

3. When molecules collide with each other, there are forces acting on them. Apart from these forces from collision, no other external forces would have effect on molecules, therefore, they move in straight lines. Collisions taking place between molecules and with the walls which are assumed as perfectly geometrically smooth, are treated as elastic.

4. In an isolated container, the molecules are distributed uniformly with no external forces acting upon it. Similarly, the directions of molecular velocities are distributed uniformly. So if the total number of molecules is N in an isolated container where the volume is V, then the average number of molecules per unit volume, say n, is:

$$n = N/V.$$

2.1.3 Statistical Thermodynamics

Statistical thermodynamics has close relationship with thermodynamics and kinetic theory. It was first developed in the last century, mainly by Boltzmann and Gibbs. Statistical thermodynamics, also called statistical mechanics, does not consider the detailed molecules as individuals, and uses probability to describe the very large number of molecules. Since molecules are numerous, even if any information about specific molecules is neglected, the average properties can be obtained. Statistical thermodynamics provides a definition of the concept of

entropy, and an explanation of the principle of the increase of entropy.

2.2 Euler Equations

Euler equations [3] are a system of nonlinear conservative equations which govern inviscid flow. They are time dependent equations. They named after Leonard Euler(1757).

A set of variables to describe a flow can be expressed either as primitive variables (also called physical variables), or conserved variables. The primitive variables are described as density $\rho(x,t)$, pressure $P(x,t)$ and velocity $u(x,t)$. The conserved variables are described as density ρ, momentum ρu and the total energy per unit volume $E = \frac{1}{2}\rho u^2 + \rho e$, where e is the internal energy.

Euler equations consist of the equations of the conservation of mass, momentum and energy. The one space dimension (1D) Euler equations are:

$$\begin{aligned} \frac{\partial \rho}{\partial t} + \frac{\partial (\rho u)}{\partial x} &= 0, \\ \frac{\partial (\rho u)}{\partial t} + \frac{\partial (\rho u^2 + P)}{\partial x} &= 0, \\ \frac{\partial E}{\partial t} + \frac{\partial (uP + uE)}{\partial x} &= 0. \end{aligned} \tag{2.1}$$

The governing partial differential equations (2.1) for the motion of a fluid is incomplete as a full description of the associated physical process. The problem is that there are more unknown variables than the equations given above, so closure conditions are needed. The key to obtaining closure conditions is to introduce thermodynamics which gives new physical variables and offers relations between variables. In equation (2.1), a new variable e is involved, the specific internal energy, which can be defined in terms of density and pressure. Therefore an extra relation is generated as a closure condition for an ideal gas equation of state:

$$P = \rho(\gamma - 1)e - \gamma P^0. \tag{2.2}$$

The internal energy is $e = E - \frac{1}{2}\rho u^2$, where γ is the adiabatic exponent set as $\gamma > 1$ and P^0 is a substance specific pressure adjustment term between liquid molecules (for an ideal gas, $P^0 = 0$).

The two space dimension (2D) compressible Euler equations are:

$$\begin{aligned}
\frac{\partial \rho}{\partial t} + \frac{\partial(\rho u_1)}{\partial x_1} + \frac{\partial(\rho u_2)}{\partial x_2} &= 0, \\
\frac{\partial(\rho u_1)}{\partial t} + \frac{\partial(\rho u_1^2 + P)}{\partial x_1} + \frac{\partial(\rho u_1 u_2)}{\partial x_2} &= 0, \\
\frac{\partial(\rho u_2)}{\partial t} + \frac{\partial(\rho u_2^2 + P)}{\partial x_2} + \frac{\partial(\rho u_1 u_2)}{\partial x_1} &= 0, \\
\frac{\partial E}{\partial t} + \frac{\partial(u_1(P+E))}{\partial x_1} + \frac{\partial(u_2(P+E))}{\partial x_2} &= 0,
\end{aligned} \tag{2.3}$$

where the velocity is $\bar{u} = (u_1, u_2)$, the internal energy is $e = E - \frac{1}{2}\rho(u_1^2 + u_2^2)$ and the rest are the same defined in 1D Euler equations.

A much simple equation of state for Euler equations is the isothermal state, rather than the ideal gas state. The isothermal 1D Euler equations are:

$$\begin{aligned}
\frac{\partial \rho}{\partial t} + \frac{\partial(\rho u)}{\partial x} &= 0, \\
\frac{\partial(\rho u)}{\partial t} + \frac{\partial(\rho u^2 + P)}{\partial x} &= 0,
\end{aligned} \tag{2.4}$$

where the pressure is $P = \rho c^2$.

2.3 Navier-Stokes Equations

Navier-Stokes equations ([3], [62], [63]) are much more complicated than Euler equations. Basically the heat conduction and viscous terms are added to the Euler equations to form the Navier-Stokes equations.

Navier-Stokes equations are a set of nonlinear partial differential equations which used to describe the motion of a Newtonian fluid. The fluid could be liquid or gas. Here we concentrate on gas as a compressible fluid. The Navier-Stokes equations were firstly started by Navier(1827). It was then further developed and summarised with the methods and hypotheses of Naviers, Poission(1831) and Sint-Venant(1843). The one space dimension compressible viscous Navier-Stokes equations are:

$$\begin{aligned} \frac{\partial \rho}{\partial t} + \frac{\partial(\rho u)}{\partial x} &= 0, \\ \frac{\partial(\rho u)}{\partial t} + \frac{\partial(\rho u^2 + P)}{\partial x} &= (\lambda + 2\mu)\frac{\partial^2 u}{\partial x^2}, \\ \frac{\partial E}{\partial t} + \frac{\partial(uP + uE)}{\partial x} &= \frac{1}{2}(\lambda + 2\mu)\frac{\partial^2(u^2)}{\partial x^2} + k\frac{(\partial^2\theta)}{\partial x^2}, \end{aligned} \tag{2.5}$$

where the pressure $P = (\gamma - 1)e$ is determined by an ideal polytropic equation of state, the internal energy is $e = E - \frac{1}{2}\rho(u^2)$, and the absolute temperature is $\theta = \theta(x,t) > 0$, such that $C_v\rho\theta = e$. An polytropic gas is also called calorically ideal gas where γ is a constant, while for a thermally ideal gas γ is a function of temperature, i.e. $\gamma = \gamma(T)$. The viscous terms depend on the constant Lame coefficients of the viscosity $\lambda > 0$ and $\mu > 0$, and the heat fluxes depend on the constant conductivity $k > 0$. Here $C_v > 0$ is the specific heat at constant volume, and is set as $C_v = 1$ for simplicity as $k \to k/C_v$.

When the right hand side of all the Navier-Stokes equations (2.5) equal to 0, i.e. the coefficients of the viscous terms λ and μ tend to be zero, and the coefficient of

heat conductivity term k tends to be zero, the 1D Navier-Stokes equations become the 1D Euler equations.

The Navier-Stokes equations and Euler equations are time dependent and consist of a continuity equation for conservation of mass, conservation of momentum and conservation of Energy. The independent variables of the NS and Euler equations are spatial coordinates and the time t, and the dependent variables are the density, the pressure, the velocity and the temperature.

2.4 The classifications of Compressible and Incompressible Fluids

In general, it is normal to classify the flow as compressible or incompressible based on the fluid which is flowing. Compressible flow is defined as variable density flow, while incompressible flow has constant density throughout. In a lot of practical problems, if the density changes 5 percent or more, the flow is treated as a compressible flow. Hydrodynamics represents the behavior of incompressible fluids, while gas dynamics represents the behavior of compressible fluids.

It is worth mentioning that the modern approach of compressible flow has gained attention since 1960. The difference between the modern approach and the classical approach of compressible flow is that apart from the classical analysis, the modern approach is supported also by many computational techniques with the treatment of noncalorically perfect gas(see [21], [23]).

Compressibility is not associated with the fluid's ability to change shape, such as that of pure shear. In order to elaborate more details about compressibility of a fluid, here we introduce a coefficient of compressibility β which is defined as:

$$\begin{aligned}\beta &= \frac{Relative\,Change\,In\,Volume}{Change\,In\,Pressure} \\ &= \lim_{\Delta p \to 0}(-\frac{\Delta v}{v\Delta p}) = -\frac{1}{v}\frac{dv}{dp}.\end{aligned} \tag{2.6}$$

Since $v = \frac{1}{\rho}$, so the coefficient β becomes

$$\beta = -\frac{1}{\rho}\frac{d\rho}{dp} = \frac{1}{\psi}, \tag{2.7}$$

where ψ is the Bulk Modulus of Elasticity which is defined as

$$\begin{aligned}\psi &= \frac{Change\,In\,Pressure}{Relative\,Change\,In\,Volume} \\ &= \lim_{\Delta p \to 0}(-\frac{v\Delta p}{\Delta v}) = -v\frac{dp}{dv},\end{aligned} \tag{2.8}$$

There are several dimensionless parameters that are used to classify the flow of a fluid. They are called Mach number, Reynolds number and Knudsen number.

2.4.1 Mach Number

Mach number is a markedly important parameter in the analysis of compressible flows. Mach number is a dimensionless parameter named after the Austrian physicist Ernst Mach. The Mach number at a point is defined as the ratio of the local velocity of the flow to the local velocity of the sound in the medium:

$$M = \frac{V}{a}, \tag{2.9}$$

where V is the local velocity and a is the local speed of sound. When the temperature increases, the speed of sound increases, thus when the Mach number equals

to 1 the speed of the fluid depends on the fluid temperature around it. For a perfect gas $P = \rho RT$, the speed of sound is:

$$a = \sqrt{\gamma RT}, \tag{2.10}$$

where γ is the adiabatic exponent, R is the gas constant, and T is the temperature.

The steady compressible flow can be classified as incompressible, subsonic, sonic, transonic, supersonic and hypersonic different flow regimes, based on the magnitude of the Mach number(see [2]):

- **incompressible:** $M < 0.3$,
- **Subsonic:** $0.3 < M < 1$,
- **Sonic:** $M = 1$,
- **Transonic:** $0.8 < M < 1.2$,
- **Supersonic:** $1.2 < M < 5$,
- **hypersonic:** $M > 5$.

2.4.2 Reynolds Number

Reynolds number is a dimensionless parameter defined as the ratio of the inertial force to the viscous force. In 1883, Osborne Reynolds firstly introduced this number to fluid dynamics as one of the principle hydrodynamic properties to classify the stability problems in the transition from laminar to turbulent flow in pipes. In 1963, Oswatitsch showed that the Reynolds number can be also interpreted as the ratio of the momentum flux to the shearing stress, which indicates that the inertial

force is not necessarily the determinative term. Here we use the first definition of Osborne Reynolds:

$$R = \frac{InertialForce}{ViscousForce}. \tag{2.11}$$

The inertial force and the viscous force can be written respectively as:

$$Mass(= \rho L^3) \cdot \ acceleration \, [\approx u_0/t = u_0/(L/u_0) = u_0^2/L]. \tag{2.12}$$

$$TangentialStress(= \mu \frac{u_0}{L}) \cdot \ surface \, (= L^2), \tag{2.13}$$

where L and u_0 are the characteristic length and characteristic velocity respectively, μ is the absolute dynamics fluid viscosity. Substitute the equations of inertial force and viscous force into equation (2.11):

$$R = \frac{\rho u_0 L}{\mu} = \frac{u_0 L}{\nu}, \tag{2.14}$$

where ν is the kinematic viscosity term which is $\nu = \frac{\mu}{\rho}$.

Therefore, the Reynolds number evaluates the relative importance of the fluid's inertia and viscosity. A high Reynolds number is produced if the viscous force is smaller than the inertial force, which is caused by the small value of ν or the big value of u_0. High values of R are related to an unstable flow, while low values of R are related to a stable flow. The stable or unstable flow is related to the local speed of the flow and the thermodynamic properties of the fluid change rate. For high Reynolds number, it is possible that the speed of flow is very high, or perhaps it is a nearly inviscid low-speed flow. When R is usually numerically very large or tends to infinite, the following flows are defined: turbulent flows, inviscid flows, potential flows and flows far removed from boundaries. When R is numerically very small, the flows are normally defined as: creeping flows, laminar flows, Stokes

flow and lubrication theory, bubble flows, and flows very close to a boundary. So Reynolds number is mostly used as a tool to describe the speed and/or viscous properties of a flow field.

2.4.3 Knudsen Number

Knudsen number is a crucial measure for molecular-structure effects, which is the ratio of the mean free path of a molecule λ to a characteristic dimension of the flow geometry L. This is:

$$Kn = \frac{\lambda}{L}. \tag{2.15}$$

The mean free path of a molecule is the average distance traveled by a molecule between collisions which occur by the random motion of the molecules. The characteristic dimension L can be easily obtained, for example, the radius of a body in fluid, or the length of a cubical box edge, or the diameter of a long pipe, etc. Since both λ and L are the same units of length, the ratio Kn is dimensionless. When λ is much less than L, i.e. $Kn << 1$, molecule-molecule collisions determine gas behavior and such that it forms as a fluid in a continuum or viscous state. Here continuum means continuum media. On the other hand, if $\lambda >> L$, i.e. $Kn >> 1$, then it turns to be molecule-surface collisions determine gas behavior, such that it is not a fluid-like state, called molecular state. Therefore, these states, or regimes can be categorized as follows [2]:

- **Continuum:** $Kn < 0.01$,
- **Molecular:** $Kn > 1$,
- **Transitional:** $0.01 < Kn < 1$.

In reality, there is no sharp change between continuum and molecular states. Knudsen number is also used to separate the line between macroscopic and microscopic models:

- **macroscopic:** $Kn < 1$,
- **microscopic:** $Kn > 1$.

It is vital to mention that the very essential condition for the continuum assumption which is required in the Navier-Stokes equations is that the mean free path of the molecules is smaller than the characteristic dimension of the flow domain. If this condition is not valid, then the fluid is not under local thermodynamic equilibrium and Newton's law of viscosity cannot be applied. For example, beyond $Kn = 0.1$, the continuum assumption of the Navier-Stokes equations will start to fall down and alternative approaches have to be used.

Chapter 3

Lattice Boltzmann Method

There are two approaches to obtain lattice Boltzmann methods. One approach to derive this method comes originally from Lattice Gas Automata (LGA), and another approach is from the Boltzmann's kinetic transport equation. One approach for the lattice Boltzmann simulation of hydrodynamics is [79]:

$$Boltzmann \rightarrow \mathbf{LBE} \rightarrow Navier - Stokes,$$

and another approach for the lattice Boltzmann simulation of hydrodynamics is:

$$Newton \rightarrow LatticeGas \rightarrow \mathbf{LBE} \rightarrow Navier - Stokes.$$

In this section these derivations are presented approximately as they developed historically.

3.1 Lattice Gas Cellular Automata

In general, to solve the problem of physical systems, the first step would be to derive the partial differential equations for the system and then solve it analytically or numerically. However most the of physical systems we are dealing with are very complicated, and most of their analytical solutions are difficult to obtain. Thus numerical solutions are an alternative way of solving complicated physical problems.

3.1.1 Cellular Automata

In the late 1940s, John von Neumann introduced the concept of cellular automata approach (also called CA), and since then this approach have been used in many different areas to model physical systems. The concept of continuum has been left behind in this approach.

Cellular automata are defined as an idealization of a physical system with discrete time and space, and only a finite set of values are taken for the physical quantities [24]. Cellular automata rules can be thought as another formation of microscopic reality which has the predicted macroscopic behavior. Cellular automata could be considered as the extremely simplified version of molecular dynamics(MD).

Cellular automata also have several disadvantages. The simulation of cellular automata is very noisy, since it is based on Boolean quantities. Another problem is that this method does not have very much flexibility to alter parameters in order to simulate more complicated physical systems.

3.1.2 Lattice Gas Cellular Automata

Lattice Gas Cellular Automata(LGCA) is a special class of cellular automata, which is one of the simplest models with discrete velocity to simulate fluid motion [25]. The remarkable difference between CA and LGCA is the update being divided into two parts which are propagation (also called streaming) and collision. Propagating describes each particle propagates to the nearest node according to the direction of its velocity. The collision procedure of LGCA is very similar with the update rule for CA. Collision refers to particles meeting in a node and how they interact and change their velocity directions based on scattering rules. After the collision, the state of each site propagates to its neighbour site. This separation, i.e. propagation and collision procedures, ensures propagation being executed and maintains the update rule simple.

In 1986, Frisch, Hasslacher and Pomeau contructed a model with fictitious particles, which each particle has the same mass [28]. The key point is that the particles moving with the same speed with 6 possible velocities. Then the particles collide when they meet, provided that the number of particles and momentum are conserved. The dynamic rule is described as only if one particle can enter the same site at the same time with the same velocity. Particles getting in the same site at the same time interact with each other and have new local distribution of particle velocities. This model is called FHP model. The FHP model is sufficient to obtain isotropic hydrodynamics, and therefore lattice gas cellular automata were brought as a model of the Navier-Stokes equations. This development has laid out the theoretical foundations of the lattice gas cellular automata, and the later development of the lattice Boltzmann methods.

The Lattice Gas is constructed as a simplified, fictitious molecular dynamic systems in which space, time and the particle velocities are all discrete (Chen and

Doolen 1998) [27]. From this point of view, the lattice gas method is normally regarded as lattice gas cellular automata. The very important quality of the lattice gas automata which is different from a cellular automata is that mass and momentum are conserved. Therefore this model is more appropriate for simulating real physical problems.

Different microscopic interactions arrive to the same form of macroscopic equations [25]. This is how the development of LGCA started. The microscopic interaction is rigorously local for the particles assigned at nodes. Particles update momentum with the vital condition that the conservation of mass and momentum are the sum up over each node. A particle propagates to its next neighbor node along its related link after each collision. The microdynamics can be viewed as a repetition of collision and propagation. The values of mass and momentum density for macroscopic state are obtained by coarse graining (the mean values over large spatial regions).

Lattice-gas cellular automata are normally based on a regular lattice with particles staying on the nodes [27]. A set of Boolean variables $n_i(x,t)(i = 1, ..., M)$ represent the particle occupation, and M is the number of directions of the particle velocity at each node:

$$n_i(x + v_i, t + 1) = n_i(x, t) + \Omega_i(n(x, t)), \tag{3.1}$$

where v_i are the local particle velocities, and Ω_i is the collision operator which is a function of all particles. At each time step, the particles experiment two sequential sub-steps, propagation and collision.

However, LGCA faces some difficulties, which are: lack of Galilean invariance, statistical noise, spurious invariants [29].

For the problem of lack of Galilean invariance, the main issue is that the continuum family of equilibria can not be parameterized with the flow speed $\vec{u}$ for a finite number of speeds. This led to the consequence that only producing a perturbative expansion can interpret hydrodynamic equilibria, but this expansion does not correspond to the form of the Navier-Stokes inertial and pressure tensors.

LGCA is a particle method, so it can not avoid to produce a fair amount of statistical fluctuations (noise). The root cause for this is LGCA is a N-body Boolean system and it generates a lot of unnecessary many-body details. However, on another side of this, the statistical noise intrinsic to LGCA dynamics is similar to true noise in actual thermodynamic systems.

For continuum fluids in a isolated system environment, mass, momentum and energy are conservative. For discrete fluids, some additional conserved quantities could be produced from the lattice discreteness. These are pure artifacts, and are so called spurious invariants.

For high Reynolds flow simulations, LGCA can not reach a good approximation, so in the early 90s, LGCA has been leveled off. Therefore, the lattice Boltzmann method was developed exactly according to the initial weaknesses of LGCA, and nowadays lattice Boltzmann method can be studied independently without the reference from LGCA.

3.2 From LGCA to Lattice Boltzmann Method

The lattice Boltzmann mothod was firstly developed from LGCA. It uses a single particle distribution function with real variables. The single particle distribution function interacts locally and propagate after collision to the next neighbor node. The lattice Boltzmann method neglects individual particle motion and particle-

particle correlations in the kinetic equations. Lattice Boltzmann equation states that the distribution function does not change the particles trajectory between collisions. However, it emphasizes the changes as a result of an 'instantaneous' interaction between colliding particles.

The advection transformation, also called free flight, streaming, originally derives from Newton's second law. The probability density $f(\boldsymbol{x}, t)$ on phase space expresses the equation of incompressible flow, with discrete velocities. The free flight transformation is:

$$\frac{\partial f_i}{\partial t} + \boldsymbol{v}_i \cdot \nabla_x f_i = 0. \tag{3.2}$$

If the initial condition of density is given at time $t = 0$, then the analytical solution is amazingly simple: $f_i(\boldsymbol{x}, \boldsymbol{v}, t) = f_i(\boldsymbol{x} - \boldsymbol{v}_i t, \boldsymbol{v}, 0)$.

In lattice Boltzmann equation, the free flight equation is always the same, and this dynamics should conserve entropy.

In comparison with this analytical solution, the numerical advection equation is much more difficult to solve, which is in fact a matter of best choice among vast approaches of approximation for different numerical applications. The main problem arises from the process of discretization, which is the change of the advection equation from continuous to discrete state that only leads the result reaching to the best approximation. Therefore, reducing the impact of discretization for solving the advection equation by the lowest computational cost is crucial for the modeling of fluid flow.

The further developments of Lattice Boltzmann method are the simplification of the collision operator and the selection of different distribution functions. This development gives much more flexibility to the application of Lattice Boltzmann method.

3.2.1 Local Equilibrium and Global Equilibrium

For global equilibrium the density is constant, while for local equilibrium it varies in space and time. The crucial property for the choice of local equilibrium is that it has to satisfy the consistency condition: the summation of the local equilibriums is equivalent to the density ρ [81].

The key issue for the derivation from the Boltzmann equation to hydrodynamics is local equilibrium, which is interpreted as a local distribution function f^e. At the local equilibrium state, the gains and losses are equivalent. Thus the collision term becomes:

$$\Omega(f^e, f^e) = 0,$$

where the superscript 'e' represents the local distribution function f is in local equilibrium. This leads to the 'detailed balance' condition:

$$f_1^{'} f_2^{'} = f_1 f_2.$$

This detailed balance condition could be interpreted as a direct/inverse collision is balanced by an inverse/direct partner. Take the logarithms of the above equation:

$$\ln f_1^{'} + \ln f_2^{'} = \ln f_1 + \ln f_2.$$

This property indicates that the quantity $\ln f$ is an additive collision invariant. At thermodynamic equilibrium, $\ln f$ has to be a function of dynamic collision invariants $I(v) \equiv [1, m\boldsymbol{v}, mv^2/2]$, namely number, momentum and energy conservation.

$$\ln f = A + B_a v_a + \frac{1}{2} C v^2, \tag{3.3}$$

where A, B_a, C are Lagrangian multipliers bearing the functional dependence on ρ, ρu_a, E which are density, momentum and energy, and they are calculated by the conservation of these quantities:

$$\begin{aligned} m\int f d\boldsymbol{v} &= \rho, \\ m\int f\boldsymbol{v} d\boldsymbol{v} &= \rho u_a, \quad a = 1, 2, 3, \\ m\int f\frac{v^2}{2} d\boldsymbol{v} &= \rho e, \end{aligned}$$

where u_a is the macroscopic flow speed, and ρe is the energy density.

3.2.2 Nonlinear Lattice Boltzmann Equation

As before mentioned, the earliest Lattice Boltzmann equation (LBE) was developed from LGCA, which was very much related to the weaknesses of LGCA, particularly statistical noise. But fortunately, not long after it was shown that the lattice Boltzmann equation can cope with many other problems that LGCA suffers. Thus lattice Boltzmann equation has taken the advantages of LGCA, and discarded the anomalies plaguing [29].

In 1988, G.McNamara and G.Zanetti firstly introduced LBE, with the initial motivation to deal with the statistical noise problem in LGCA [39]. The fundamental idea is straightforward, which is to replace the Boolean occupation numbers n_i with the associated ensemble-averaged populations:

$$f_i = \langle n_i \rangle ,$$

where $\langle\,\rangle$ means the ensemble averaging. The concept has been changed from tracking single Boolean molecules to the time history of a collective population

which expresses a 'cloud' of microscopic states.

Mathematically, the Boolean occupation numbers can be separated into two parts, the average part and the fluctuating part:

$$n_i = f_i + g_i,$$

where the average of fluctuating g_i is zero, i.e. $\langle g_i \rangle = 0$. Thus,

$$\Delta_i f_i = \Omega_i(f) + G_i,$$

where Ω_i is the collision operator, and G_i is the sum of all contributions from interparticle correlations.

For the purpose of simplicity, the earliest Lattice Boltzmann Equation (LBE) assumed that there is no correlations between particles for a collision, i.e. $G_i = 0$. Therefore it left a nonlinear, finite difference equation for the one particle distribution f_i:

$$\Delta_i f_i = \Omega_i(f_1, .., f_m),$$

where m is the m-th order of polynomial of f. This nonlinear LBE is a transcription of LGCA microdynamics accompanied with the replacement $n_i \rightarrow f_i$. The distribution f_i as defined before, is the averaged, smooth quantity, and as a consequence, the effect of averaging populations is that the statistical noise has been removed away. However, on the physical side, the physics of particle correlations ('non-Boltzmann effects') is lost. Thus, some of the fundamental concerns, such as the breakdown of molecular chaos, long time tails, and related points are not in any consideration.

3.2.3 The Quasilinear Lattice Boltzmann Equation

The crucial development in the Chapman-Enskog treatment which leads from kinetic theory to hydrodynamics, is the low Knudsen, small mean free path assumption in discrete form [29]:

$$f_i = f_i^e + f_i^{ne}. \tag{3.4}$$

The non-equilibrium component f_i^{ne} corresponding to the equilibrium f_i is calculated as the order of $O(k)$, where k is the Knudsen number. In the late 80's, nearly at the same time, Higuera and Jimenez expanded the equation with a low Mach number expansion into the lattice Chapman-Enskog treatment as follows [29]:

$$f_i = f_i^{e0} + f_i^{e1} + f_i^{e2} + f_i^{ne} + O(kMa^2), \tag{3.5}$$

where the superscripts 0, 1, 2 stand for the order of the Mach number expansion. The collision operator around global equilibria f_i^{e0} can be expanded as:

$$\Omega_i(f) = \Omega_i^0 + \Omega_{ij}^0 \phi_j + \frac{1}{2}\Omega_{ijk}^0 \phi_j \phi_k, \tag{3.6}$$

where

$$\phi_i = f_i - f_i^{e0},$$

$$\Omega_{ij} = \partial \Omega_i / \partial f_j,$$

and

$$\Omega_{ijk} = \partial^2 \Omega_i / \partial f_j \partial f_k.$$

This superscript 0 means it is defined at $f_i = f_i^{e0}$. The collision operator at global

equilibria is

$$\Omega_i^0 = 0.$$

And without the terms higher than $O(kMa^2)$,

$$\Omega_i(f) = \Omega_{ij}^0 f_j^1 + \frac{1}{2}\Omega_{ijk}^0 f_j^1 f_k^1 + \Omega_{ij}^0 f_j^{ne},$$

while at a local equilibrium $f_i = f_i^e$, i.e. $f_i^{ne} = 0$, the above equation left as:

$$\Omega_{ij}^0 f_j^1 + \frac{1}{2}\Omega_{ijk}^0 f_j^1 f_k^1 = 0.$$

Therefore,

$$\Omega_i = \Omega_{ij}^0 f_j^{ne} = \Omega_{ij}^0 (f_j - f_j^e),$$

Eventually, this leads to the quasilinear LBE introduced by Higuera and Jimenez,

$$\Delta_i f_i = A_{ij}(f_j - f_j^e),$$

where $A_{ij} \equiv \Omega_{ij}^0$. Although this equation seems as a linear equation, it is a nonlinear equation which represents the nonlinear Navier-Stokes dynamics. The quadratic nonlinearity is embedded in the local equilibrium term f_i^e.

The LBE developed by McNamara and Zanetti, and Higuera and Jimenez have reduced two defects of LGCA: statistical noise and the complexity of the collision rule.

3.2.4 Lattice Boltzmann Methods

To solve the Boltzmann equation analytically and numerically, the main problem is how to manage the nonlinear integral collision operator. Because of the realistic

interactions between particles, the integral collision operator expressed in Boltzmann equation is very complicated. At the hydrodynamic level which includes turbulence, the realistic form of the collision operator is not really necessary to keep all the details, and most details contained in operator Ω play no role. In 1954, Bhatnagar, Gross and Krook introduced in ([31], [59]), a much simpler collision operator. In this collision operator, some mathematically simple terms are chosen, where these terms consistent with the conservation laws of mass, momentum and energy, and meanwhile, keep certain essential qualities of collisions, such as persistence of velocity. This simpler form of the collision operator is suitable from low density to high density, even the intermediate region is included. In addition, this form is also applicable to physically more complicated situations.

Here we give some details about how the Boltzmann equation collision operator changed into the simpler Bhatnagar-Gross-Krook(BGK) relaxation collision operator [30]. In the Boltzmann equation there are two parts for each collision term. One part describes particles absorbed from a definite velocity range by collisions, and another part describes the particles emitted into that range after the collisions. For BGK operator, the absorption term is nearly the same as in Boltzmann equation, but the emission term is substituted by a term representing a Maxwellian distribution of the emitted particles, where the particles meet the condition that density, mass velocity, and temperature fulfill the conservation laws of mass, momentum and energy. The BGK collision operator is:

$$\Omega[f] = -\frac{1}{\tau}(f - f^e), \tag{3.7}$$

where f^e is a local equilibrium associated with the local conserved quantities density ρ, speed u and temperature T, while τ is a time scale which relates collision

relaxation to the local equilibrium. In principle, τ is a complicated functional of the distribution function f, but here τ related to the BGK equation is to consider the simplification which τ is a constant value for this relaxation scale.

This simplified BGK collision operator looks like a linear operator, since the explicit particle-particle quadratic coupling is being removed in the process. But in reality it is not the case as its appearing, and the truth is that in BGK collision operator the local equilibrium depends exponentially on the fluid speed and temperature, which both are linear functions of the particle distribution. This property of hidden nonlinearity is very important for obtaining analytical solutions and has a very strong effect on the lattice Boltzmann equation.

The following equation is the Bhatnagar-Gross-Krook model Boltzmann equations in continuum kinetic theory, and it is the famous LBGK for a short name:

$$\frac{\partial f}{\partial t} + v\frac{\partial f}{\partial x} = -\frac{1}{\tau}[f - f^e]. \tag{3.8}$$

The equilibrium f_i^e is the local equilibrium distribution with a Maxwellian form:

$$f_i^e = \frac{\rho}{(2\pi v_T)^{d/2}} exp[-\frac{(v-u)^2}{2(v_T)^2}], \tag{3.9}$$

where d is the spatial dimension. The thermal speed v_T with the fluid temperature T is:

$$v_T = \sqrt{\frac{K_B T}{m}}.$$

From the above equation, we can see that the local equilibrium is entirely dominated by the local hydrodynamic quantities, ρ, T, and u.

The propagating operator is linear, and the collision operator contains nonlinearity. In the collision operator, the local Maxwellian f^e gives nonlinearity and

that is completely local in configuration space. The conservative laws are embedded on the local equilibrium, and the local equilibria has to ensure that it takes the same density and momentum as the actual distribution function:

$$\begin{aligned} \sum_i f_i^e &= \sum_i f_i = \rho, \\ \sum_i f_i^e c_{ia} &= \sum_i f_i c_{ia} = \rho u_a. \end{aligned} \tag{3.10}$$

Unlike the lattice Boltzmann equation only applies to low density situation, LBGK has much wider areas for applications which opens up from low to high density situation. LBGK has all the properties of hydrodynamics. LBGK also can be applied to most complexities of velocity space, which includes multiphase and complex boundary conditions, and does not have conflicts with the hydrodynamic content of the theory.

Here we give some elaboration of the difference between LBGK and LBE. LBE does not need the full equilibrium distribution, instead only the second-order term in the Mach number expansion. Apart from this, LBE uses a constant, uniform density ρ, not local value of ρ, therefore LBE bears weak density fluctuations in the equilibria.

As given above LBGK is a single time relaxation scheme, and that is a very valuable point comparing with other schemes. However, this simplification based on the single time relaxation is also its disadvantage, which is all modes decay at the same time rate ω^{-1}. The consequence of this effect is that unphysical short-wave oscillations may be generated. This unphysical short-wave needs to be filtered out, and this leads to the fact that spatial resolution would be lost. The generation of oscillations also depends on the initial and physical conditions. Therefore numerical stability may be reduced because of the effect of oscillation.

Numerical instabilities also may be generated when velocity gradients are large. In addition, this single relaxation time indicates that mass, momentum and heat transfer all occur at the same rate. Therefore, this condition only applies for ideal gas. Another limitation for LBGK is that the Prandtl number must be fixed, which is far from the real physics.

Despite the disadvantages mentioned above, the continuum limit of LBGK can reproduce the Navier-Stokes equation and is a viable tool for numerical fluid dynamics. LBGK is not a fundamental equation, but is a useful model for numerical dynamics. LBGK is much more simpler, elegant and efficient model than LBE after all.

The discrete velocity Boltzmann equation is:

$$\frac{\partial f_i}{\partial t} + v_i \frac{\partial f_i}{\partial x} = -\frac{1}{\tau}[f_i - f_i^e]. \tag{3.11}$$

This discretization of LBGK accepts a time step is chosen such that $\delta_t \gg \tau$. For small τ, the Chapman-Enskog approximation can deliver the equation 3.11 to the compressible Navier-Stokes equation with kinematic viscosity $\nu \sim \tau c_1^2$, where c_1 is the thermal velocity. The relaxation time τ is proportional to the kinematic viscosity ν for LBM.

Chapter 4

Entropy

The concept of entropy firstly appeared in the second law of thermodynamics, as one of the most important thermodynamics properties, and then it was introduced in the development of statistical physics during the 19th century. These two developments of entropy are rather symbiotically related, especially by the work of Boltzmann.

4.1 Entropy in Thermodynamics

Entropy was firstly introduced by Clausius in 1867 as a mathematical quantity, S . Entropy describes the heat transfer during a reversible process through the function [20]:

$$dS = \frac{\delta Q}{T}, \tag{4.1}$$

where T is the absolute temperature, and Q is the amount of the heat where the exchange occurs. The entropy of a perfect gas is:

$$S = C_V \ln T + R \ln V + constant, \tag{4.2}$$

where C_v is the specific heat capacity at constant volume, V is the volume and R per mole of gas is a constant for all gases. The above equation (4.2), shows that if the volume is constant, the entropy S increases as $\ln T$ goes up, and if the temperature is constant, the entropy S increases as $\ln V$ increases.

Adiabatic processes are irreversible processes. In an adiabatic process, there is no heat transfer between the system and the surroundings. In adiabatic processes, entropy always increases.

For all irreversible adiabatic processes the change of entropy are always positive, so the following equation holds:

$$dS \geq \frac{\delta q}{T}. \tag{4.3}$$

If there is no irreversible adiabatic process, then the total entropy change equals to the change of entropy in the exchange of heat process. If the system is thermally insulated such that $\delta q = 0$, and the volume is fixed, then we arrive to the very important conclusion:

$$dS \geq 0. \tag{4.4}$$

In words, it means that "in any closed system whose volume and internal energy are fixed, the entropy S tends to a maximum, and when this is achieved all change ceases and the system is in equilibrium" [19].

4.2 The Statistical Approach

The statistical explanation of entropy is associated with the microscopic states of a system. This idea was firstl introduced by Ludwig Boltzmann, and further

explored by Maxwell (1831-1879). The statistical concept states that macroscopic phenomena can be approached from microscopic dynamics, i.e. a macroscopic state can be represented by many different microscopic states.

Here, microscopic state refers to configurations of molecular motion, i.e. a state in which all the details about atoms and molecules are specified [20]. In the microscopic point of view, to describe one gram of helium gas would require around 10^{23} parameters, while in macroscopic terms, it only need 3 parameters. However, it is not essential to express the velocity and the position of all the atoms and molecules associated.

It is important to mention that the numbers of molecules with certain velocities (or certain velocity ranges) do not change with time, if the gas is in equilibrium. In the real physical world, the velocity of each molecule changes frequently before and after each collision. But, as Boltzmann showed in some models, "these collisions are such as to maintain the equilibrium distribution of velocities in the gas as a whole" [19].

A macroscopic state can be defined from density, momentum, pressure, temperature, energy and similar macroscopic quantities. Normally a huge number of microscopic states correspond to a macroscopic state. These microstates are being treated as indistinguishable states at the macrostates level. These microstates are named as 'realizations' of the macrostates.

The justification of entropy equation was proved by Planck (1858-1947) as follows. First, assume entropy S is:

$$S = f(W). \tag{4.5}$$

Here, f refers as a universal function of the argument W. Now let us take two

isolated systems 1 and 2, with entropies S_1 and S_2, and the associated microstates are W_1, W_2 respectively. Next these two systems combine into one composite system. The total entropy becomes:

$$S_{12} = S_1 + S_2. \tag{4.6}$$

And it is possible to combine the microstate of system 1 with any of the microstates of system 2 to give a distinguishable microstate:

$$W_{12} = W_1 W_2. \tag{4.7}$$

Now combine the equations (4.5), (4.6) and (4.7), we arrive at the general solution of this equation is:

$$f(W_{12}) = f(W_1 W_2) = f(W_1) + f(W_2). \tag{4.8}$$

The general solution of this equation is:

$$S = f(W) = k \ln W, \tag{4.9}$$

where k is a arbitrary constant.

Entropy also is interpreted in some other aspects by researchers, as disorder and spread. When entropy is high, it is to be considered as great disorder, meanwhile when entropy is low, the system is an ordered system. The explanation of entropy, in the idea of spread by Guggenheim, said that for example, high entropy can be interpreted as having the elements of an assembly spread over a big range of energy levels.

4.3 H-Function: Boltzmann-Gibbs-Shannon entropy

4.3.1 The Gibbs and Boltzmann H-Functions

The concept of entropy H function is an important step for the development of LBM (see [47], [48], [76]). The classical expressions for entropy were firstly developed by Gibbs and Boltzmann [5]. Gibbs established the general theory of equilibrium of complex media by using entropy maximum. After Boltzmann proved his H-theorem in 1872, the expression for the H-function became well-known:

$$H = \int f(x,v) \ln f(x,v) \mathrm{d}x\mathrm{d}v,$$

where $f(x,v)$ is a distribution density of particles in phase space, x is the coordinate of a particle, and v is the velocity. The H-Function is a monotonically decreasing function in time for an ideal gas.

Gibbs H-Function expression is based on the probability density in the full phase space of the system:

$$H_G = \int W_N \log W_N d\tau, \tag{4.10}$$

where $W_N(x_1, p_1; x_2, p_2; ...; x_N, p_N; t)$ is the probability density, p is the momentum of a particle.

4.3.2 Shannon's Information Theory

In 1928, R.V.L.Hartley developed the logarithmic measure of information $H = n \log s$ initially for electronic communication in the paper [7]. Hartley eliminated

all the psychological factors and their variations in order to compose a definite quantitative measure of information which solely stands on physical considerations, as Hartley called "Quantitative Expression for Information". In the equation $H = n \log s = \log s^n$, H stands for the amount of information in a particular system which is related to n selections. The small letter s refers to the number of symbols available at each selection, and s^n is the number of distinguishable sequences.

C.E.Shannon further developed Hartley's idea and formed information theory in mathematics. Shannon started with the key question on how to measure the uncertainty in the selection of the event. This measure, say $H(p_1, p_2, ...p_n)$ needs to fulfill three properties:

1. H should be continuous in the p_i.

2. If all the p_i are equal, $p_i = \frac{1}{n}$, then H is a monotonic increasing function of n.

3. If a choice can be divided into two successive choices, the original H is the weighted sum of the individual values of H,

where $\{p_1, p_2, ...p_n\}$ are the probabilities of occurrence of a set of possible events with the property $\sum_{i=1}^{n} p_i = 1$. The H which satisfies the above three properties can be expressed in the form:

$$H = -K \sum_{i=1}^{n} p_i \log p_i, \tag{4.11}$$

where K is a positive constant.

The derivation of H is shown below [9]. Firstly, define $H(\frac{1}{n}, \frac{1}{n}, ..., \frac{1}{n}) = A(n)$. In the property 3 given above, it states that a choice can be decomposed from s^m

equally likely possibilities into a series of m choices from s equally likely possibilities and get:

$$A(s^m) = mA(s).$$

And similarly

$$A(t^n) = nA(t),$$

where n can be chosen as arbitrarily large, and select an m in order to satisfy:

$$s^m \leq t^n \leq s^{(m+1)}.$$

And then take the logarithms and divide by $n \log s$:

$$\frac{m}{n} \leq \frac{\log t}{\log s} \leq \frac{m}{n} + \frac{1}{n}.$$

Since n is chosen arbitrarily large in the first place, so this inequality can be rewritten as:

$$\left| \frac{m}{n} - \frac{\log t}{\log s} \right| < \epsilon,$$

where ϵ is arbitrarily small. In property 2 it is requested that H is a monotonic increasing function of n, i.e. $A(n)$ is also a monotonic increasing function, so:

$$A(s^m) \leq A(t^n) \leq A(s^{(m+1)})$$

$$mA(s) \leq nA(t) \leq (m+1)A(s).$$

Divided by $nA(s)$

$$\frac{m}{n} \leq \frac{A(t)}{A(s)} \leq \frac{m}{n} + \frac{1}{n},$$

or

$$\left|\frac{m}{n} - \frac{A(t)}{A(s)}\right| < \epsilon.$$

Thus,

$$\left|\frac{A(m)}{A(n)} - \frac{A(t)}{A(s)}\right| < 2\epsilon,$$

and $A(t) = K \log t$. Assume now that we have a choice from n possibilities with commeasurable probabilities $p_i = \frac{n_i}{\sum n_i}$, where n_i are integers. The choice can be divided from $\sum n_i$ possibilities into a choice from n possibilities $p_1, p_2, ..., p_n$. If the ith item was selected, then n_i is with equal probabilities for the choice:

$$K \log \sum n_i = H(p_1, ..., p_n) + K \sum p_i \log n_i,$$

and finally:

$$\begin{aligned} H &= K\left[\sum p_i \log(\sum n_i) - \sum p_i \log n_i\right] \\ &= -K \sum p_i \log \frac{n_i}{\sum n_i} \\ &= -K \sum p_i \log p_i. \end{aligned}$$

When $K = 1$, i.e.$H = -\sum p_i \log p_i$ this expression plays a very important role in information theory as a measure of information, choice and uncertainty. This H can be regarded as the entropy in statistical mechanics where p_i is the probability of a system being in a cell i of its phase space.

4.4 The Kullback and Leibler Entropy

The Boltzmann-Gibbs-Shannon entropy has the following properties which are: (i)Additivity [75]: The total entropy of the system is the sum of the entropies

of the independent subsystems. This is a conditional statement, saying 'if the systems are independent, then the entropy of the joint system equals to the sum of the entropies of the subsystems'. (ii) Trace-Form: The total entropy is the sum of all the states, i.e. the sum over the convex functions $f(p_i, p_i^*)$. (iii)Convexity of entropy for the reference entropy H, and concavity for entropy S. S.Kullback and R.A.Leibler introduced the relative entropy or else called the Kullback-Leibler divergence between the current distribution P and some 'reference' distribution Q ([8], [10]):

$$D_{KL}(P||Q) = \sum_i p_i \log \frac{p_i}{q_i}. \tag{4.12}$$

4.5 The Entropic Lattice Boltzmann Method

Introducing entropy to lattice Boltzmann method gives the entropic lattice Boltzmann method (ELBM)([18], [74]). ELBM numerical discretized solution of the kinetic equation is slightly different from the LBGK numerical solution:

$$f_i(x + v_i\Delta t, t + \Delta t) = (1 - \beta)f_i(x, t) + \beta\tilde{f}_{i,\alpha}(x, t), \tag{4.13}$$

with $\tilde{f}_{i,\alpha} = (1 - \alpha)f_i + \alpha f_i^{eq}$. The parameter α is determined such that a constant entropy condition is satisfied. To find the value of $\alpha = \alpha(f)$, the entropic functional $S(f)$ has to be involved, which is:

$$S(f) = S(\tilde{f}) = S((1 - \alpha)f + \alpha f^{eq}). \tag{4.14}$$

Inaccuracy in the solution of this equation will bring artificial viscosity. A substantial issue of the value α is to secure that entropy does not decrease.

Chapter 5

Flux-corrected Transport and Median Filters

5.1 Flux-corrected Transport

Flux-corrected transport (FCT) was created to improve the reliability and the physically acceptable results of the convection algorithms by Boris and Book three decades ago ([32], [33], [34], [35], [36], [37]). Since the traditional Fluid Dynamics approaches have many defects, such as the fact that mass density sometimes produces negative populations, this is not physically reasonable in reality. Nowadays many of the monotonic preserving and non-oscillatory fluid transport algorithms build partly on this principle.

Flux correction is also normally called flux limiter. The main idea about this invention is to reduce the impact of truncation error considerations and locally replace with conservative monotonicity enforcement. Particularly this monotonicity enforcement will be applied in those places where the solution was not smooth, as well as where high order solutions would break physically-motivated upper and

lower bounds on the solution.

FCT is a nonlinear finite difference technique. A transport algorithm called 'Sharp And Smooth Transport Algorithm' (SHASTA) generates high diffusion, so the demand of creating antidiffusion for removing this diffusive errors is highly required. Consequently, the limiter was invented to control the antidiffusive fluxes to maintain positivity, as a nonlinear ingredient.

In a finite difference algorithm if all the operations can be represented as flux, then it is certainly conservative, since the amount of flux that moves from one point will not be changed to the next point. Therefore, transportative fluxes can be used for the approximation of advection.

5.1.1 Brief History of Flux Limiters

Boris and Book worked in the area of time dependent fluid dynamics, especially relative to supersonic flow, such as shocks, contact discontinuities and sharp gradients. The numerical method they implemented is a finite-difference approach. To find an approximation of a finite difference of differential equation, the simple approach is to expand the derivatives of time and space function in Taylor series on a uniformed spacing δx mesh ([32], [37]).

$$f(x \pm \Delta x) = f(x) \pm \frac{\partial f}{\partial x}\Delta x + \frac{\partial f^2}{\partial x^2}(\Delta x)^2 \pm .....,$$

Thus,

$$f(x + \Delta x) - f(x - \Delta x) = 2\frac{\partial f}{\partial x}\Delta x + O(\Delta x)^3,$$

rearrange it:

$$\frac{\partial f(x,t)}{\partial x} = \frac{1}{2\Delta x}[f(x + \Delta x, t) - f(x - \Delta x, t)] + O(\Delta x)^2,$$

and for the time derivative:

$$\frac{\partial f(x,t)}{\partial t} = \frac{1}{2\Delta t}[f(x,t+\Delta t) - f(x,t-\Delta t)] + O(\Delta t)^2.$$

So for the passive advection equation

$$\frac{\partial \rho}{\partial t} + u\frac{\partial \rho}{\partial x} = 0. \tag{5.1}$$

The finite difference approximation is

$$\rho(x,t+\Delta t) = \rho(x,t-\Delta t) - \varepsilon[\rho(x+\Delta x,t) - \rho(x-\Delta x,t)], \tag{5.2}$$

where $\varepsilon = u\frac{\Delta t}{\Delta x}$ is the Courant number. This approximation is a second-order leapfrog scheme. The special feature of the Taylor series expansion is that it produces accurate different schemes for slowing varying profiles. Beside that, it provides tools to analyze amplitude and phase error. The limitation of Taylor series expansion is that it cannot be applied when discontinuities are present, where dispersive ripples make their appearances. The reason why it does not work is because it does not ensure positivity of variables which only accepts positive values. Examples are mass, energy density and temperature. When close to discontinuities, positivity is even harder to achieve.

Here it is important to give some reference about discontinuity. Shocks, contact discontinuities and slip lines(tangential discontinuities) are physically discontinuous if dissipation is not involved. In classical physics, a physical quantity is normally continuous and dissipation can not be completely absent. Similarly in nature there are no absolute discontinuities.

In numerical analysis, the changes of the finite difference approach are discon-

tinuous. The level of discontinuity can vary. The difference of a 'real' discontinuity and non-discontinuity depends on the relative and absolute change in a variable if it exceeds some threshold value, and it also depends on primary of the problem as well as one's standard.

The requirement for shocks to meet the Rankine-Hugoniot conditions is that viscous dissipation generates entropy at a shock front. The weak solutions state the zero viscosity limit. Therefore, any numerical scheme must include some dissipation to fulfill the jump conditions.

Shocks for this type of equations are self-steepening. A shock wave increases the temperature of the medium through which is traveling, and consequently, the speed of sound increases (The speed of sound is proportional to the square root of the specific heat). Thus, information travels faster and this causes the signals in the region behind a shock to have a tendency to get closer to the shock. Comparing with shocks, other discontinuities are not self-steepening, such as contact surfaces. The numerical diffusion tends to smear out for shear surfaces and interfaces between two different media, or between two regions in the same medium with different properties, and as a result, it is more complicated to simulate than shocks.

5.1.2 The algorithms of FCT

A historic background of algorithms composed with flux corrected transport technique is given in paper [32] for solving continuity equations by using Eulerian finite difference method. For a FCT algorithm, there are mainly two stages: a transport or convective stage, and an anti-diffusive or corrective stage. These two stages have the properties of being conservative and non-negative. The advantage of the combination of these two stages is that the usual dispersively produced

ripples is highly reduced in the regions of sharp gradients and shocks.

The fundamental principle for the antidiffusion stage is described as follows [37]:

" The antidiffusion stage should generate no new maxima or minima in the solution, nor should it accentuate already existing extrema."

This description guarantees that the antidiffusion is nonnegative and this is done by maintaining the correction of antidiffuive mass fluxes. The fluxes $f_{j+\frac{1}{2}}$ are constrained term by term. Therefore "no antidiffusive flux transfer of mass can push the density value at any grid point beyond the density value at neighboring points", that is where the origin of the name 'flux-corrected transport' comes from. The fluxes which will be strongly corrected by the following formula are [37]:

$$A^C_{i+\frac{1}{2}} = S_{max}(0, min(|A_{\frac{1}{2}}|, S(q^{td}_{i+2} - q^{td}_{i+1})\Delta x, S(q^{td}_i - q^{td}_{i-1})\Delta x)), \tag{5.3}$$

$$f^C_{j+\frac{1}{2}} = sgn\Delta_{j+1/2} max[0, min(\Delta_{j-1/2} sgn\Delta_{j+1/2}, \frac{1}{8}|\Delta_{j+1/2}|, \Delta_{j+3/2} sgn_{j+1/2}\Delta_{j+1/2})], \tag{5.4}$$

where

$$\Delta_{j+1/2} = \rho^1_{j+1} - \rho^1_j,$$

and the corrected fluxes $f^c_{j+\frac{1}{2}}$ replace the fluxes in equation:

$$\bar{\rho}^1_j = \rho^1_j - f_{j+\frac{1}{2}} + f_{j-\frac{1}{2}}. \tag{5.5}$$

The FCT algorithm has much better performance comparing with some general schemes, such as 'one sided' first order scheme, second-order Lax-Wendroff two step scheme, and second order Leapfrog scheme. All these algorithms including FCT are linear operations beside the stage of the flux correction. However, this

restriction of assumption leads to the consequence of 'clipping and "terracing" phenomena.

5.1.3 Summary

This new class of Eulerian, finite-difference algorithms are appropriate to solve continuity and continuity like equations. FCT algorithms provide not only second order advection, but also keep the dilation terms nonnegative and conservative. The application of this method can be easily extended to $2D$ and $3D$, and combined with even more or less standard transport algorithms to improve results.

There are two stages in FCT algorithms, the transport stage and the flux-corrected antidiffusion stage. The continuity equation is solved by using three point formula, and in general strong diffusion is generated, and a large numerical error is formed at the first stage. Therefore at the second stage, the numerical error is being rectified by antidiffusion and flux correcting procedures.

The flux correction helps the algorithm to produce nonnegative and stable results as well as minimizing the diffusion. The diffusion introduced in stage I is larger than any dispersive error. The antidiffusion cancels the dispersion. In other words, the local large diffusive flux is equivalent and of opposite sign to the local dispersion error.

5.2 Median, Conservative and Mean Filters

Here, the history of median, conservative and mean filters in image processing will be given ([50], [51]). In general, there is a tradeoff between preservation of image detail and noise elimination which the noise represents as unwanted black or white pixel. Mean filters also lose information in their quest for noise elimination,

and the trick is to minimize information loss. Ideally, a filter that adapts to the underlying pixel values is desired.

However, an adaptive filter alters its basic behavior depending on the underlying pixel values, which allows it to retain image detail while still removing noise. The typical criteria for determining filter behavior involve some measure of local brightness and contrast.

Another useful adaptive filter is the adaptive median filter. The primary strength of the adaptive median filter is the removal of salt-and-pepper noise, but it also attempts to smooth other types of noise and to avoid the distortion of small image structures. 'Salt and pepper' noise is also called impulse noise, which is typically seen in images, representing randomly in a form of black and white pixels. Noisy pixels can only take the maximum and the minimum values. In image restorations, specially for the areas with fine details and high contrast, a minimum or low rank has a tendency of darkening an image, and a maximum or high rank has a tendency of brightening an image.

Median, mean and conservative filters were originally developed for image restorations. Each filter has its own unique and special effect on noise reduction for an image. These sufficient qualities they have are good enough to bring them into our area of research. The vital point by using these filters for deviation of local equilibrium is to make the best adjustment between preservation of details and impulse noise elimination.

Mean filter is to calculate the mean(average) value of its neighbors including itself and replace each pixel value with the corresponding average. Mean filter is one of the simplest type of low-pass filter.

$$\bar{x} = \frac{1}{n} \sum_{i=1}^{n} x_i, \tag{5.6}$$

where n is the length of a window (or kernel), which formulates the size and pattern of neighborhood when the average is computed. For example, a 1×3 window in $1D$ is shown:

1	1	1

The size of the window dominates the level of smoothing effect. The larger the size is, the greater the smoothing effect the filter has.

The concept of median filter was primarily developed by Tukey for the utility of noise suppression in images. It is a nonlinear order filter which selects the middle pixel value from the monotonically increasing sequence and replaces the central pixel with the median value. Mathematically, median value is obtained from the classical definition. If the window is an even number, then the median would be the average of the two middle pixels in an ordered sequence. If it is an odd number, then the median would be the middle pixel value in an ordered sequence. For example, an odd window is $\{11, 21, 108, 5, 9\}$, and after sorting them in numerical order, the median value 11 will replace the central pixel value. An even window is $\{2, 11, 21, 108, 5, 9\}$, and after sorting them in numerical order, the median value 10 will replace the central pixel value. If the value 108 presented a valid pulse, then the result would suffer the loss of information. On another side, if it were an impulse noise, the median filter would produce a desirable result.

A conservative filter assures that each central pixel is restricted within the boundary defined by its nearby neighbors. It firstly identifies the maximum and the minimum values of the neighbors of the central pixel within an given window. If the central pixel value is greater than the maximum value, then it is replaced by the maximum value. If the central pixel value is smaller than the minimum value, then it is replaced by the minimum value. The values of central pixels that

satisfy the boundary conditions remain unchanged. For example, given a set of $1D$ 1×5 window, $\{21, 2, 99, 9, 0\}$, the central pixel is 99, with the maximum value of its neighbors 21, and the minimum value 0, and obviously the central pixel will be updated to 21 by the conservative filter.

Figure 5.2 illustrates the performance of mean and median and conservative filters operating on discrete step functions, ramp function, pulse functions and triangle functions with a window of three pixels. Notice that for the boundary conditions of these three filters, we leave the first and the last pixels untouched. Median and conservative filters are sensitive for preserving sharp edges on step functions and have considerable ability of removing impulse noise for one pulse. Mean filter smooths out local noise variations on most of the functions, but it loses detail information, such as lack of edge preservation and smearing local structure. The undesirable blurring effect of mean filter can reduce the original detail information.

The choice of windows length for all these filters can be varied. In general the starting point would be three. If there is no significant information loss, then the windows length would be increased to five and so on. The stop point of increasing windows length would be that the filter would do more harm than good, and it is also worthy considering the capability of the equipment on the increasing computational expenses. The basic principle of filters with window length n is that regions in which the signal period is smaller than half of the window length n will be altered.

A mean filter is simple and can be implemented easily with computational efficiency. However, it is not very successful for clearing up impulse noise in general, because an unrepresentative value in the neighborhood can influence the mean value significantly. Though median and conservative filters behave accidentally

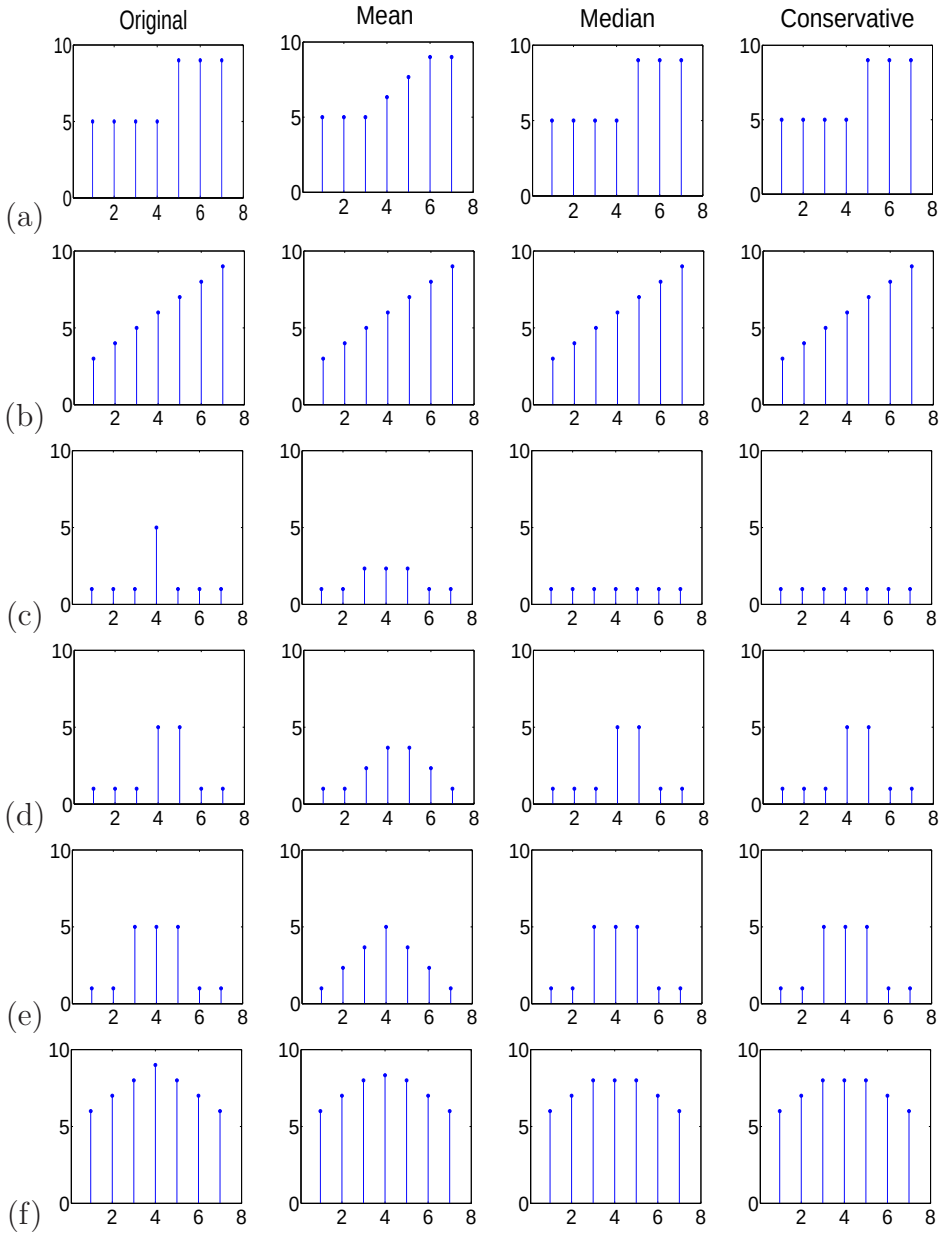

Figure 5.1: Examples of mean, median and conservative filters with windows length 3 on (a)step (b)ramp (c)single pulse (d)double pulse (e)triple pulse (f)triangle

the same on all the functions presented on the example shown above, they can yield very different results with different windows length in other applications. A conservative filter keeps the original information unchanged slightly more than a median filter, therefore it is considerably effective on removing extreme high or low noise. Median filter takes actually the median value of one of the points in the neighborhood(or maybe itself), such that it does not create unrealistic values and is more reasonable robust average for erasing impulse noise. The drawback for median filter is that if the noise level is above 50 percent, then the result will be affected by the filter.

Chapter 6

Nonequilibrium Entropy Limiters

A non-equilibrium entropy filter ([42], [43], [44], [45], [77]) is introduced to suppress the spurious oscillations near sharp gradients in high order schemes. The main concept for building nonequilibrium entropy limiter schemes is to control a scalar quantity which is the value of nonequilibrium entropy. Nonequilibrium entropy is the difference between the state entropy $S(f)$ where f is at some site, and its corresponding quasi-equilibrium entropy $S(f^*) : \Delta S(f) := S(f^*) - S(f)$, where f^* is the quasiequilibrium. There are some flux limiter functions examples in papers ([55], [57], [58]).

The core structure for general limiters in this model is established on the representation of distributions f in the form:

$$f = f^* + \parallel f - f^* \parallel \frac{f - f^*}{\parallel f - f^* \parallel}. \tag{6.1}$$

In this equation $f - f^*$ describes the nonequilibrium part of the distribution, which is formed in 'norm $\times$ direction' where $\parallel f - f^* \parallel$ represents the norm of this nonequilibrium component. The essence of limiters that can perform on a given distribution f is that the norm of the nonequilibrium component $f - f^*$

will be changed accordingly, but its direction and the quasiequilibrium would not be affected, especially the macroscopic variables which are kept the same, as f and f^* coincide in moments. We use ϕ to represent a limiter, and after limiter transformations, the distribution f has the form:

$$f \mapsto f^* + \phi \times (f - f^*), \tag{6.2}$$

under the condition that the limiter function ϕ has to be sufficiently smooth and $\phi > 0$. By applying the nonequilibrium entropy as the variable of limiter ϕ, the above equation becomes:

$$f \mapsto f^* + \phi(\Delta S) \times (f - f^*), \tag{6.3}$$

where $\Delta S = S(f^*) - S(f)$. Notice that, in non-entropic lattice Boltzmann models, the non-entropic equilibria is evaluated from the discrete Kullback entropy:

$$S_K(f) = -\sum_i f_i \ln\left(\frac{f_i}{f_i^*}\right), \tag{6.4}$$

where $-S_K(f) = \Delta S(f)$. The entropy function is a very useful function for the analysis of kinetic equation ([64], [81]). Kullback entropy ([67], [66]) in quadratic approximation,

$$-S_K(f) = \sum_i f_i \ln\left(\frac{f_i}{f_i^*}\right) \approx \sum_i \frac{(f_i - f_i^*)^2}{f_i^*}. \tag{6.5}$$

There is a vast range of choices on how to construct non-equilibrium entropy filters, examples such as positivity rule, Ehrenfests' regulation [42]. We will elaborate the details about limiters which apply in 3 velocities and 5 velocities. One

type of limiters is based on pointwise correction, and another is based on several neighborhoods correction where the value of a select site will be decided by its nearby neighbors.

The adaptive nonequilibrium entropy limiters have the property that they can easily pick up the highly noisy ones which are far from equilibrium states and transform them into or near equilibrium states, thus the spurious oscillations are reduced accordingly. The disadvantage of these limiters is that they bring up additional dissipation, but still all this dissipation can be estimated by the assessment of nonequilibrium entropy production.

6.1 Positivity Rule

To keep the positivity of probabilities or populations valid, we need to build some positive rules for the populations of f ([42], [53], [54]). After collision, if f is far from f^*, and the population of f become nonpositive, then this may cause the populations to be nonphysical. The important fact is that even when one site population of f_i losses its positivity, the whole sites of f are considered by some authors as nonphysical. In this condition, it is vital and extremely important to add a positivity rule to keep the populations of f positive.

There are some methods to build positivity rules. One of the simple ways is to substitute nonpositive populations of f by the closest nonnegative state which is from the straight line [43]:

$$\{\lambda f(x) + (1-\lambda)\Pi^*(f(x)), \quad \lambda \in \mathbb{R}\}, \tag{6.6}$$

This is defined by two points, $f(x)$ and its corresponding quasiequilibrium state. For the quasiequilibrium f_M^*, an equilibration operation is the projection Π^* of

the distribution f into the corresponding quasiequilibrium state: $\Pi^*(f) = f^*_{m(f)}$, where $m(f) = M$. The value of λ depends on x, apart from the value of f. This positivity rule is not applied for each site of f, only for those values of populations which are nonpositive, therefore it is a pointwise application. A positivity rule is a simple and efficient way to preserve the populations of f positive, but by its nature, it also affect the accuracy of approximation. The basic reason is that though it keeps the populations of f positive, it also brings additional dissipation, since it moves the nonpositive state of f near or closer to quasiequilibrium state. However, it is nearly unavoidable to introduce additional dissipation, if we want to keep the populations conservative. This positivity rule is one of the minimal necessary modifications to keep all the populations physical. Therefore a positivity rule is applied for each LBGK model simulation here.

6.2 Ehrenfests' Regularisation

Ehrenfests regularisation ([40], [42], [70]) is a pointwise correction limiter. As a start, we consider the nonequilibrium entropy for each site:

$$\Delta S(f) := S(f^*) - S(f),$$

where f^* is the corresponding quasiequilibrium at the same point. The local deviation of f from the corresponding quasiequilibrium is being controlled through a pre-specified threshold value δ and a number of sites k. For each time step, we select k sites with largest ΔS, then compare with the pre-defined threshold value δ. In other words, there will be a number of k sites such that the values of limiter ϕ are zero, and we set the values of f for these sites to be the quasiequilibrium values. Here we need to mention that, the number of k sites, is not selected

randomly from the range which are $\Delta S(f)(x) > \delta$, but instead that we sort all the sites which fulfill this condition in descending order, and then take the first k sites from this sorted range, and leave the rest of sites unchanged.

The LBGK equation with Ehrenfests' step is constructed as following:

$$f_i(\boldsymbol{x} + \boldsymbol{v}_i\delta t, t + \delta t) = \begin{cases} f_i^*(x,t) + (2\beta - 1)(f_i^*(x,t) - f_i(x,t)), & \Delta S \leq \delta, \\ f_i^{eq}(\boldsymbol{x}, t), & \text{otherwise.} \end{cases} \tag{6.7}$$

where $\beta = 1/(2\nu + 1)$.

Therefore, the limiter $\phi(\Delta S)$ for Ehrenfests' regularisation is set as [45]:

$$\phi(\Delta S)(x) = \begin{cases} 1, & \Delta S \leq \delta, \\ 0, & \text{otherwise.} \end{cases} \tag{6.8}$$

The number of sites selected should be less or equal to $\mathfrak{o}(Nh/L)$, where N is the total number of sites, h is the step of the space discretisation and L is the macroscopic characteristic length. When this condition is satisfied, the change of accuracy order "on average" could be avoided.

6.3 Smooth Limiters

Ehrenfests' regularisation contributes localised pointwise corrections with limited sites. Smooth limiters are based on a different type of concept, which treat the limiter ϕ as a real function of $\Delta S(f)$. In this concept, the function ϕ has a lot of options to choose. There are two types of categories that limiters belong to [44]:

1. Ensemble-independent ϕ. The value of the limiter $\phi(\Delta S(f))$ depends on local value of ΔS only, not on the entire values or its neighbors of f_i, i.e.$\Delta S(f_i)$ (the i^{th} site). For example, Ehrenfests' regularisation, the lim-

iter ϕ is ensemble-independent, since when the k sites are being selected, the values of ϕ are set as zeros, and the derivations of f return to their corresponding quasiequilibrium values f^*, which are not relevant to the whole ensemble or its neighbors.

2. Ensemble-dependent ϕ. The value of the limiter $\phi(\Delta S(f))$ depends on the values of the entire ensemble or the neighbors of f_i.

The first smooth limiter, named **Smooth limiter** 1, introduced here is constructed as following [46]:

$$\phi(\Delta S) = 1/(1 + \alpha \Delta S^k), \tag{6.9}$$

where $\alpha = \frac{\delta}{E(\Delta S)^k}$, and $E(\Delta S)$ is the average value of ΔS. In this function, there are two conditions needed to be fulfilled which are $\alpha > 0$ and $k > 0$. This limiter is an ensemble-dependent limiter, since it involves the average value of ΔS, i.e. the entire ensemble. The second smooth limiter, named **Smooth limiter** 2, is constructed as [44]:

$$\phi(\Delta S) = \frac{1 + (\Delta S/(\delta E(\Delta S)))^{k-1/2}}{1 + (\Delta S/(\delta E(\Delta S)))^k}, \tag{6.10}$$

where $E(\Delta S)$ is defined the same as above. For smooth limiter 2, the restrictions are $k \geq 1$ and $\delta \geq 1$. Similarly, this limiter is also an ensemble-dependent limiter. The performance of the smooth limiter 2 has the following qualities:

1. $\phi(\Delta S) \approx 1$, when ΔS is small,
2. $\sqrt{(\delta E(\Delta S)/\Delta S)}$, when $\Delta S \gg \delta E(\Delta S)$.

Both of these two smooth limiters are unlike Ehrenfests' regularisation which only corrects certain points, but instead each point is being corrected by the

limiters. Therefore they introduce more dissipation than other limiters. By the nature of their definitions, these two smooth limiters produce more modification than Ehrenfests' regularization.

6.4 Smooth Double Monotonic Nonequilibrium Entropy Limiters

The monotonic properties are vital for both theory and application of entropy, according to the second law of thermodynamics. There are two essential descriptions of the monotonic properties for the non-equilibrium entropy limiters [44]:

1. One of the core roles that a non-equilibrium entropy filter plays is to keep the entropy non-negative, which satisfies the dissipation condition. Another role is to ensure the distribution to finally reach equilibrium, which enhances the stabilization of the distribution by this functionality. Notice that to satisfy this property, the value of ϕ should be bounded at all times with $0 \leq \phi \leq 1$.

2. A monotonic non-equilibrium entropy filter should not change the order of the states for any distributions in a line with the same moments. Before the limiter transformation any two distributions f and f' with the relationship $f' - (f')^* = x(f - f^*)$ for $x > 0$, such that $\Delta S(f) > \Delta S(f')$, then after the limiter transformation this non-equilibrium entropy order should not be altered. For example, for the limiter (6.3), the non-equilibrium entropy $\Delta S = \Delta S(f^* + x\phi(\Delta S(f^* + x(f - f^*)))(f - f^*))$ should be a monotonically increasing function with the interval $x \in [0, 1]$.

The quadratic approximation is given by:

$$\Delta S(f^* + x(f - f^*)) = x^2 \Delta S(f), \tag{6.11}$$

$$\begin{aligned} &\Delta S(f^* + x\phi(\Delta S(f^* + x(f - f^*)))(f - f^*)) \\ &= \Delta S(f^* + x\phi(x^2 \Delta S(f))(f - f^*)) \\ &= x^2 \phi^2 (x^2 \Delta S(f)). \end{aligned} \tag{6.12}$$

In the equation (6.12),the term $y\phi(y^2 s)$ must be a monotonically increasing function with the conditions that $y > 0$ for any $s > 0$.

A limiter that satisfies these two monotonic conditions, named as 'double monotonic' limiter. In general the first condition is easy to be satisfied, but not all could fulfill the second condition. For example the limiter $\phi = 1/(1 + \alpha \Delta S^k)$ fulfills the first condition, but not the second condition if $k > 1/2$.

The double monotonic function for smooth functions in quadratic approximation can also be derived from the system of differential inequalities [78]:

$$\begin{aligned} \phi(x) + 2x\phi'(x) &\geq 0; \\ \phi'(x) &\leq 0. \end{aligned}$$

We combine these two inequalities and rewrite them into: $\phi'(x) = -\frac{\eta(x)}{2x}\phi(x)$ with the condition $0 \leq \eta(x) \leq 1$. This equation can be really easily solved:

$$\begin{aligned} \frac{\phi'(\chi)}{\phi(\chi)} &= -\frac{\eta(\chi)}{2\chi} \\ (\ln(\phi(\chi)))' &= -\frac{\eta(\chi)}{2\chi}, \end{aligned} \tag{6.13}$$

with the boundary condition of interval $\chi \in [0, x]$,

$$\ln(\phi(\chi)) = \int_0^x -\frac{\eta(\chi)}{2\chi} d\chi, \tag{6.14}$$

And finally, the general solution of these inequalities for double monotonic filters is:

$$\phi(\chi) = \exp\left(-\frac{1}{2}\int_0^x \frac{\eta(\chi)}{\chi} d\chi\right). \tag{6.15}$$

There are two essential conditions that have to be provided. One is the that integral exists, another is the given initial condition $\phi(0) = 1$, which implies physically that when the limit of non-equilibrium entropy tends to zero, a limiter would not change the flow. Let $\eta(x)H(x - \Delta S_t)$ be a Heaviside step function with threshold value ΔS_t, then the general solution (6.15) produces the threshold limiter. For example, set $\eta(\chi) = \chi^k/(\Delta S_t^k + \chi^k)$, and substitute into the equation (6.15), we get

$$\begin{aligned} \phi(x) &= \exp\left(-\frac{1}{2}\int_0^x \frac{\chi^{k-1}}{(\Delta S_t^k + \chi^k)} d\chi\right) \\ &= \exp\left(\ln(\frac{\Delta S_t^k + x^k}{\Delta S_t^k})^{-\frac{1}{2k}}\right) \\ &= \left(1 + \frac{x^k}{\Delta S_t^k}\right)^{-\frac{1}{2k}}. \end{aligned} \tag{6.16}$$

Thus, the non-equilibrium entropy function would be:

$$\phi(x) = \left(1 + \frac{x^k}{\Delta S_t^k}\right)^{-\frac{1}{2k}}. \tag{6.17}$$

There are two different approaches for approximation from this threshold limiter according to the value of x ([78], [80]).

$$\phi(x) = 1 - \frac{1}{2k}\frac{x^k}{\Delta S_t^k} + o(x^k); \tag{6.18}$$

$$\phi(x) = \sqrt{\frac{\Delta S_t}{x}} + o(x^{-k}). \tag{6.19}$$

If the value of x is reasonably small, the equation (6.18) is the approximation up to kth order. The macroscopic equations are equivalent to the LBM macroscopic equations without limiters up to the $(k+1)$st order in powers of deviation from equilibrium. If the value of x is large, the equation (6.19) is the approximation up to kth order. This double monotonic limiter is a local one point correction limiter. By the primary properties of this double monotonic limiter, the quadratic approximation brings accuracy without additional care, and stabilization by transforming the distribution to equilibrium.

6.5 Nonequilibrium Entropic Median and Mean Filters

Among a vast number of choices of limiters, a median entropy filter is preferred due to its effective noise reduction ([42], [43], [44], [45], [78]). Comparing with pointwise correction of non-equilibrium entropy at the 'most non-equilibrium' points, such as Ehrenfests' regulations, median entropy filters have the property of using local structure. A median entropy filter can correct local non-monotone irregularities, but at the same time keeping regular fragments untouched. A median entropy filter engages in reduction of 'salt and pepper noise' by treating monotone

increase or decrease of non-equilibrium entropy as regular fragments. In terms of non-equilibrium entropy, 'salt' is the maximum(or high rank) filter of the non-equilibrium entropy, where ΔS is bigger than the median value, and 'pepper' is the minimum(or low rank) of non-equilibrium entropy. In the application of non-equilibrium entropy, the 'salt' noise can be removed, but the 'pepper' noise will not be touched.

In the non-equilibrium entropy field, median filter considers each site in turn and concerns its nearby neighbors. The median value is represented as ΔS_{med}. For each point, firstly, it makes all the values of its surrounding neighborhood into numerical order by given a range of its surrounding, then this point is replaced by the middle value. For example, if a site has 3 nearest neighbors including itself, and then after sorting the values of these 3 points, $\Delta S : \Delta S_1 \leq \Delta S_2 \leq \Delta S_3$, the median value is $\Delta S_{med} = \Delta S_2$. Similarly, for 5 nearest neighbors(including itself) after sorting the median is $\Delta S_{med} = \Delta S_3$, For 15 nearest neighbors, after sorting the median is $\Delta S_{med} = \Delta S_8$, and so on. The median entropy filter replaces the non-equilibrium entropy value ΔS at the point with the values of the median calculated ΔS_{med}, and then substitutes this median value into the homothety coefficient $\sqrt{\Delta S_{med}/\Delta S}$ into equation (6.3) to update f, ie. we set up $\phi(\Delta S) = \sqrt{\Delta S_{med}/\Delta S}$ ([44], [78]),

$$f(\boldsymbol{x}) \mapsto f^*(\boldsymbol{x}) + \sqrt{\frac{\Delta S_{med}}{\Delta S}}(f(\boldsymbol{x}) - f^*(\boldsymbol{x})). \tag{6.20}$$

This is the general structure for entropy median filter. The vital issue for median filter is to control the non-equilibrium entropy limitation(or constraints) and substitute by the related median value accordingly when ΔS exceeds some range. There could be many possible ways to build non-equilibrium entropy median filters according to one's interest. We establish three types of median entropy filter,

named as smooth, maximum and general median entropy filters. There are three fundamental elements associated here, ΔS, ΔS_{med} and a predefined value δ. The specific constraint for each filter is described as follows:

$\Delta S > \delta$, and $\Delta S > \Delta S_{med}$, smooth median entropy filter,
$(\Delta S - \Delta S_{med}) > \delta$, maximum median entropy filter,
$\parallel \Delta S - \Delta S_{med} \parallel > \delta$, general median entropy filter.

Notice, for the smooth median entropy filter, is also called median entropy filter for short abbreviation. For the maximum filter, the constraint is set as the difference between the value of non-equilibrium entropy and the median non-equilibrium entropy, and this is greater than the predefined value δ. The general filter has some de-efficiency of filtering. Apart from having the same condition as maximum filter, it also alters the situation when $(\Delta S_{med} - \Delta S) > \delta$, as this will cause the total entropy decrease. The smaller the value of ΔS , the closer the entropy tends to maximum. In this case, the second law of thermodynamics is not being respected.

Similarly, the constraint for the mean entropy filter is $\Delta S > \delta$, and $\Delta S > k\Delta S_{mean}$. Thus, the mean entropy filter is $\phi(\Delta S) = \sqrt{k\Delta S_{mean}/\Delta S}$, and then,

$$f(\boldsymbol{x}) \mapsto f^*(\boldsymbol{x}) + \sqrt{\frac{k\Delta S_{mean}}{\Delta S}}(f(\boldsymbol{x}) - f^*(\boldsymbol{x})). \tag{6.21}$$

From the primary nature of the constraint of each filter, additional dissipation is introduced to each filter according to the predefined value δ. Following the second law of thermodynamics, the value of ΔS which is bigger than the value of ΔS_{med} will be updated by the median entropy filters apart from the general filter.

6.6 Numerical Experience on Three-velocity Set

In this section, we present some numerical results to illustrate the experiments of median entropy filter. In the first part the discretized velocities and explicit equilibria are given, and then in the second part the 1D shock tube is introduced to demonstrate the experiments.

6.6.1 Velocities and Equilibria

In one dimension, the vector velocity is discretized into a set of 3 components corresponding to static, left and right moving populations f_i, where $i = 1, 2, 3$. In order to make the simulation easier to model, we set these three components of velocity as: $\{v_1, v_2, v_3\} := \{0, -1, 1\}$ and a lattice with spacing and time step $\delta t = 1$. Another important factor is to give explicit definition of entropy, $S = -H$, where H is an H function:

$$H = f_1 \log(f_1/4) + f_2 \log(f_2) + f_3 \log(f_3). \tag{6.22}$$

For this entropy, the quasiequilibrium is as follows,

$$\begin{aligned} f_1^* &= \frac{2\rho}{3}\big(2 - \sqrt{1+3u^2}\big), \\ f_2^* &= \frac{\rho}{6}\big((3u-1) + 2\sqrt{1+3u^2}\big), \\ f_3^* &= -\frac{\rho}{6}\big((3u+1) - 2\sqrt{1+3u^2}\big), \end{aligned}$$

where

$$\rho := \sum_i f_i, \qquad u := \frac{1}{\rho}\sum_i v_i f_i.$$

To see how this equilibrium is derived, see [49]. The entropy functional is:

$$S(f) = -\sum_i f_i \log \frac{f_i}{W_i}, \quad i = 1, 2, 3.$$

The weights for quasiequilibrium are $\{\frac{4}{6}, \frac{1}{6}, \frac{1}{6}\}$, and the weights for the entropy are taken as the same proportion of quasiequilibrium $\{4, 1, 1\}$. Notice that, W_1 is the weight corresponding to the static population with the zero velocity, and W_2 is the weight corresponding to the left moving population, and W_3 is the weight corresponding to the right moving population. The governing equations for LBGK are:

$$f_i(x + v_i, t + 1) = f_i(x, t) + (2\beta - 1)(f_i^*(x, t) - f_i(x, t)), \quad i = 1, 2, 3. \tag{6.23}$$

where $\beta = 1/(2\nu + 1)$, with ν defined as kinematic viscosity.

6.6.2 Shock Tube

For a compressible althermal fluid, the 1D shock tube is one of an ideal model for hydrodynamics codes. In the shock tube, the computational domain is the interval $[0, 1]$, and it is discretized as 801 equally spaced lattice sites. For simplicity, the initial density ratio is set as $1 : 2$, such that

$$0 \leq x \leq 400, \quad \rho = 1.0;$$
$$400 < x \leq 801, \quad \rho = 0.5.$$

In these tests, there are three types of pictures demonstrated which are density profile, the total entropy, and the total nonequilibrium entropy.

To see how well the different filters behave with additional dissipation, we set

up the LBGK model without any limiters as a starting point to compare with the LBGK models with limiters. The kinematic viscosity is fixed as $\nu = 10^{-9}$ for all the limiters, but has been varied for LBGK. Figure 6.1 clearly proves that the lower value of kinematic viscosity is, the more spurious oscillations in the nearby neighborhoods of shocks will be produced.

From figure 6.2 to figure 6.4, the general median entropy filter, the maximum median entropy filter and the smooth median entropy filters are presented with 3 neighbors including itself. It is obvious that the smooth median filter is more effective for reducing the spurious oscillations in both post-shock and shock regions under the same conditions comparing with the other two filters. The maximum median entropy filter suppresses spurious oscillations in the post-shock region better than the general median entropy filter. The general median filter has an ill condition, because it takes the absolute value, $\parallel \Delta S - \Delta S_{med} \parallel > \delta$. When $\Delta S_{med} - \Delta S > \delta$, it means when the site of entropy is much closer than the median value entropy, it will be selected by this filter and then by replacing this median value. This behaviour brings the fragments further away from the equilibrium state. Therefore, the general median entropy filter is not an optimal choice for reducing spurious oscillations. Figure 6.5 shows the performance of the smooth median entropy filter with different numbers of neighborhood.

All the three median entropy filters introduce additional local dissipation in thin zones around shocks in the shock tube. This has similar effect to bring additional global dissipation in the simulation. In particular, median entropy filter has the advantage of applying for the shape of shock tube. The reason for that is a shock tube does not have many peaks and troughs, so that the limiter would not smooth out important fragments and keep the original shape as close as possible.

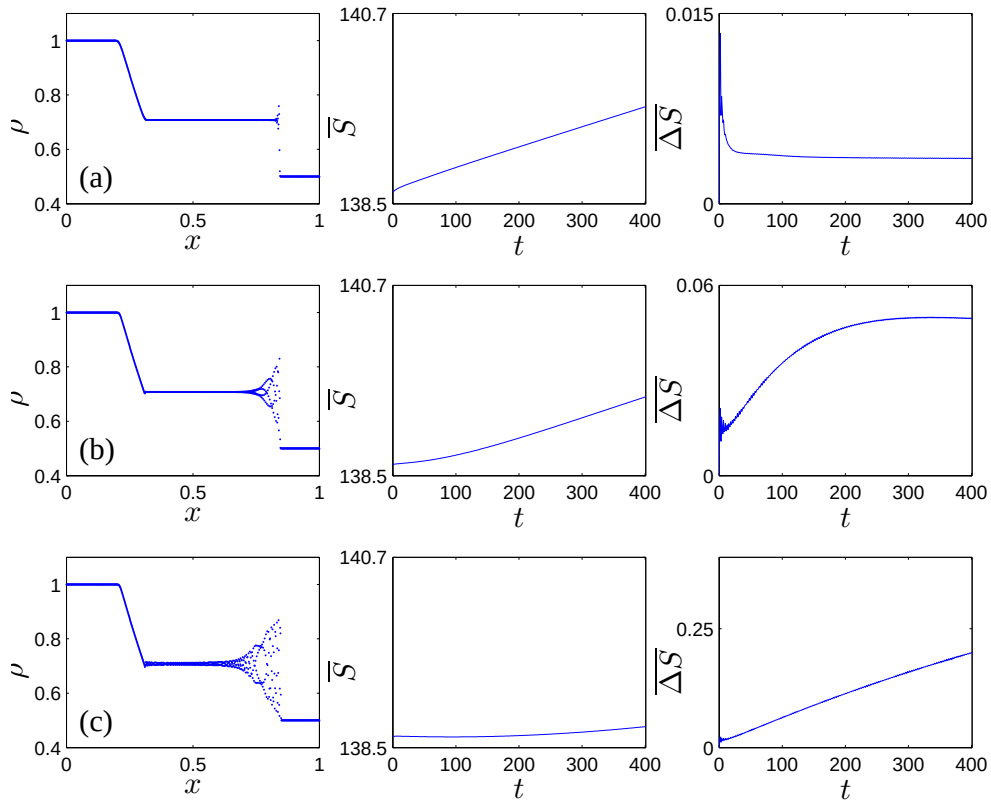

Figure 6.1: The isothermal shock tube simulation, total entropy $\overline{S}$ and nonequilibrium entropy $\overline{\Delta}S$ time histories are displayed above using **LBGK** only after 400 time steps. The viscosity is (a) $\nu = 0.066$ (b) $\nu = 0.0066$ (c) $\nu = 0.00066$.

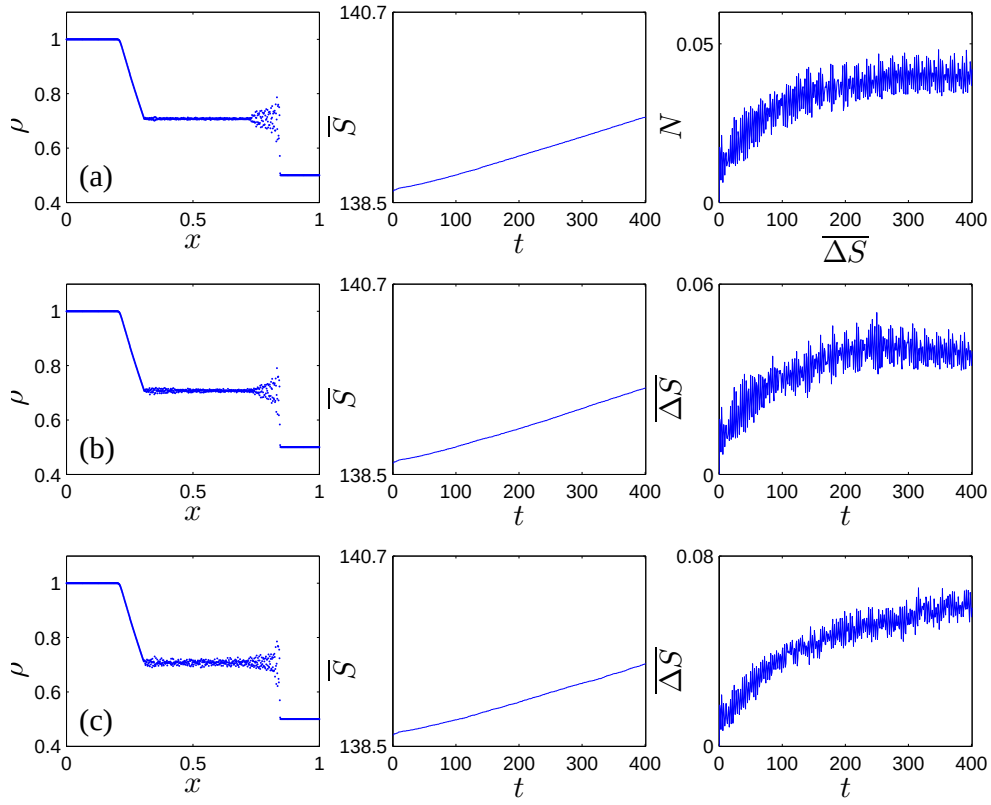

Figure 6.2: The isothermal shock tube simulation, total entropy $\overline{S}$ and nonequilibrium entropy $\overline{\Delta}S$ time histories are displayed above for $\nu = 10^{-9}$ after 400 time steps using **general median entropy filter**. The nearest neighbors including the site itself is $m = 3$, and the threshold is (a) $\delta = 10^{-5}$ (b) $\delta = 10^{-4}$ (c) $\delta = 10^{-3}$.

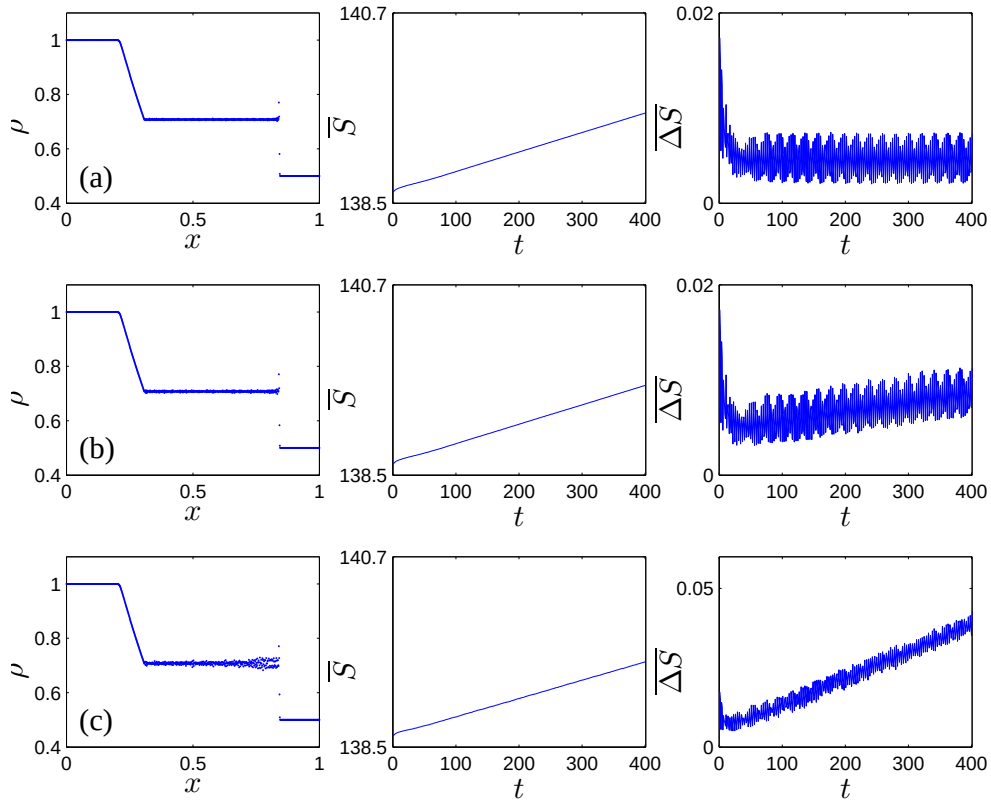

Figure 6.3: The isothermal shock tube simulation, total entropy $\overline{S}$ and nonequilibrium entropy $\overline{\Delta}S$ time histories are displayed above for $\nu = 10^{-9}$ after 400 time steps using **the maximum median entropy filter**. The nearest neighbors including the site itself $m = 3$, and the threshold (a) $\delta = 10^{-5}$ (b) $\delta = 10^{-4}$ (c) $\delta = 10^{-3}$.

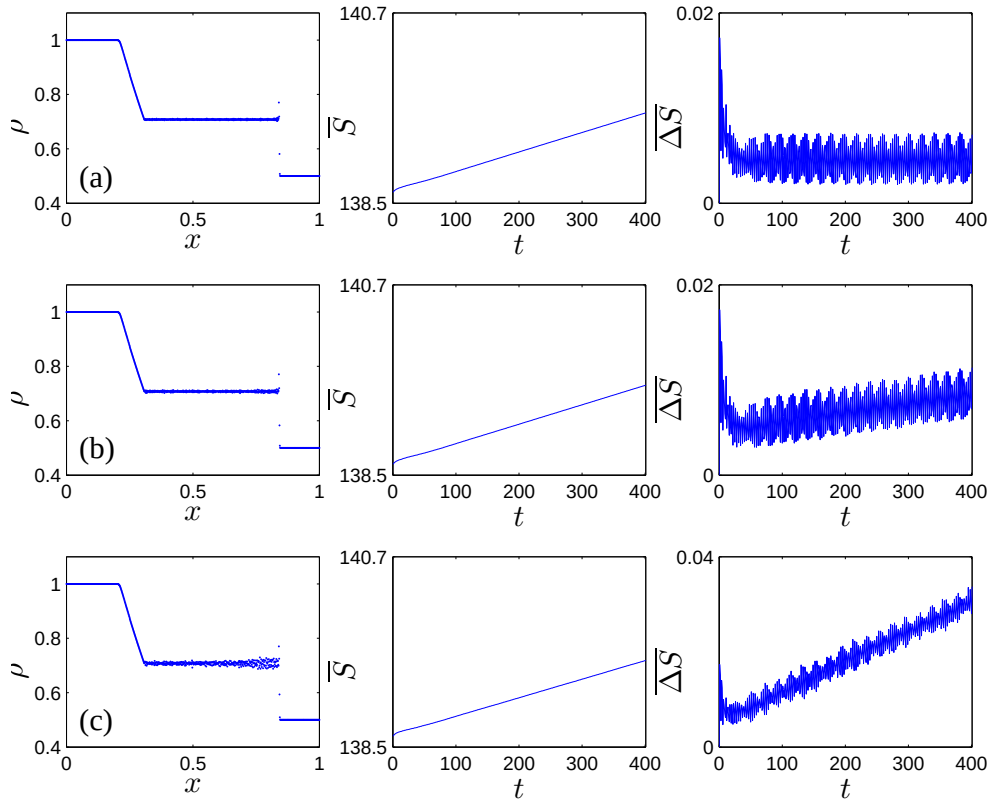

Figure 6.4: The isothermal shock tube simulation, total entropy $\overline{S}$ and nonequilibrium entropy $\overline{\Delta}S$ time histories are displayed above for $\nu = 10^{-9}$ after 400 time steps using **the smooth median entropy filter**. The nearest neighbors including the site itself is $m = 3$, and the threshold is (a) $\delta = 10^{-5}$ (b) $\delta = 10^{-4}$ (c) $\delta = 10^{-3}$.

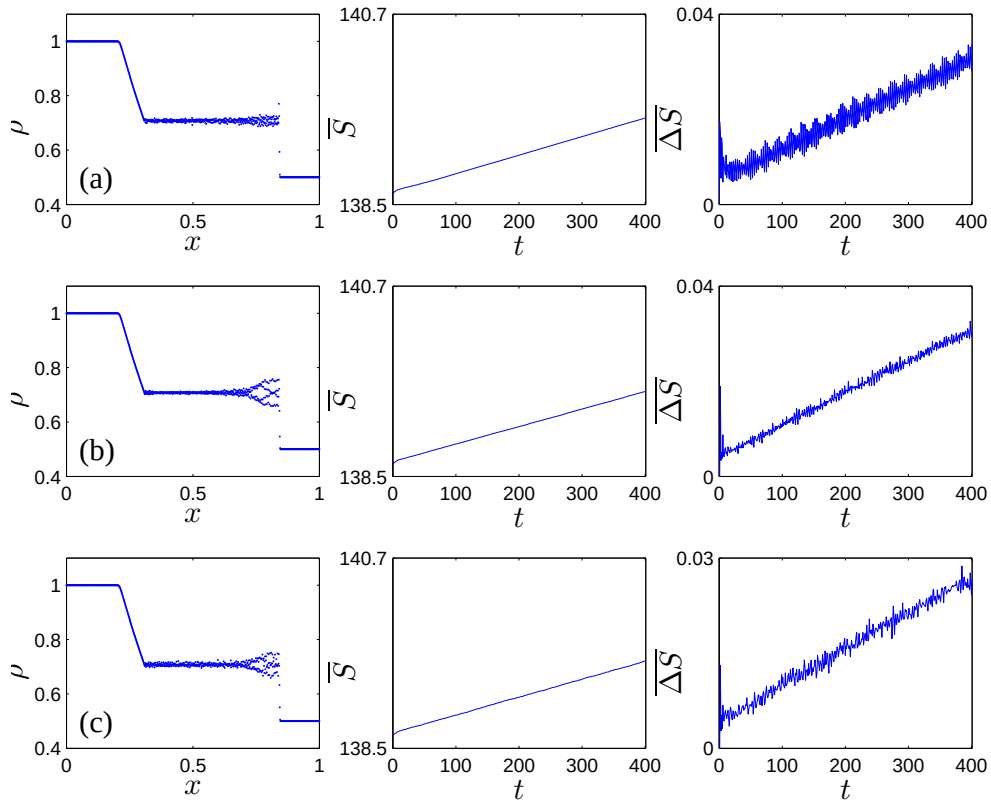

Figure 6.5: The isothermal shock tube simulation, total entropy $\overline{S}$ and nonequilibrium entropy $\overline{\Delta}S$ time histories are displayed above for $\nu = 10^{-9}$ after 400 time steps using **the smooth median entropy filter**. The threshold is $\delta = 10^{-4}$, and the nearest neighbors including the site itself is (a) $m = 3$ (b) $m = 5$ (c) $m = 7$

Chapter 7

Lattice Boltzmann Methods with Five-Velocity Set

The nonequilibrium entropy limiters for LBM with discrete five-velocities sets are based on non-entropic equilibria, with the condition that Kullback entropy is employed. The discrete five-velocity sets have to be chosen such that they can give a stable and complete Galilean invariant LB scheme.

7.1 Weights and Velocities

The lattice is set with spacing and time step $\delta t = 1$. The entropy function H is the same as before:

$$H = \sum_{i=1}^{N} f_i \ln(\frac{f_i}{W_i}). \tag{7.1}$$

With a five-velocity set, the entropy function is:

$$H = f_1 \log(\frac{f_1}{W_1}) + f_2 \log(\frac{f_2}{W_2}) + f_3 \log(\frac{f_3}{W_3}) + f_4 \log(\frac{f_4}{W_4}) + f_5 \log(\frac{f_5}{W_5}). \tag{7.2}$$

The constraints for weights W_i are $W_i > 0$ and $\sum_i^N W_i = 1$. The weights W_i

and the reference temperature T_0 need to fulfill the constitutive relations for the pressure P^{eq} and the energy flux Q^{eq}:

$$\begin{aligned} P^{eq} &= \sum_{i=1}^{N} f_i^{eq} v_i^2 = \rho T_0 + \rho u^2, \\ Q^{eq} &= \sum_{i=1}^{N} f_i^{eq} v_i^3 = 3\rho T_0 u + \rho u^3. \end{aligned} \tag{7.3}$$

The weights and the reference temperature are ([38]):

$$\begin{aligned} W_0 &= \frac{-3m^4 - 3n^4 + 54m^2n^2 - (m^2+n^2)D_5}{75m^2n^2}, \\ W_{\pm m} &= \frac{9m^4 - 6n^4 - 27m^2n^2 + (3m^2 - 2n^2)D_5}{300m^2(m^2-n^2)}, \\ W_{\pm n} &= \frac{9n^4 - 6m^4 - 27m^2n^2 + (3n^2 - 2m^2)D_5}{300n^2(n^2-m^2)}, \\ T_0 &= \frac{3m^2 + 3n^2 + D_5}{30}, \end{aligned} \tag{7.4}$$

where D_5 is:

$$D_5 = \sqrt{9m^4 - 42n^2m^2 + 9n^4}. \tag{7.5}$$

There are 3 discrete five-velocity sets we will use here: $\{v_1, v_2, v_3, v_4, v_5\} := \{-3, -1, 0, 1, 3\}$, $\{v_1, v_2, v_3, v_4, v_5\} := \{-5, -2, 0, 2, 5\}$, $\{v_1, v_2, v_3, v_4, v_5\} := \{-7, -3, 0, 3, 7\}$. The corresponding populations $\{f_1, f_2, f_3, f_4, f_5\}$ stand for: f_1, f_2 left moving populations, f_3 static, and f_4, f_5 right moving populations.

7.2 Equilibria, LBGK and Shock Tube

The non-entropic quasiequilibrium f^* is:

$$f_i^* = \rho W_i \{1 + \frac{\boldsymbol{v}_i U}{T_0} + \frac{U^2}{2T_0^2}(\boldsymbol{v}_i^2 - T_0) + \frac{U^3 \boldsymbol{v}_i}{6T_0^3}(\boldsymbol{v}_i^2 - 3T_0)\}, \tag{7.6}$$

where

$$\rho := \sum_i f_i, \quad U := \frac{1}{\rho} \sum_i v_i f_i. \tag{7.7}$$

The governing equations for LBGK ([59], [60], [61]) are given as follows:

$$f_i(x + v_i, t + 1) = f_i^*(x, t) + (2\beta - 1)(f_i^*(x, t) - f_i(x, t)), \tag{7.8}$$

where $\beta = 1/(2\nu + 1)$.

For five-velocity sets we use shock tube test also. The computational domain is again the interval $[0, 1]$, which is discretized into 801 uniform space lattice sites. The initial density is set:

$$\rho = \begin{cases} x \leq 400, & \rho = 1.0; \\ otherwise, & \rho = 0.5. \end{cases} \tag{7.9}$$

The kinematic viscosity is fixed as $\nu = 10^{-9}$ for all the limiters introduced. It is important to mention that, for each five-velocity set, the time step is different. Since when the velocity gets bigger, after certain time steps, the shock tube gets unstable. So the time step will set as $100\sqrt{3}/c_s$, where c_s is the speed of sound, which is $c_s = \sqrt{T_0}$. The number of time steps for the 3 five-velocity sets $\{-3, -1, 0, 1, 3\}$, $\{-5, -2, 0, 2, 5\}$, $\{-7, -3, 0, 3, 7\}$ are respectively $150, 90, 60$. These five-velocity sets would not be used normally, because they are unstable and are used to test the filters here. The bounce back boundary conditions are applied in the computation.

7.3 Figure description

In the following section, we will illustrate some examples for the 6 limiters introduced in chapter 6 on the 3 five-velocity sets using non-entropic polynomial

quasiequilibria.

There are mainly two types of figure we will illustrate here. One panel shows the comparison of LBGK which has no limiters, and LBGK with the 6 limiters which we proposed in the previous chapter. Another panel shows the comparison of shock tube density profiles only. On the first panel we illustrate vertically the shock tube density profile ρ, the velocity profile U, the sum of entropy $\bar{S}$, the total nonequilibrium entropy $\bar{\Delta S}$ and finally the nonequilibrium entropy in histograms(80). The sum of entropy $\bar{S}$ is $\bar{S}(t) = \sum_x S(x,t)$, and the total nonequilibrium entropy is $\bar{\Delta S}(t) = \sum_x \Delta S(x,t)$. The second panel is the comparison of shock tubes with different threshold values. Apart from these two types of panel, we also demonstrate some statistical tables for each limiter with the same velocity set. These tables include the average nonequilibrium, the average velocity, and the calculation of Mach number and Reynolds number.

7.4 Results Discussion

For the first type of panel, we generally compare the LBGK with a limiter which behaves reasonably well such that, with the predefined threshold values, the limiter can remove the spurious oscillations effectively. For the second type of panel, the comparison of shock tube density profiles can clearly exhibit how the limiter behaves in different threshold values. The tables display the accurate values for the average nonequilibrium entropy and velocity, as well as Mach and Reynolds numbers.

There are two parts in the shock tube density profile we can pay more attention to in these figures, which are the shock region and post shock region. It is very important to mention that both the post shock and shock regions should not be

extremely smooth. In other words, it simply means we have introduced too much additional dissipation by the limiter. Especially when the maximum velocity in the velocity set is big, the shock tube and velocity profiles give very unstable performance with much bigger oscillations (sharp gradients) when only LBGK is applied with no limiters. The velocity profile performs very similarly to the shock tube density profile.

The total entropy $\bar{S}$ for the LBGK with no limiters decreases with time. Although the positivity rule is enforced in LBGK, after a certain number of time steps, some of the values of populations still decrease because of the rounding error, even though the range of decrease for the total entropy is under 0.6. As we can see that the total entropy with any one of the limiters grows in time.

The total entropy in paper [44] is in the range from 1215 to 1217, but the figures here are in the range from 138 to 140. The reason for the difference between these two ranges is the norm for the entropy and equilibrium is distinct. In other words, the scale of the sum of entropy is different, but the proportion keeps the same. In the following we will show the reason for this.

$$S(f) = -\sum_i f_i log(\frac{f_i \alpha}{w_i}) = -\sum_i f_i log(\frac{f_i}{w_i}) - \sum_i f_i log(\alpha), \tag{7.10}$$

where α is a constant. Similarly,

$$S(f^*) = -\sum_i f_i^* log(\frac{f_i^* \alpha}{w_i}) = -\sum_i f_i^* log(\frac{f_i^*}{w_i}) - \sum_i f_i^* log(\alpha). \tag{7.11}$$

Since ΔS is:

$$\Delta S = S(f) - S(f^*), \tag{7.12}$$

therefore,

$$\Delta S = -\sum_i f_i log(\frac{f_i}{w_i}) + \sum_i f_i^* log(\frac{f_i^*}{w_i}) - \sum_i f_i log(\alpha) + \sum_i f_i^* log(\alpha). \quad (7.13)$$

Since $\sum_i f_i = \sum_i f_i^*$, so the above equation becomes:

$$\Delta S = -\sum_i f_i log(\frac{f_i}{w_i}) + \sum_i f_i^* log(\frac{f_i^*}{w_i}). \quad (7.14)$$

From the above equations, we can clearly see that, the difference of norm in entropy would not affect the non-equilibrium entropy. The difference is that, Brownlee uses 3 velocities $\{-1, 0, 1\}$, with the weight for equilibrium $\{1/6, 4/6, 1/6\}$, and the weight for entropy $\{1, 4, 1\}$. The weights for equilibrium and entropy are the same proportion. Here, we use the same weight scale for both equilibrium and entropy.

The total nonequilibrium entropy always increases with time in LBGK with no limiters, however LBGK with any one of the limiters we introduced behave differently with time. The scales of the total nonequilibrium entropy for LBGK with no limiter and LBGK with limiters are very different. The range for LBGK with no limiter is $0 \leq \bar{\Delta S} \leq 0.6$, and the range for LBGK with limiters is much smaller and varies when different limiters are applied.

The histograms of nonequilibrium entropy ΔS for both LBGK without limiter and LBGK with limiters have the same scale, which are divided into 80 bins. Note that the domain in the $y-$axis is fixed up to 15, but the actual domain, especially the points close to zero, should be $0 \leq N \leq 800$. The fact is that the majority of points are concentrated around zero. In order to show closely the points which are not close to zero, we cut the domain to 15. So when the tail is long and fat in the histograms, the shock tube and velocity profiles have more oscillations in the

shock regions.

For the total nonequilibrium entropy time histories as shown, we can see that in each one of them there is a turning point, which sometimes is a local minimum point, sometimes a local maximum point. When the shock tube starts to be active, the total nonequilibrium entropy begins to accumulate from the first time step to say, time step N_s, where the turning point takes place, and this is the place where the maximum number of points are being filtered to the distribution f. The smoother the shock tube is, the less the tendency for the total nonequilibrium entropy to increase dramatically, or even sometimes gets to decrease, as the time steps increase. Further more, the turning points mostly appear when the shock region is formed, and the maximum number of points are being filtered.

The small waves or vibrations appear in figures for LBGK with limiters, caused by the process from continuous equation to discretization, i.e the Gibbs phenomena.

The Ehrenfests' regularization is a point-wise correction limiter of nonequilibrium entropy, therefore it brings additional dissipation locally and it is an ensemble independent limiter. As we can see the figures for the 3 five-velocity sets, when 5 sites are selected with highest $\Delta S > \delta$, Ehrenfest's regularization is efficient to reduce the spurious oscillations in the shock regions, but not very helpful in the post shock regions. But when 10 and 19 sites are selected, for velocity sets $\{-5, -2, 0, 2, 5\}$ and $\{-7, -3, 0, 3, 7\}$, the spurious oscillations can be efficiently removed for both shock and post shock regions. Notice that for velocity set $\{-7, -3, 0, 3, 7\}$, the table for the smooth limiter 2, the values of average nonequilibrium entropy and velocity, and Mach and Reynolds numbers for the threshold from $\delta = 10^{-3}$ to $\delta = 10^{-5}$ are the same. The reason is that limiter picks exactly the same 5 sites for all these 3 different threshold values.

The smooth limiter 1 and smooth limiter 2 are both ensemble dependent limiters. Notice that the k_2 and k_3 are different from Ehrenfests' regularization k_1. As we can see, the smooth limiter 1 for all these 3 velocity sets can remove the spurious oscillations effectively and there are no heavy tails in the nonequilibrium entropy histograms. However the smooth limiter 2 gives too smooth performance for these velocity sets.

The smooth median limiter, the maximum median limiter and the mean limiter are all ensemble dependent limiters. The concept of constructing the smooth median and maximum median limiters determines that the nonequilibrium entropy of neighbors have more influence on the performance of the limiters than any other limiters. The performance of these two median limiters are very gentle and effective in general, while not introducing too much additional dissipation at the same time remove the spurious oscillations efficiently.

The conclusions are given here from the figures and tables which are displayed. The positivity rule is always enforced on both LBGK without limiters and LBGK with limiters, to ensure the populations are positive and to keep a minimum loss of density during the process of simulation. The construction of nonequilibrium entropy limiter schemes is based on controlling a scalar quantity, i.e. the nonequilibrium entropy. We use the computations of LBGK without limiters as a frame of reference comparing with the computations of LBGK with limiters. The conclusion is that for the 6 nonequilibrium entropy limiters we have introduced in previous Chapter, median entropy limiters are recommended as a preferred limiter, since they give reasonably gentle and effective performance which removes the spurious oscillations in both shock and post shock regions, at the same time not bringing too much dissipation.

7.5 Velocity set $\{-3, -1, 0, 1, 3\}$

7.5.1 Ehrenfests' Regularisation

Velocity set $\{-3, -1, 0, 1, 3\}$ LBGK compares with Ehrenfests' limiter				
parameters	average ΔS	average U	Mach	Reynolds
none	7.8533×10^{-4}	4.4015×10^{-1}	3.4449×10^{-1}	3.5212×10^{11}
$\delta = 10^{-2}, k_1 = 5$	3.7575×10^{-4}	4.4014×10^{-1}	3.4448×10^{-1}	3.5211×10^{11}
$\delta = 10^{-3}, k_1 = 5$	7.2349×10^{-5}	4.4178×10^{-1}	3.4577×10^{-1}	3.5343×10^{11}
$\delta = 10^{-4}, k_1 = 5$	5.8848×10^{-5}	4.4204×10^{-1}	3.4597×10^{-1}	3.5363×10^{11}
$\delta = 10^{-4}, k_1 = 10$	2.4617×10^{-5}	4.4287×10^{-1}	3.4662×10^{-1}	3.5430×10^{11}
$\delta = 10^{-4}, k_1 = 19$	1.3941×10^{-5}	4.4341×10^{-1}	3.4704×10^{-1}	3.5473×10^{11}

7.5.2 Smooth Limiter 1

Velocity set $\{-3, -1, 0, 1, 3\}$ LBGK compares with smooth limiter 1				
parameters	average ΔS	average U	Mach	Reynolds
none	7.8533×10^{-4}	4.4015×10^{-1}	3.4449×10^{-1}	3.5212×10^{11}
$\delta = 10^{-3}, k_2 = 0.5$	5.8779×10^{-4}	4.4089×10^{-1}	3.4507×10^{-1}	3.5271×10^{11}
$\delta = 10^{-2}, k_2 = 0.5$	1.4362×10^{-5}	4.4276×10^{-1}	3.4653×10^{-1}	3.5421×10^{11}
$\delta = 10^{-1}, k_2 = 0.5$	1.1596×10^{-5}	4.4378×10^{-1}	3.4733×10^{-1}	3.5502×10^{11}
$\delta = 10^{-3}, k_2 = 1$	2.9912×10^{-4}	4.4210×10^{-1}	3.4602×10^{-1}	3.5368×10^{11}
$\delta = 10^{-2}, k_2 = 1$	1.6991×10^{-5}	4.4334×10^{-1}	3.4699×10^{-1}	3.5467×10^{11}
$\delta = 10^{-1}, k_2 = 1$	8.4356×10^{-6}	4.4395×10^{-1}	3.4747×10^{-1}	3.5516×10^{11}

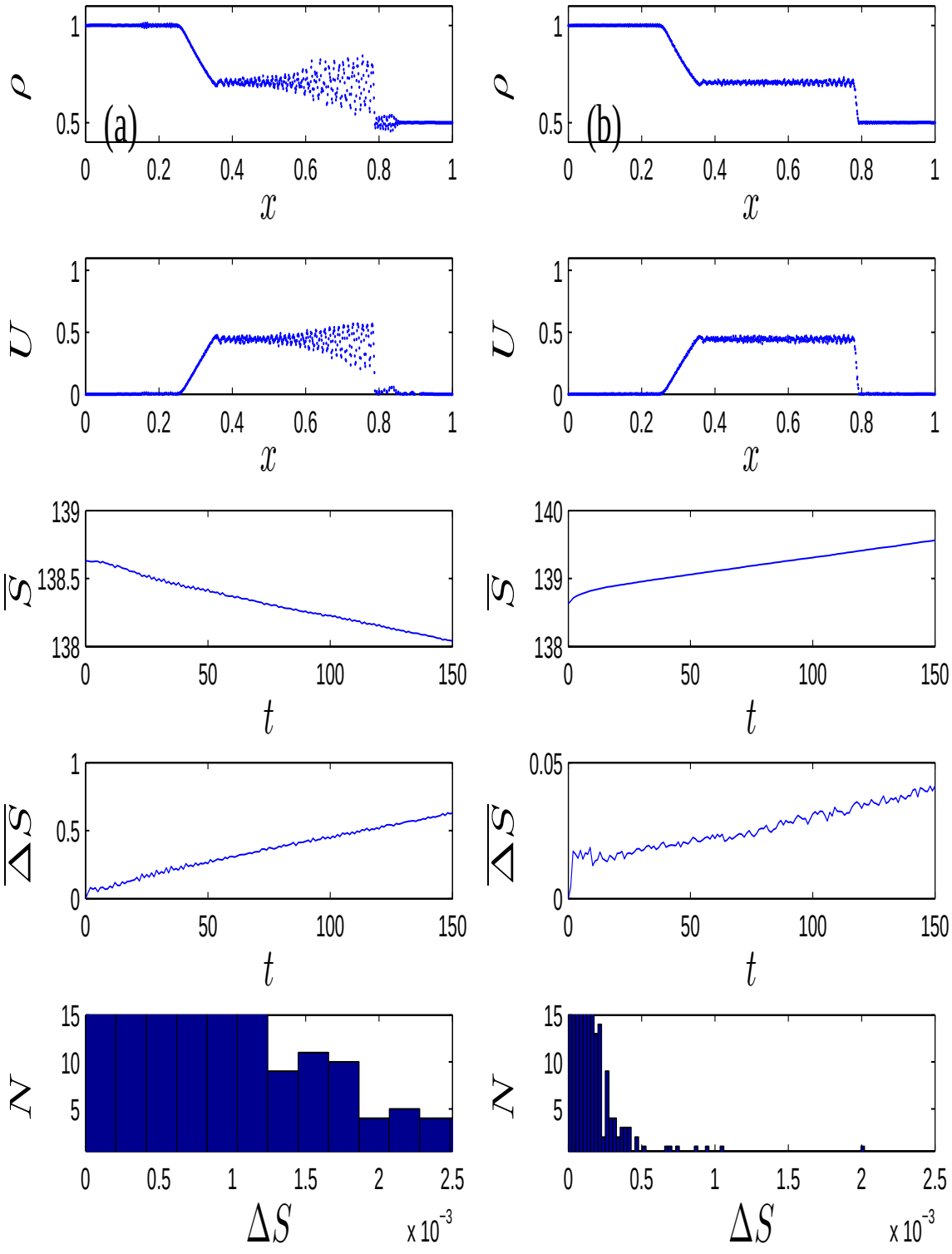

Figure 7.1: Velocity set $\{-3,-1,0,1,3\}$, (a) LBGK vs (b)Ehrenfests' with $k_1 = 5$ and $\delta = 10^{-4}$.

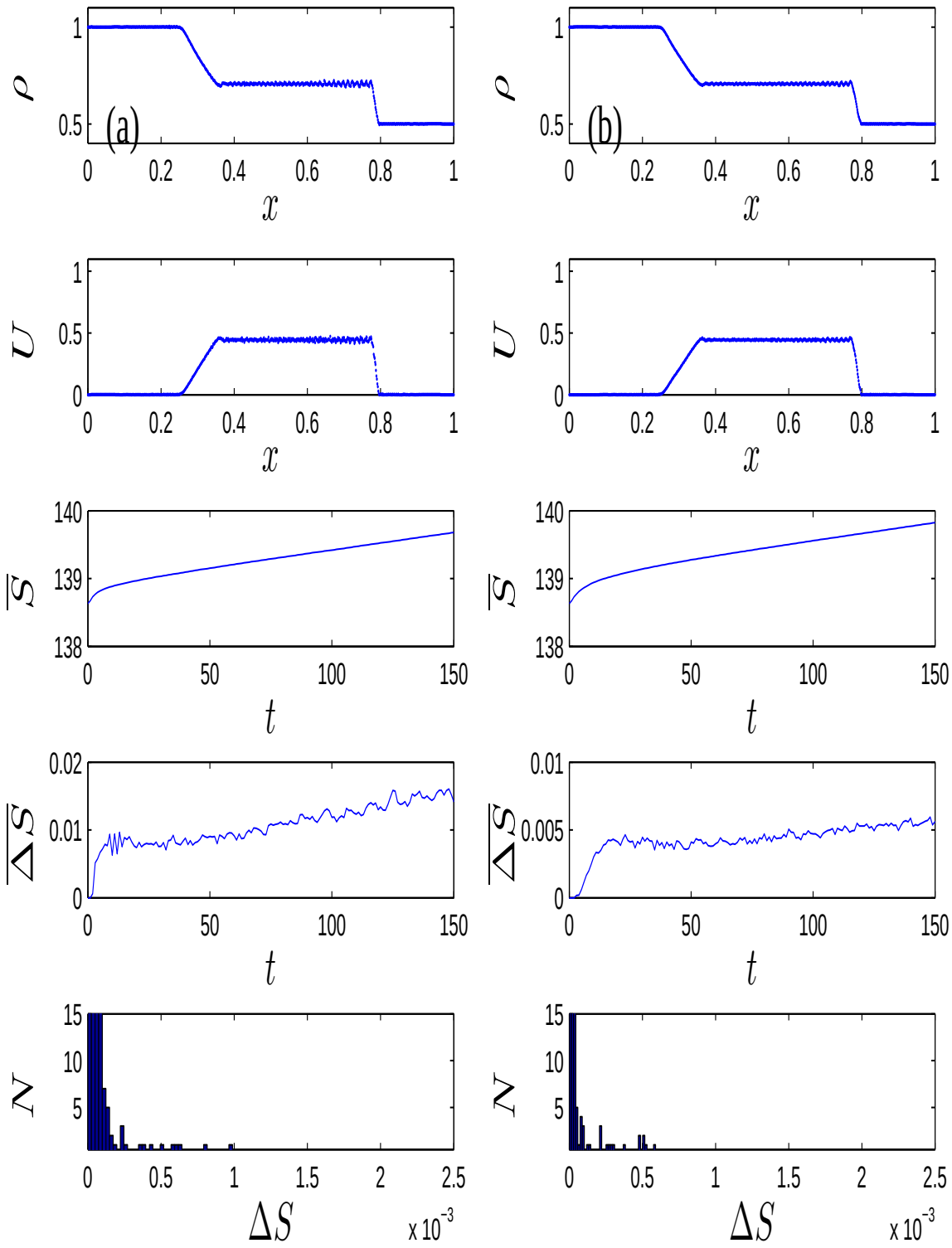

Figure 7.2: Velocity set $\{-3,-1,0,1,3\}$, Ehrenfests' with $\delta = 10^{-4}$, (a) $k_1 = 10$ and (b) $k_1 = 19$.

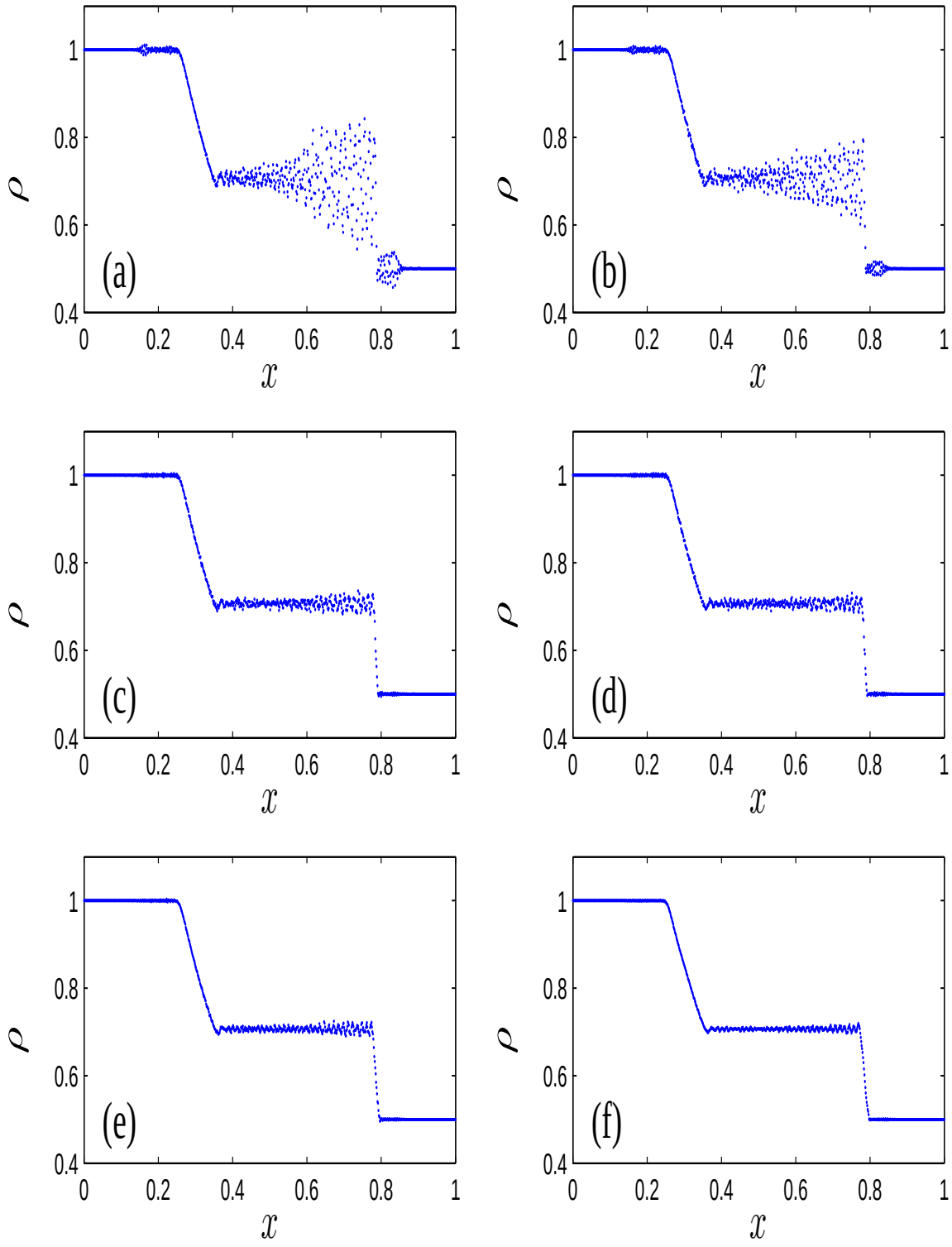

Figure 7.3: Velocity set $\{-3,-1,0,1,3\}$, (a) LBGK with no limiter, and Ehrenfests' with (b) $k_1 = 5, \delta = 10^{-2}$, (c) $k_1 = 5, \delta = 10^{-3}$, (d) $k_1 = 5, \delta = 10^{-4}$, (e) $k_1 = 10, \delta = 10^{-4}$, and (f) $k_1 = 19, \delta = 10^{-4}$.

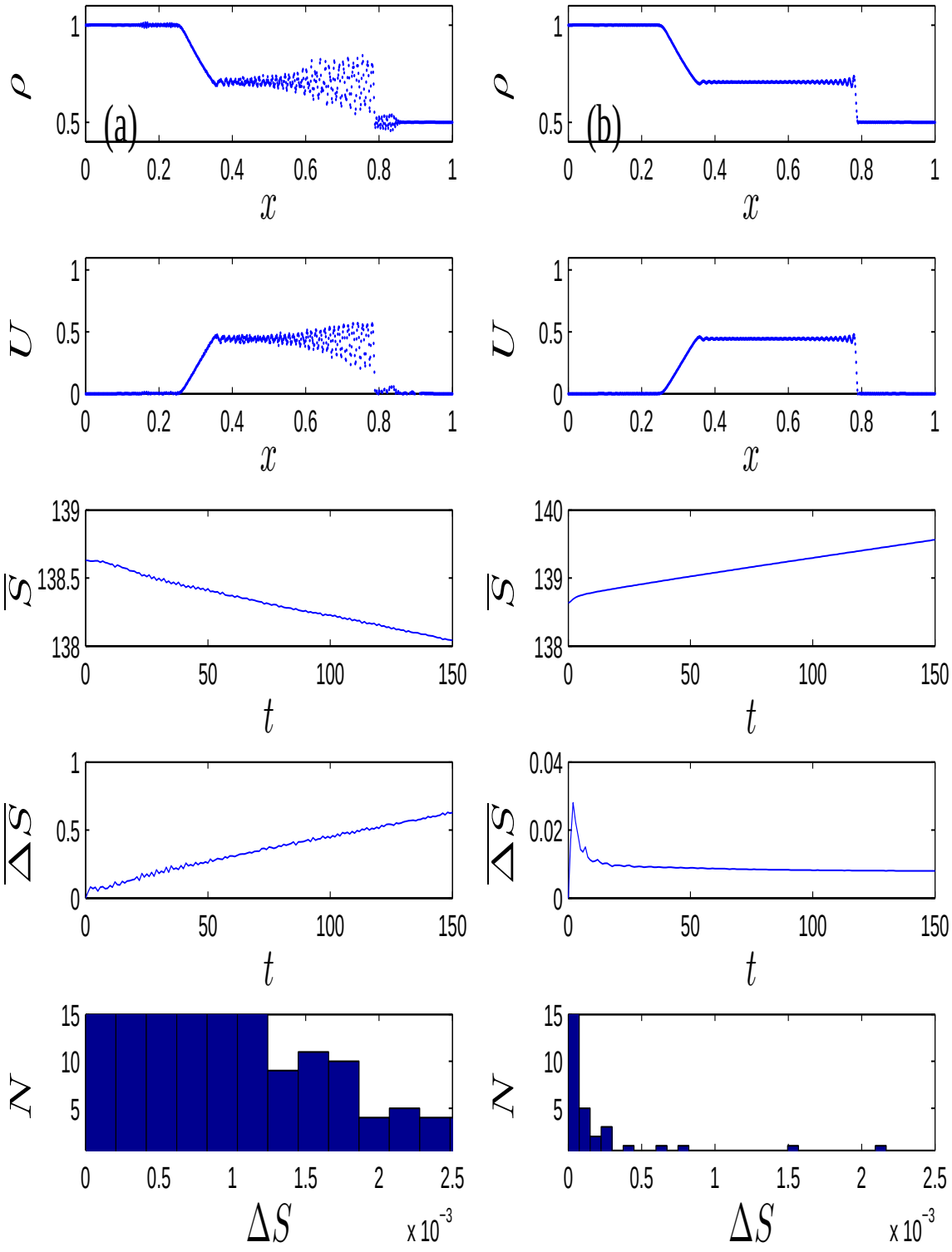

Figure 7.4: Velocity set $\{-3,-1,0,1,3\}$, (a) LBGK vs (b) Smooth limiter 1 with $k_2 = 0.5$ and $\delta = 5 \times 10^{-2}$.

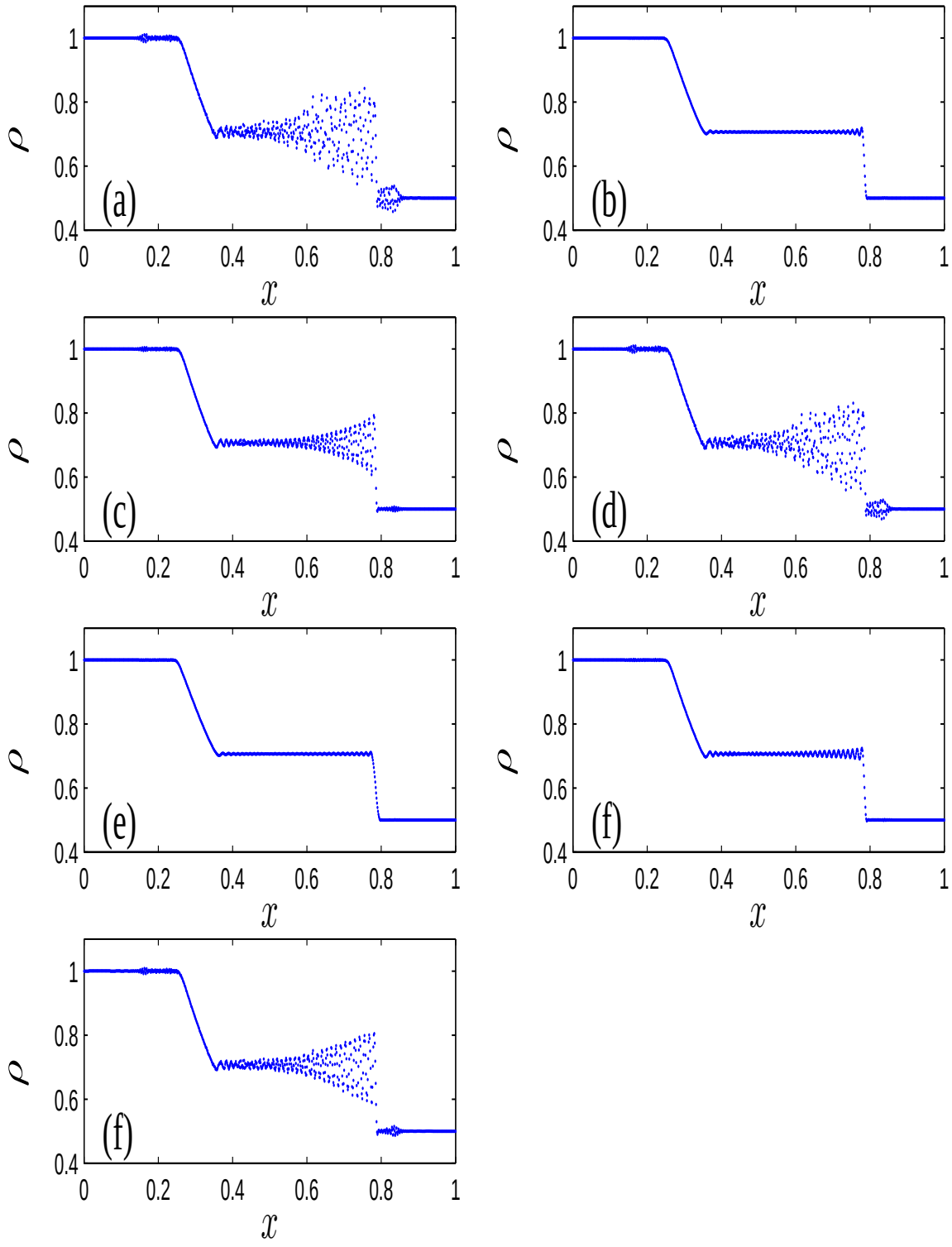

Figure 7.5: Velocity set $\{-3, -1, 0, 1, 3\}$, (a) LBGK with no limiter, and Smooth limiter 1 with (b) $k_2 = 0.5, \delta = 10^{-1}$, (c) $k_2 = 0.5, \delta = 10^{-2}$, (d) $k_2 = 0.5, \delta = 10^{-3}$, (e) $k_2 = 1, \delta = 10^{-1}$, (f) $k_2 = 1, \delta = 10^{-2}$, and (g) $k_2 = 1, \delta = 10^{-3}$.

7.5.3 Smooth Limiter 2

Velocity set $\{-3,-1,0,1,3\}$ LBGK compares with Smooth limiter 2				
parameters	average ΔS	average U	Mach	Reynolds
none	7.8533×10^{-4}	4.4015×10^{-1}	3.4449×10^{-1}	3.5212×10^{11}
$\delta = 1, k_3 = 1$	2.5807×10^{-5}	4.4321×10^{-1}	3.4689×10^{-1}	3.5457×10^{11}
$\delta = 1.5, k_3 = 2$	2.5854×10^{-5}	4.4333×10^{-1}	3.4698×10^{-1}	3.5466×10^{11}
$\delta = 2, k_3 = 2$	5.4419×10^{-5}	4.4327×10^{-1}	3.4693×10^{-1}	3.5461×10^{11}
$\delta = 2, k_3 = 3$	1.3975×10^{-5}	4.4340×10^{-1}	3.4703×10^{-1}	3.5472×10^{11}

7.5.4 Median Limiter

Velocity set $\{-3,-1,0,1,3\}$ LBGK compares with Median filter				
parameters	average ΔS	average U	Mach	Reynolds
none	7.8533×10^{-4}	4.4015×10^{-1}	3.4449×10^{-1}	3.5212×10^{11}
$\delta = 10^{-3}, m_1 = 11$	8.1732×10^{-5}	4.4231×10^{-1}	3.4618×10^{-1}	3.5385×10^{11}
$\delta = 10^{-4}, m_1 = 11$	2.7753×10^{-5}	4.4286×10^{-1}	3.4662×10^{-1}	3.5429×10^{11}
$\delta = 10^{-5}, m_1 = 11$	1.9153×10^{-5}	4.4343×10^{-1}	3.4706×10^{-1}	3.5475×10^{11}
$\delta = 10^{-4}, m_1 = 5$	5.3409×10^{-5}	4.4321×10^{-1}	3.4689×10^{-1}	3.5457×10^{11}
$\delta = 10^{-4}, m_1 = 21$	1.8045×10^{-5}	4.4365×10^{-1}	3.4723×10^{-1}	3.5492×10^{11}

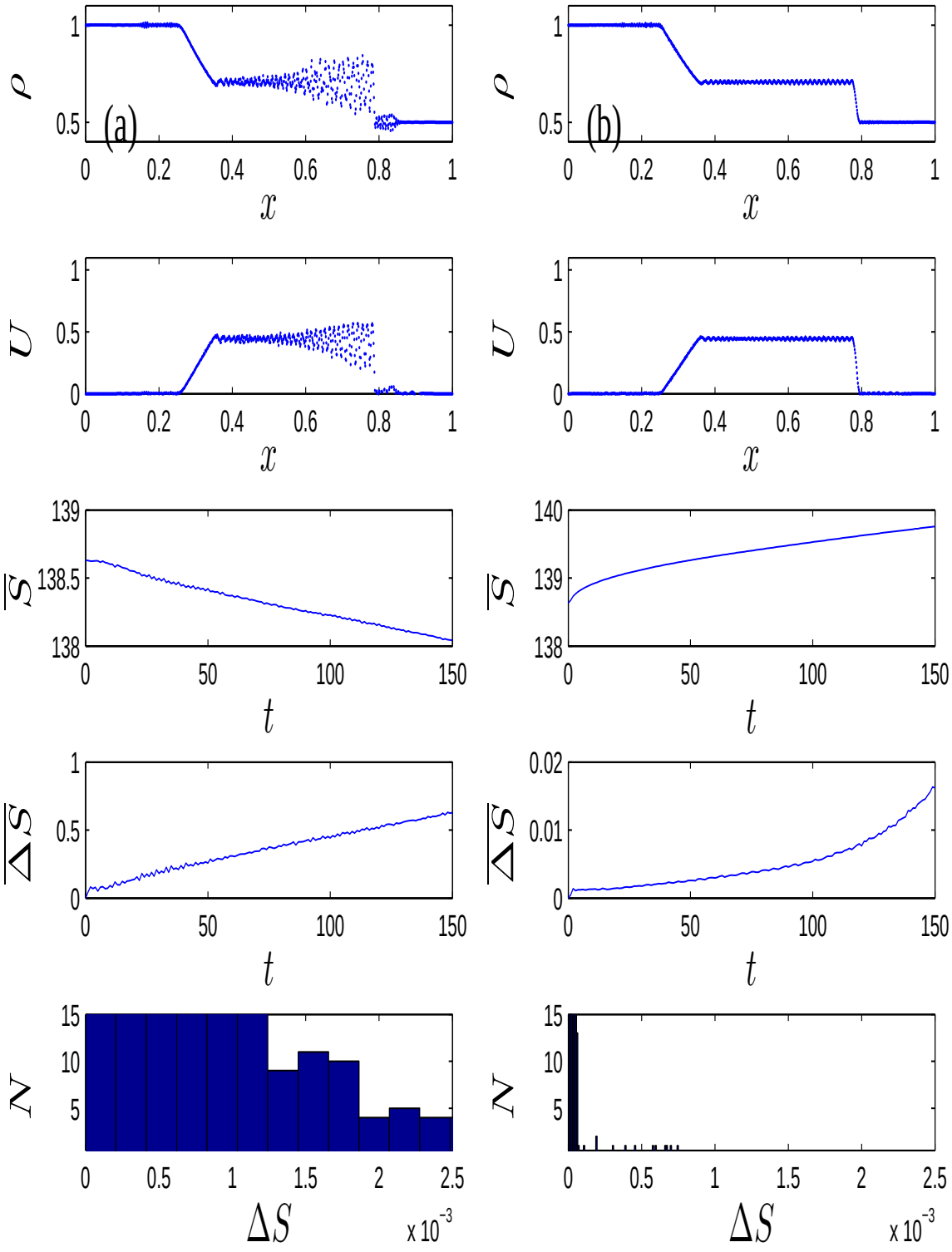

Figure 7.6: Velocity set $\{-3, -1, 0, 1, 3\}$, (a) LBGK vs (b) Smooth limiter 2 with $k_3 = 2.0$ and $\delta = 1.5$.

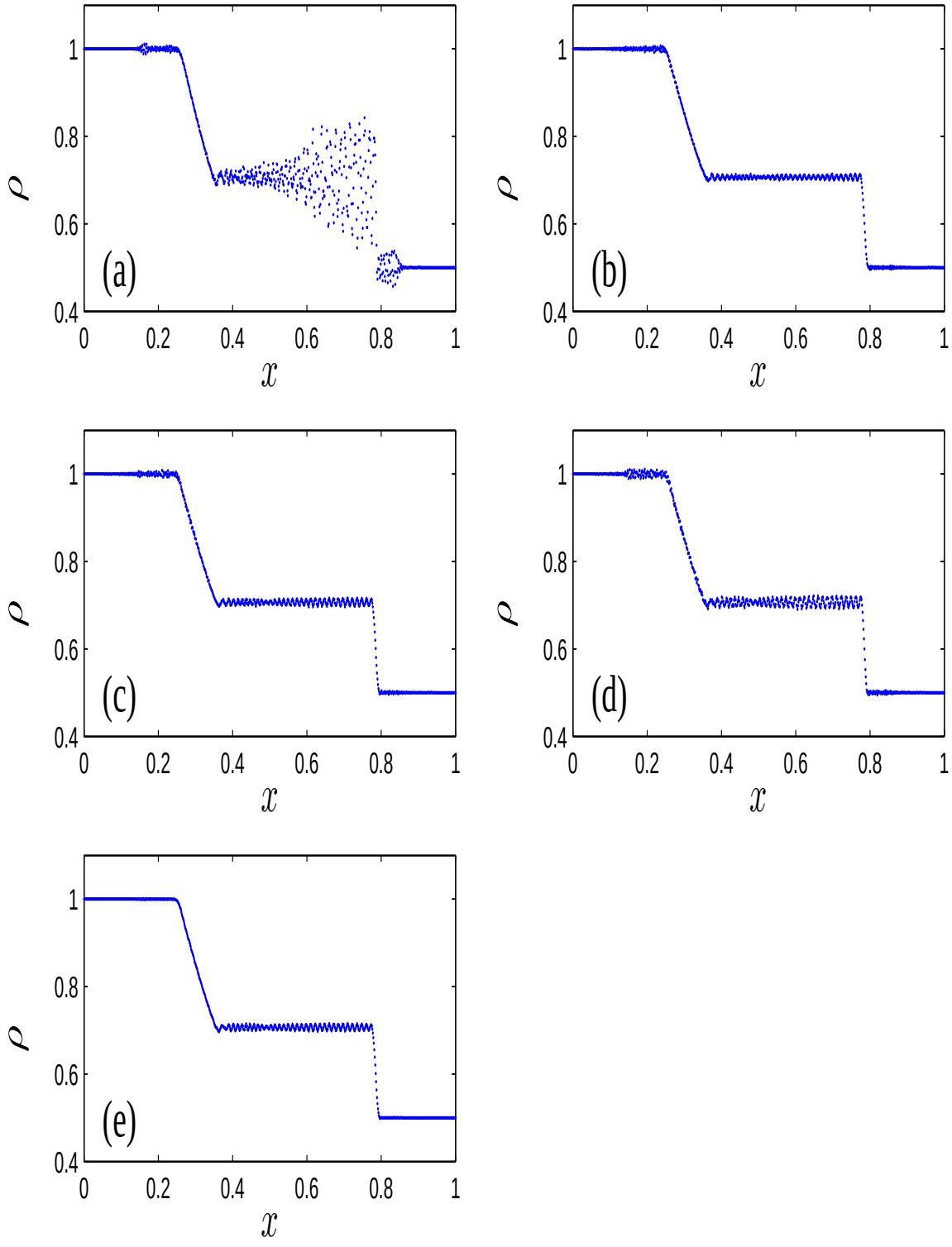

Figure 7.7: Velocity set $\{-3,-1,0,1,3\}$, (a) LBGK with no limiter, and Smooth limiter 2 with (b) $k_3 = 1.0, \delta = 1.0$, (c) $k_3 = 2.0, \delta = 1.5$, (d) $k_3 = 2.0, \delta = 2.0$, (e) $k_3 = 3.0, \delta = 2.0$.

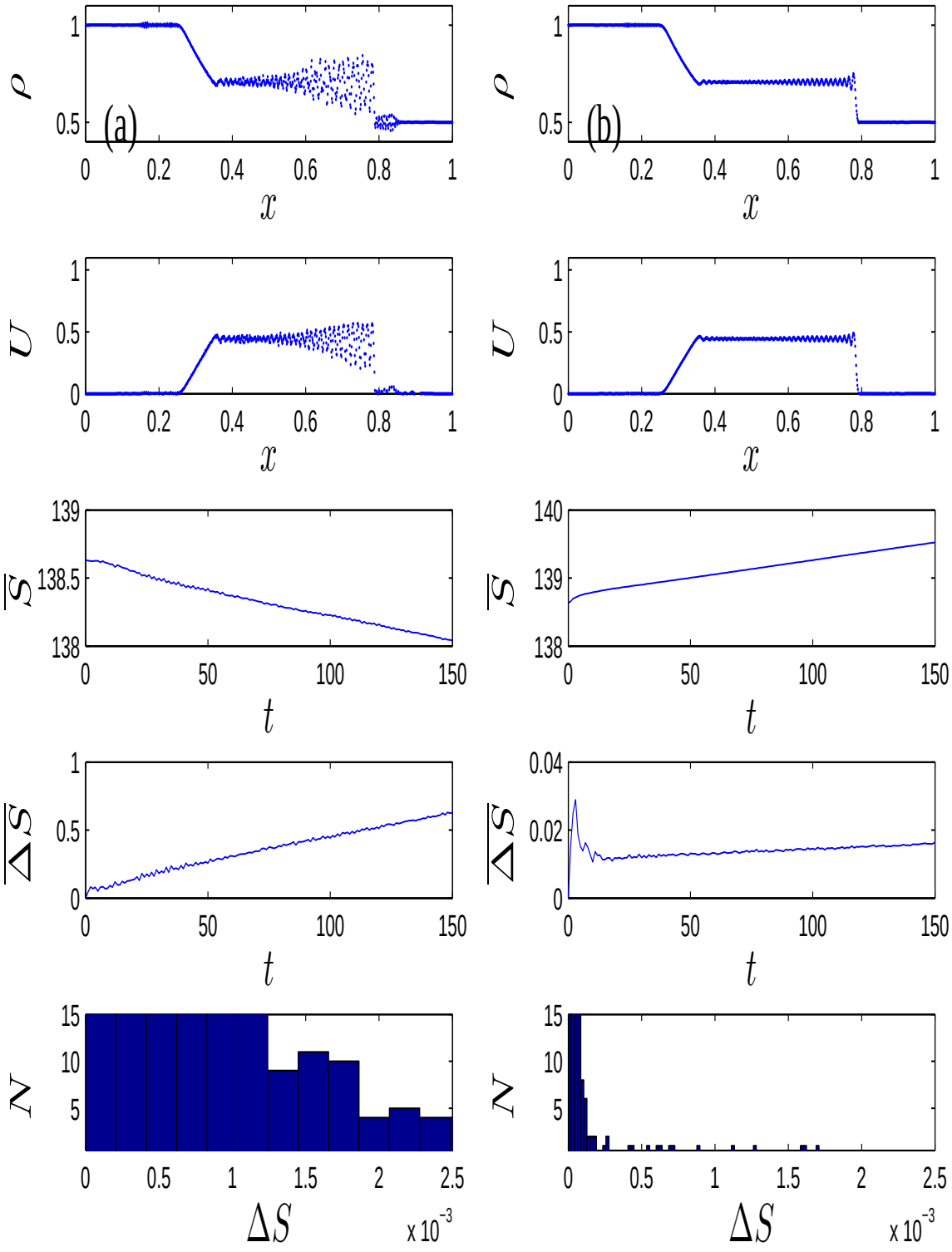

Figure 7.8: Velocity set $\{-3,-1,0,1,3\}$, (a) LBGK vs (b) Median limiter with $m_1 = 11$ and $\delta = 10^{-4}$.

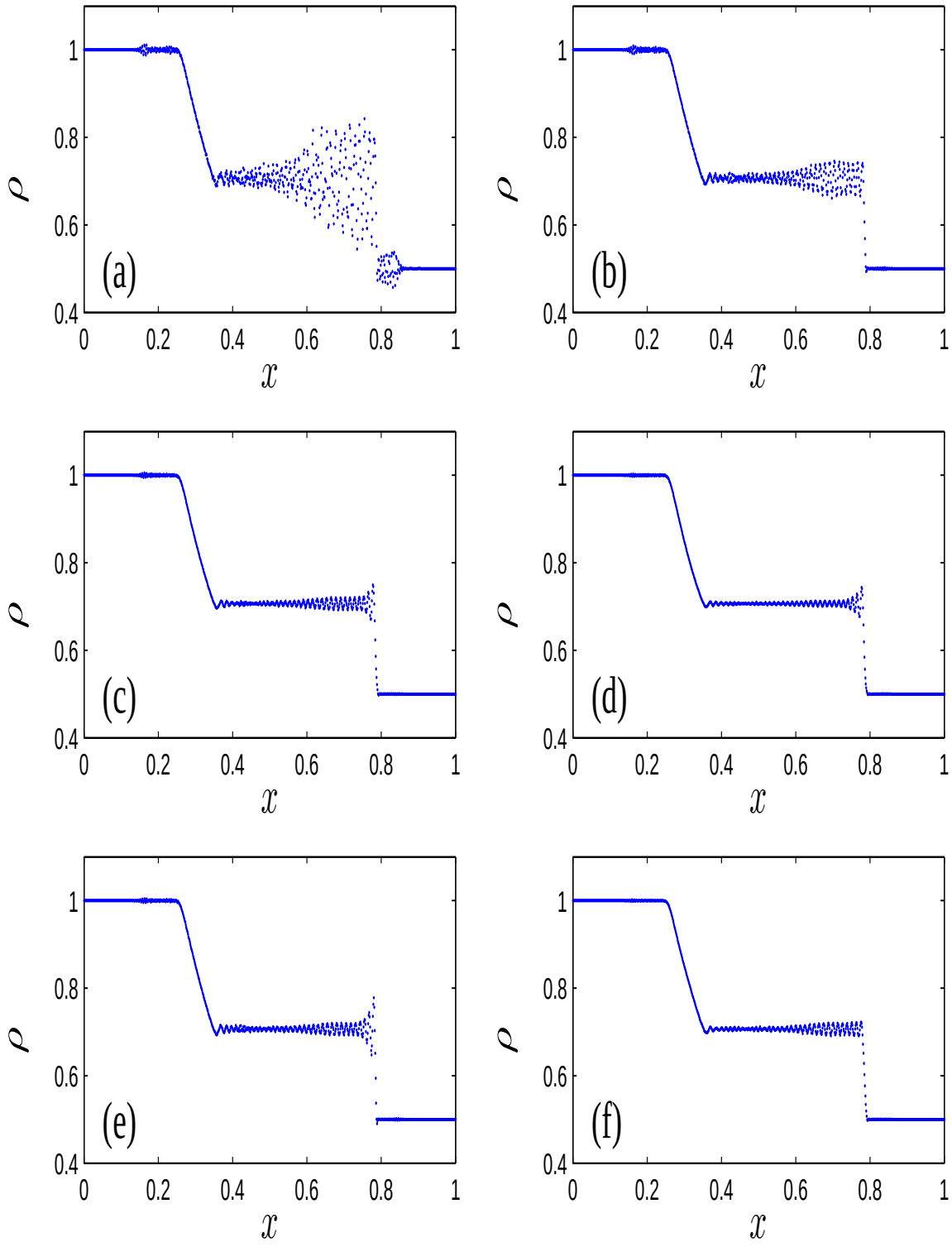

Figure 7.9: Velocity set $\{-3,-1,0,1,3\}$, (a) LBGK with no limiter, and Median limiter with (b) $m_1 = 11, \delta = 10^{-3}$, (c) $m_1 = 11, \delta = 10^{-4}$, (d) $m_1 = 11, \delta = 10^{-5}$, (f) $m_1 = 5, \delta = 10^{-4}$, and (e) $m_1 = 21, \delta = 10^{-4}$.

7.5.5 Maximum Median Limiter

Velocity set $\{-3,-1,0,1,3\}$ LBGK compares with maximum median filter				
parameters	average ΔS	average U	Mach	Reynolds
none	7.8533×10^{-4}	4.4015×10^{-1}	3.4449×10^{-1}	3.5212×10^{11}
$\delta = 10^{-3}, m_2 = 11$	6.2667×10^{-5}	4.4255×10^{-1}	3.4637×10^{-1}	3.5404×10^{11}
$\delta = 10^{-4}, m_2 = 11$	3.2568×10^{-5}	4.4353×10^{-1}	3.4714×10^{-1}	3.5483×10^{11}
$\delta = 10^{-5}, m_2 = 11$	1.8143×10^{-5}	4.4383×10^{-1}	3.4737×10^{-1}	3.5506×10^{11}
$\delta = 10^{-4}, m_2 = 5$	5.5164×10^{-5}	4.4306×10^{-1}	3.4677×10^{-1}	3.5445×10^{11}
$\delta = 10^{-4}, m_2 = 21$	1.8882×10^{-5}	4.4326×10^{-1}	3.4693×10^{-1}	3.5461×10^{11}

7.5.6 Mean Limiter

Velocity set $\{-3,-1,0,1,3\}$ LBGK compares with mean filter				
parameters	average ΔS	average U	Mach	Reynolds
none	7.8533×10^{-4}	4.4015×10^{-1}	3.4449×10^{-1}	3.5212×10^{11}
$\delta = 10^{-2}, k_4 = 1$	4.0609×10^{-4}	4.4032×10^{-1}	3.4462×10^{-1}	3.5225×10^{11}
$\delta = 10^{-3}, k_4 = 1$	6.3290×10^{-5}	4.4330×10^{-1}	3.4696×10^{-1}	3.5464×10^{11}
$\delta = 10^{-4}, k_4 = 1$	1.2743×10^{-5}	4.4352×10^{-1}	3.4713×10^{-1}	3.5482×10^{11}
$\delta = 10^{-5}, k_4 = 1$	8.7041×10^{-5}	4.4393×10^{-1}	3.4745×10^{-1}	3.5514×10^{11}
$\delta = 10^{-3}, k_4 = 1.5$	6.6680×10^{-5}	4.4320×10^{-1}	3.4688×10^{-1}	3.5456×10^{11}

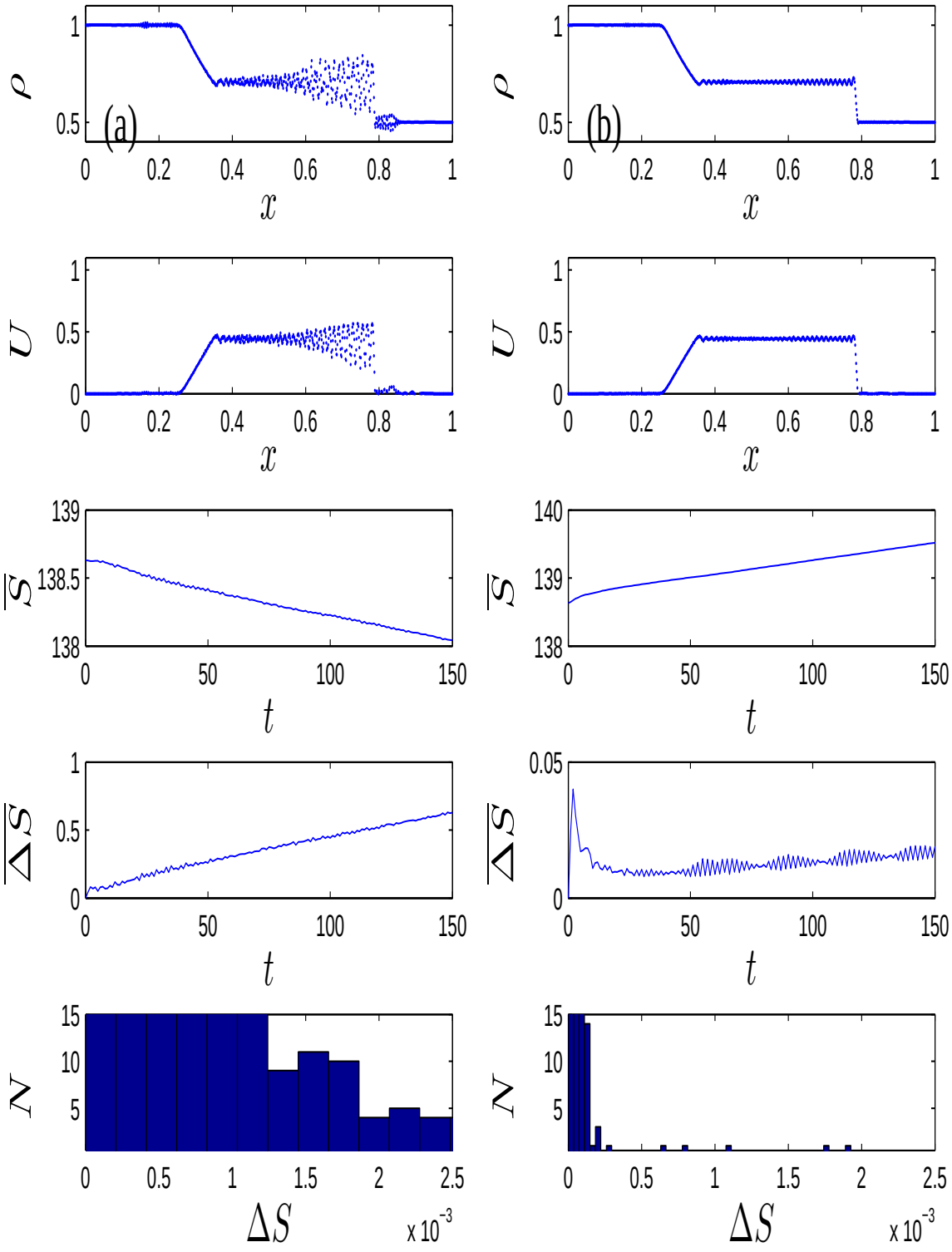

Figure 7.10: Velocity set $\{-3,-1,0,1,3\}$, (a) LBGK vs (b) maximum median limiter with $m_2 = 11$ and $\delta = 10^{-4}$.

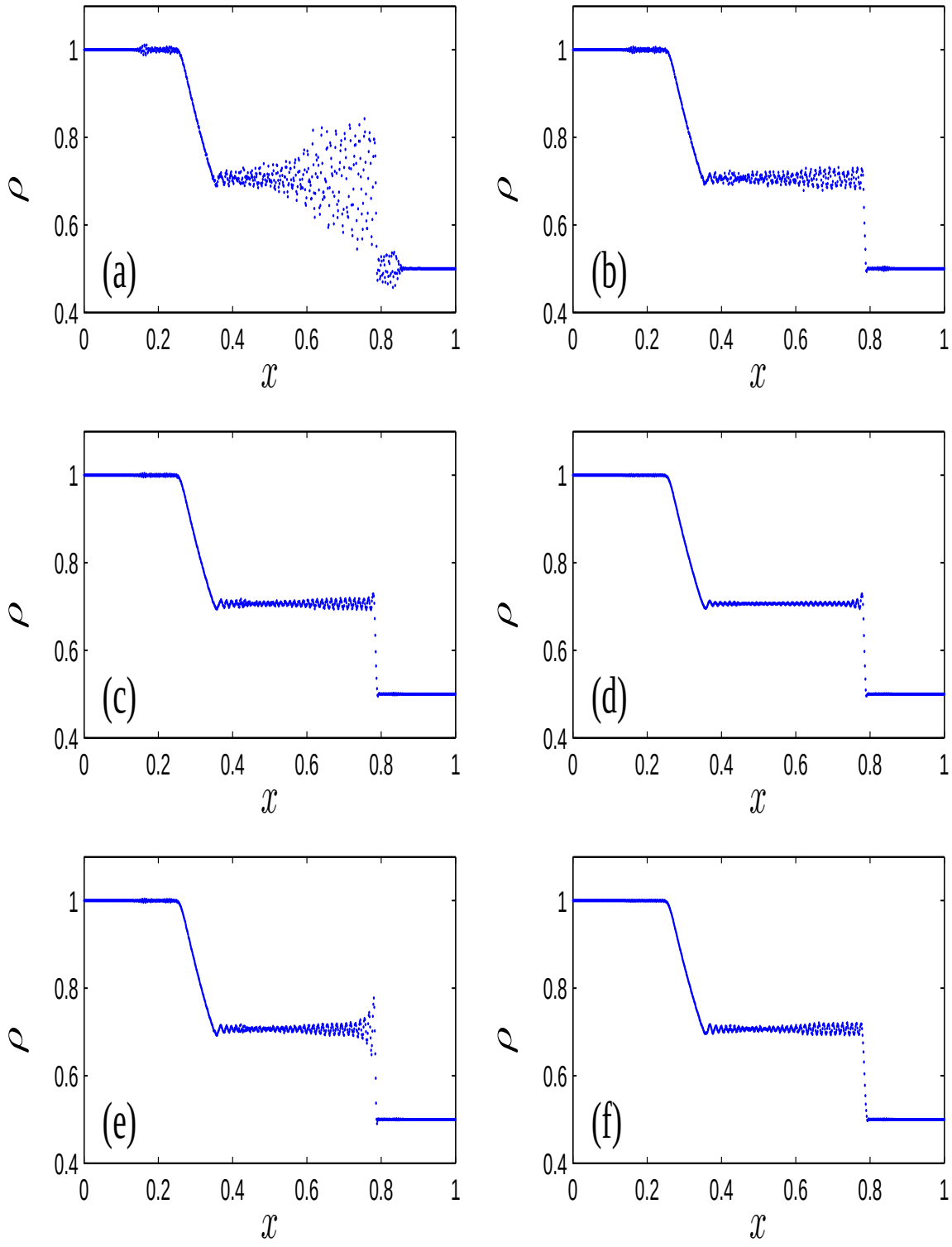

Figure 7.11: Velocity set $\{-3,-1,0,1,3\}$, (a) LBGK with no limiter, and maximum median limiter with (b) $m_2 = 11, \delta = 10^{-3}$, (c) $m_2 = 11, \delta = 10^{-4}$, (d) $m_2 = 11, \delta = 10^{-5}$, (f) $m_2 = 5, \delta = 10^{-4}$, and (e) $m_2 = 21, \delta = 10^{-4}$.

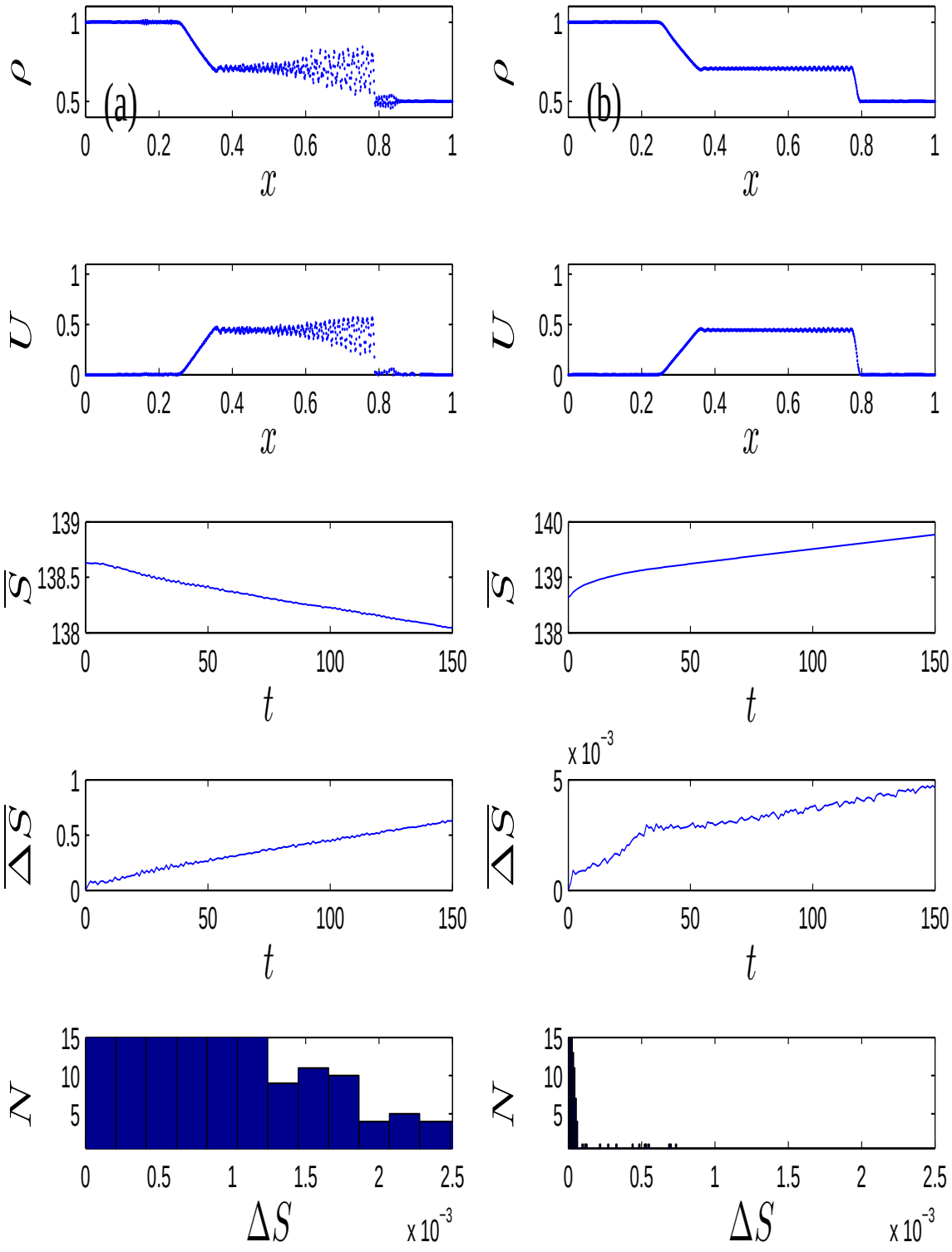

Figure 7.12: Velocity set $\{-3,-1,0,1,3\}$, (a) LBGK vs (b) mean limiter with $k_4 = 1$ and $\delta = 10^{-4}$.

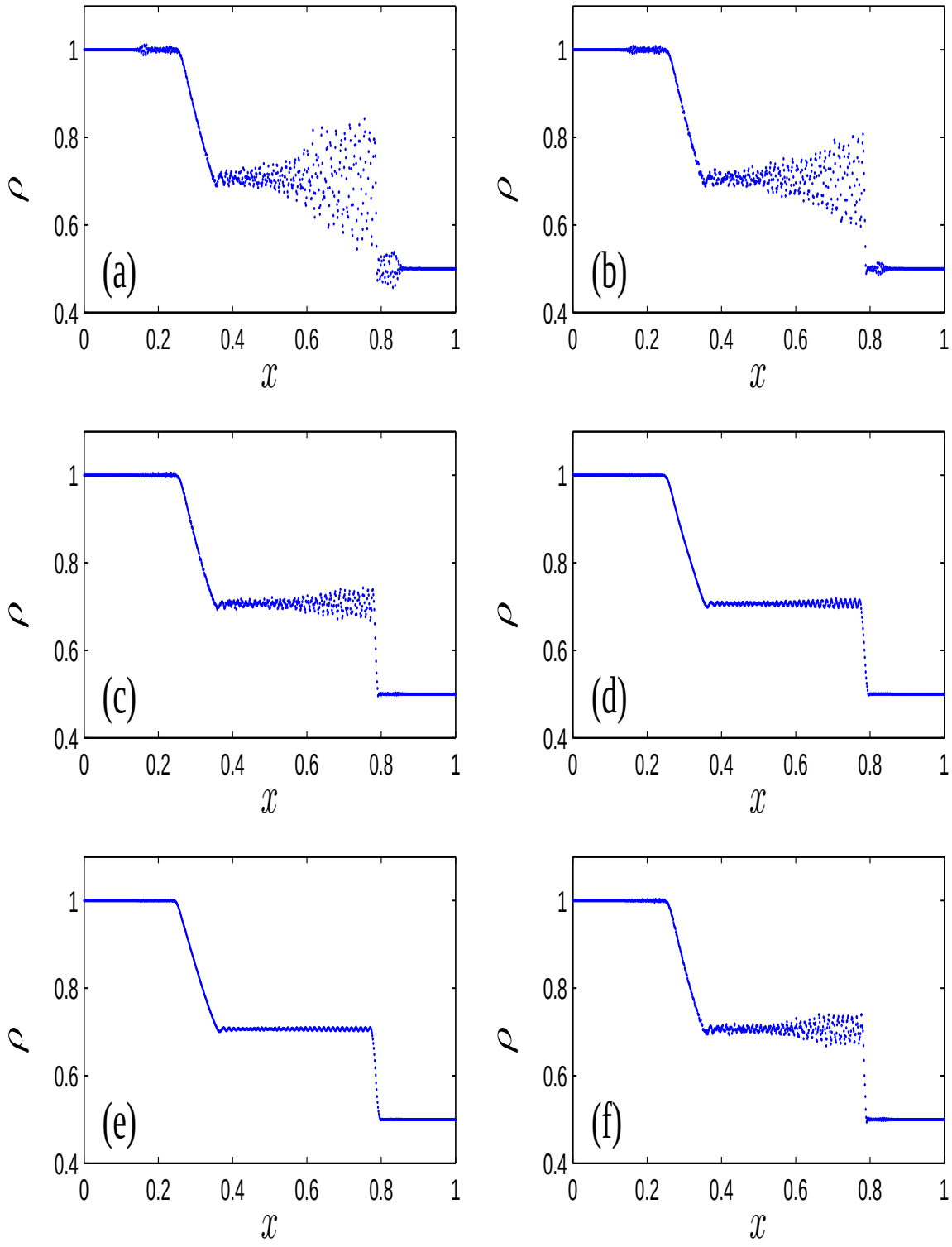

Figure 7.13: Velocity set $\{-3,-1,0,1,3\}$, (a) LBGK with no limiter, and mean limiter with (b) $k_4 = 1, \delta = 10^{-2}$, (c) $k_4 = 1, \delta = 10^{-3}$, (d) $k_4 = 1, \delta = 10^{-4}$, (e) $k_4 = 1, \delta = 10^{-5}$, and (f) $k_4 = 1.5, \delta = 10^{-3}$.

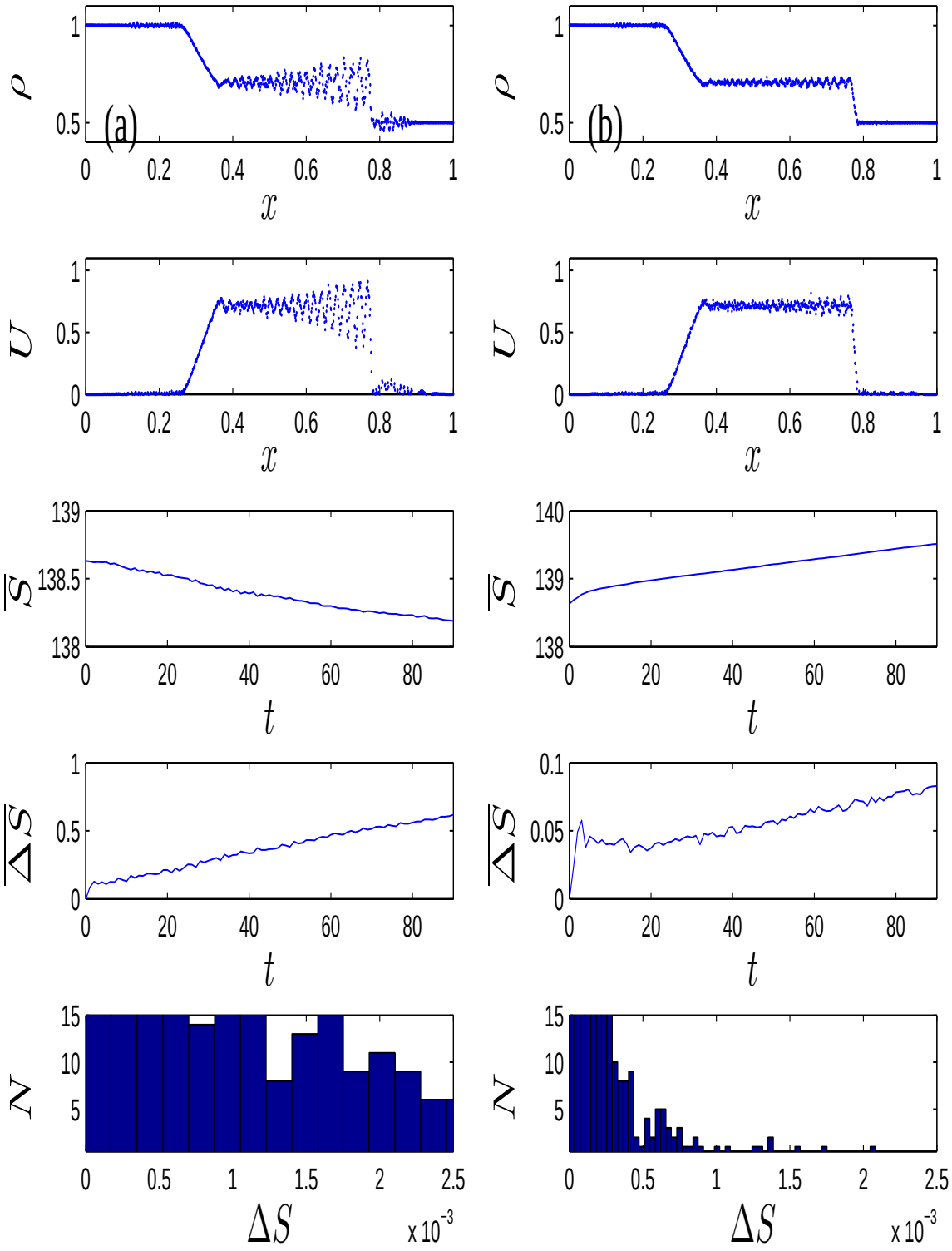

Figure 7.14: velocity set $\{-5,-2,0,2,5\}$, (a) LBGK vs (b)Ehrenfests' with $k_1 = 5$ and $\delta = 10^{-3}$.

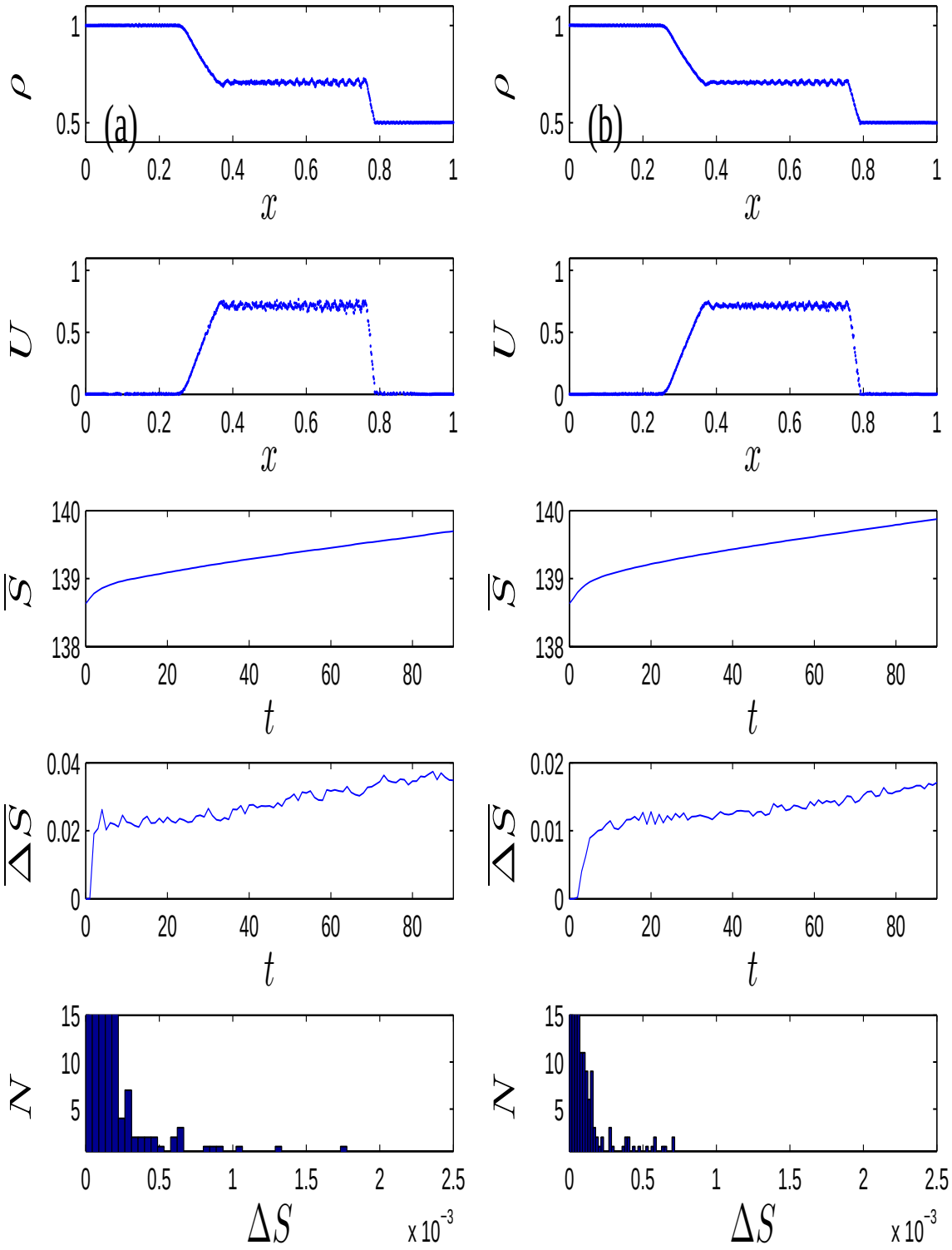

Figure 7.15: velocity set $\{-5, -2, 0, 2, 5\}$, Ehrenfests' with $\delta = 10^{-4}$, (a) $k_1 = 10$ and (b) $k_1 = 19$.

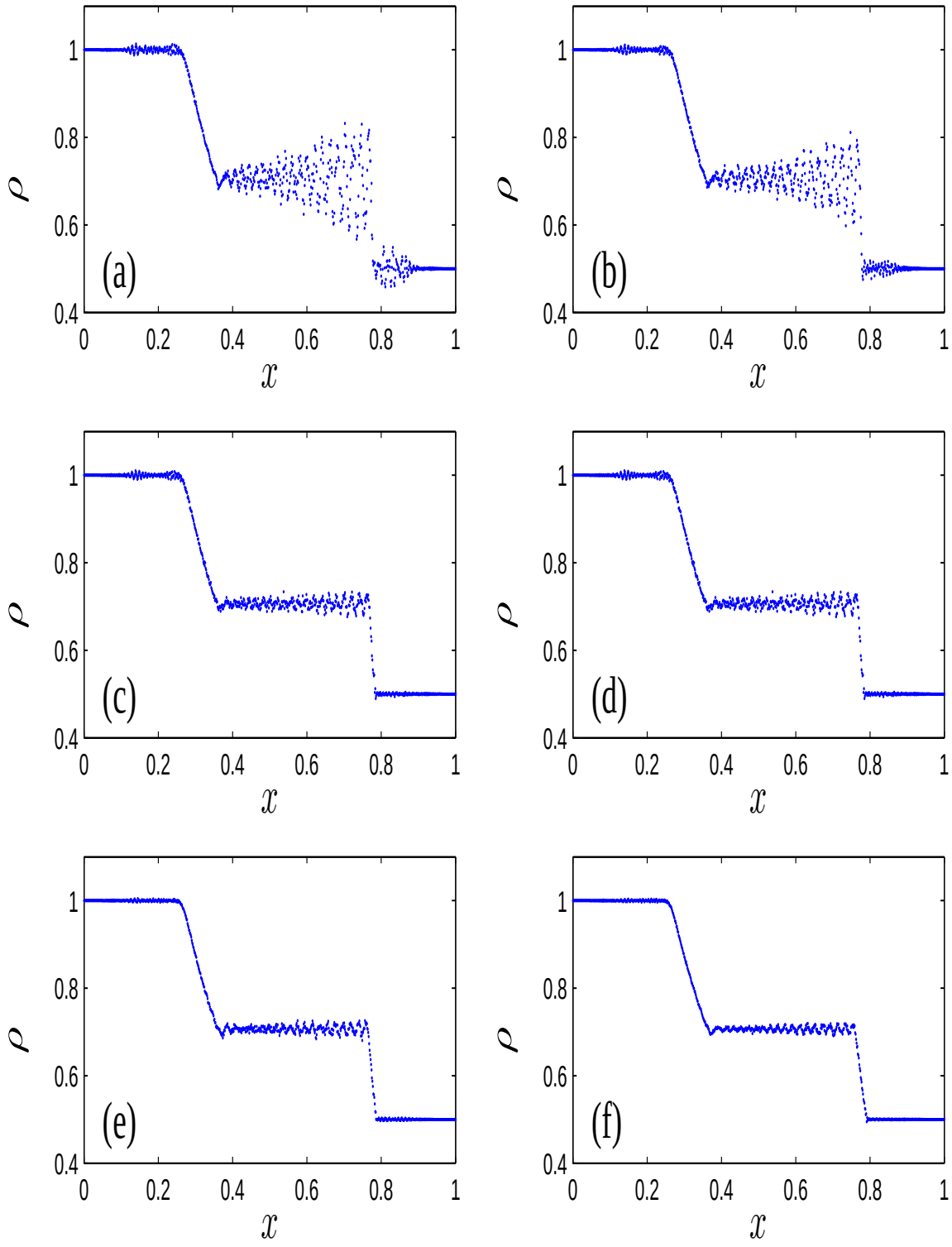

Figure 7.16: velocity set $\{-5,-2,0,2,5\}$, (a) LBGK with no limiter, and Ehrenfests' with (b) $k_1 = 5, \delta = 10^{-2}$, (c) $k_1 = 5, \delta = 10^{-3}$, (d) $k_1 = 5, \delta = 10^{-4}$, (e) $k_1 = 10, \delta = 10^{-4}$, and (f) $k_1 = 19, \delta = 10^{-4}$.

7.6 Velocity set $\{-5, -2, 0, 2, 5\}$

7.6.1 Ehrenfests' Regularisation

velocity set $\{-5, -2, 0, 2, 5\}$ LBGK compares with Ehrenfests' limiter				
parameters	average ΔS	average U	Mach	Reynolds
none	7.7357×10^{-4}	7.1514×10^{-1}	3.4811×10^{-1}	5.7211×10^{11}
$\delta = 10^{-2}, k_1 = 5$	4.9367×10^{-4}	7.1136×10^{-1}	3.4627×10^{-1}	5.6909×10^{11}
$\delta = 10^{-3}, k_1 = 5$	1.1570×10^{-4}	7.1324×10^{-1}	3.4718×10^{-1}	5.7059×10^{11}
$\delta = 10^{-4}, k_1 = 5$	1.1570×10^{-4}	7.1324×10^{-1}	3.4718×10^{-1}	5.7059×10^{11}
$\delta = 10^{-4}, k_1 = 10$	5.5118×10^{-5}	7.1362×10^{-1}	3.4737×10^{-1}	5.7090×10^{11}
$\delta = 10^{-4}, k_1 = 19$	3.2546×10^{-5}	7.1365×10^{-1}	3.4738×10^{-1}	5.7092×10^{11}

7.6.2 Smooth Limiter 1

velocity set $\{-5, -2, 0, 2, 5\}$ LBGK compares with smooth limiter 1				
parameters	average ΔS	average U	Mach	Reynolds
none	7.7357×10^{-4}	7.1514×10^{-1}	3.4811×10^{-1}	5.7211×10^{11}
$\delta = 10^{-2}, k_2 = 0.5$	2.5096×10^{-4}	7.1348×10^{-1}	3.4730×10^{-1}	5.7079×10^{11}
$\delta = 5.5 \times 10^{-2}, k_2 = 0.5$	3.7111×10^{-5}	7.1374×10^{-1}	3.4743×10^{-1}	5.7100×10^{11}
$\delta = 10^{-1}, k_2 = 0.5$	2.2322×10^{-5}	7.1384×10^{-1}	3.4748×10^{-1}	5.7107×10^{11}
$\delta = 10^{-2}, k_2 = 1$	4.3749×10^{-5}	7.1395×10^{-1}	3.4753×10^{-1}	5.7116×10^{11}
$\delta = 2 \times 10^{-2}, k_2 = 1$	2.3412×10^{-5}	7.1385×10^{-1}	3.4748×10^{-1}	5.7108×10^{11}
$\delta = 10^{-1}, k_2 = 1$	1.5078×10^{-5}	7.1418×10^{-1}	3.4764×10^{-1}	5.7134×10^{11}

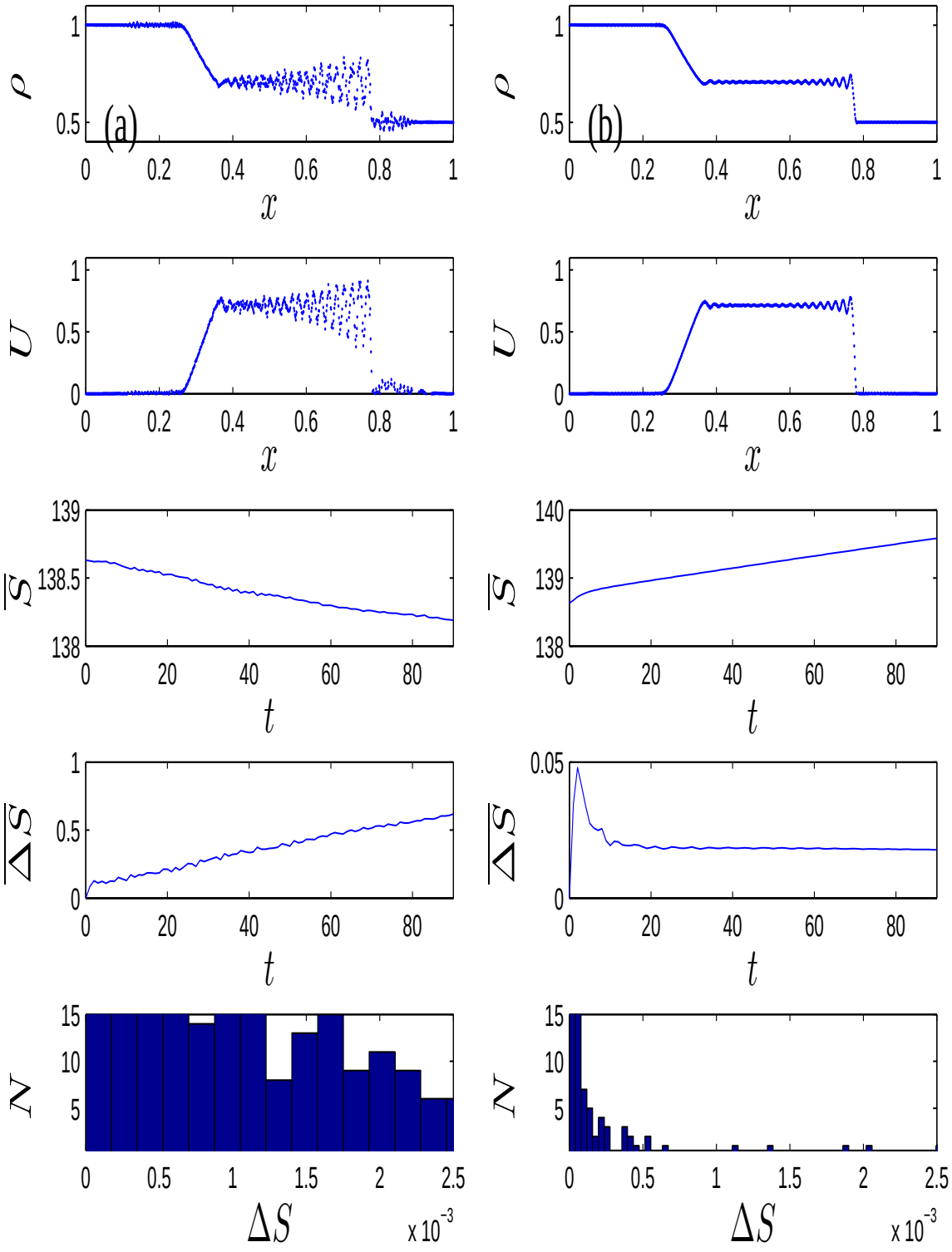

Figure 7.17: velocity set $\{-5,-2,0,2,5\}$ (a) LBGK vs (b) Smooth limiter 1 with $k_2 = 0.5$ and $\delta = 5.5 \times 10^{-2}$.

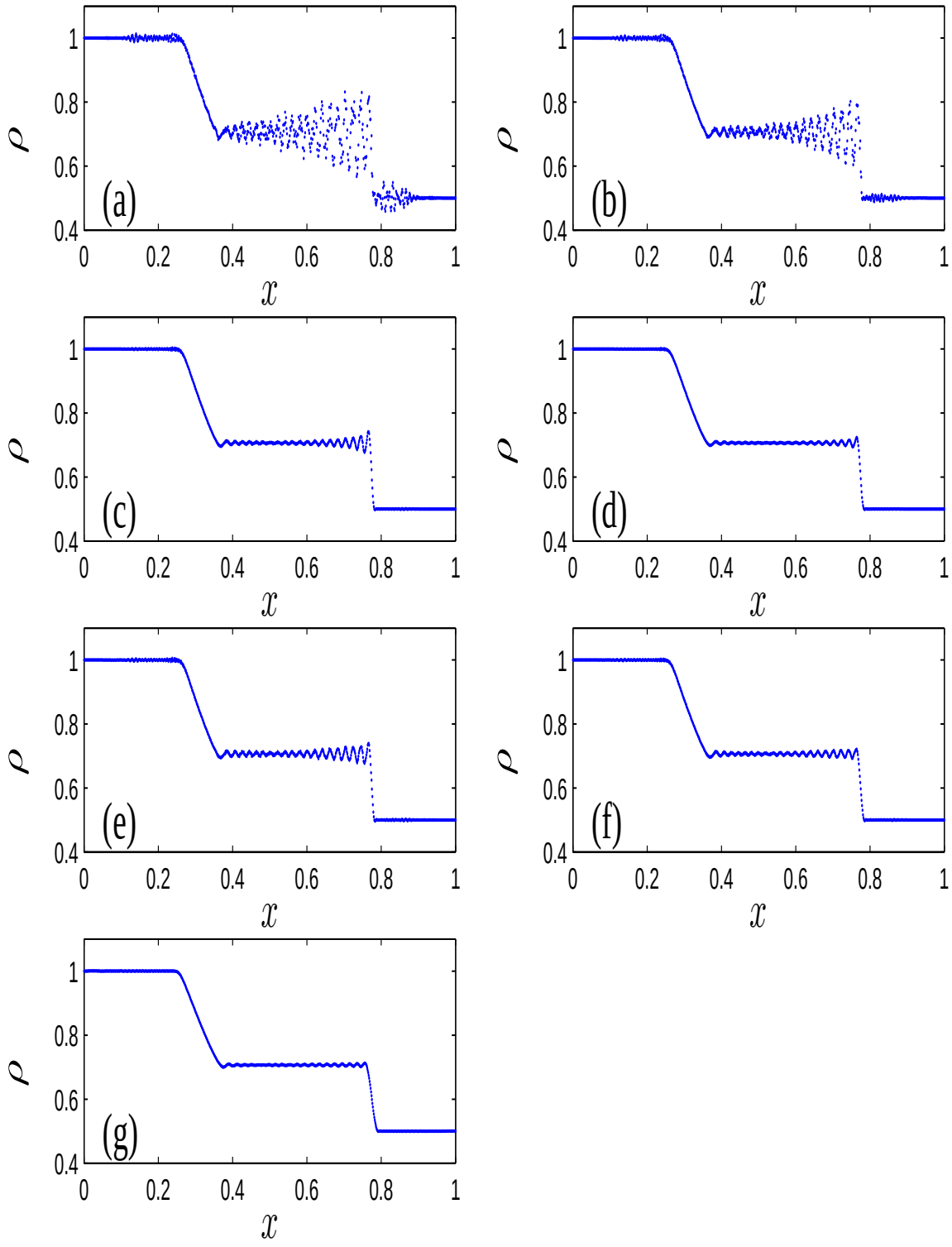

Figure 7.18: velocity set $\{-5, -2, 0, 2, 5\}$ (a) LBGK with no limiter, and Smooth limiter 1 with (b) $k_2 = 0.5, \delta = 10^{-2}$, (c) $k_2 = 0.5, \delta = 5.5 \times 10^{-2}$, (d) $k_2 = 0.5, \delta = 10^{-1}$, (e) $k_2 = 1, \delta = 10^{-2}$, (f) $k_2 = 1, \delta = 2 \times 10^{-2}$, and (g) $k_2 = 1, \delta = 10^{-1}$.

7.6.3 Smooth Limiter 2

velocity set $\{-5,-2,0,2,5\}$ LBGK compares with Smooth limiter 2				
parameters	average ΔS	average U	Mach	Reynolds
none	7.7357×10^{-4}	7.1514×10^{-1}	3.4811×10^{-1}	5.7211×10^{11}
$\delta = 1, k_3 = 1$	3.6927×10^{-5}	7.1510×10^{-1}	3.4809×10^{-1}	5.7208×10^{11}
$\delta = 1.5, k_3 = 2$	2.5208×10^{-5}	7.1376×10^{-1}	3.4744×10^{-1}	5.7101×10^{11}
$\delta = 2, k_3 = 2$	3.1184×10^{-5}	7.1390×10^{-1}	3.4751×10^{-1}	5.7112×10^{11}
$\delta = 2, k_3 = 3$	2.1221×10^{-5}	7.1353×10^{-1}	3.4733×10^{-1}	5.7083×10^{11}

7.6.4 Median Limiter

velocity set $\{-5,-2,0,2,5\}$ LBGK compares with Median filter				
parameters	average ΔS	average U	Mach	Reynolds
none	7.7357×10^{-4}	7.1514×10^{-1}	3.4811×10^{-1}	5.7211×10^{11}
$\delta = 10^{-3}, m_1 = 11$	1.2370×10^{-4}	7.1537×10^{-1}	3.4822×10^{-1}	5.7230×10^{11}
$\delta = 10^{-4}, m_1 = 11$	4.0581×10^{-5}	7.1415×10^{-1}	3.4763×10^{-1}	5.7132×10^{11}
$\delta = 10^{-5}, m_1 = 11$	3.4737×10^{-5}	7.1367×10^{-1}	3.4740×10^{-1}	5.7094×10^{11}
$\delta = 10^{-4}, m_1 = 5$	1.6755×10^{-4}	7.1374×10^{-1}	3.4743×10^{-1}	5.7099×10^{11}
$\delta = 10^{-4}, m_1 = 21$	3.9443×10^{-5}	7.1360×10^{-1}	3.4736×10^{-1}	5.7088×10^{11}

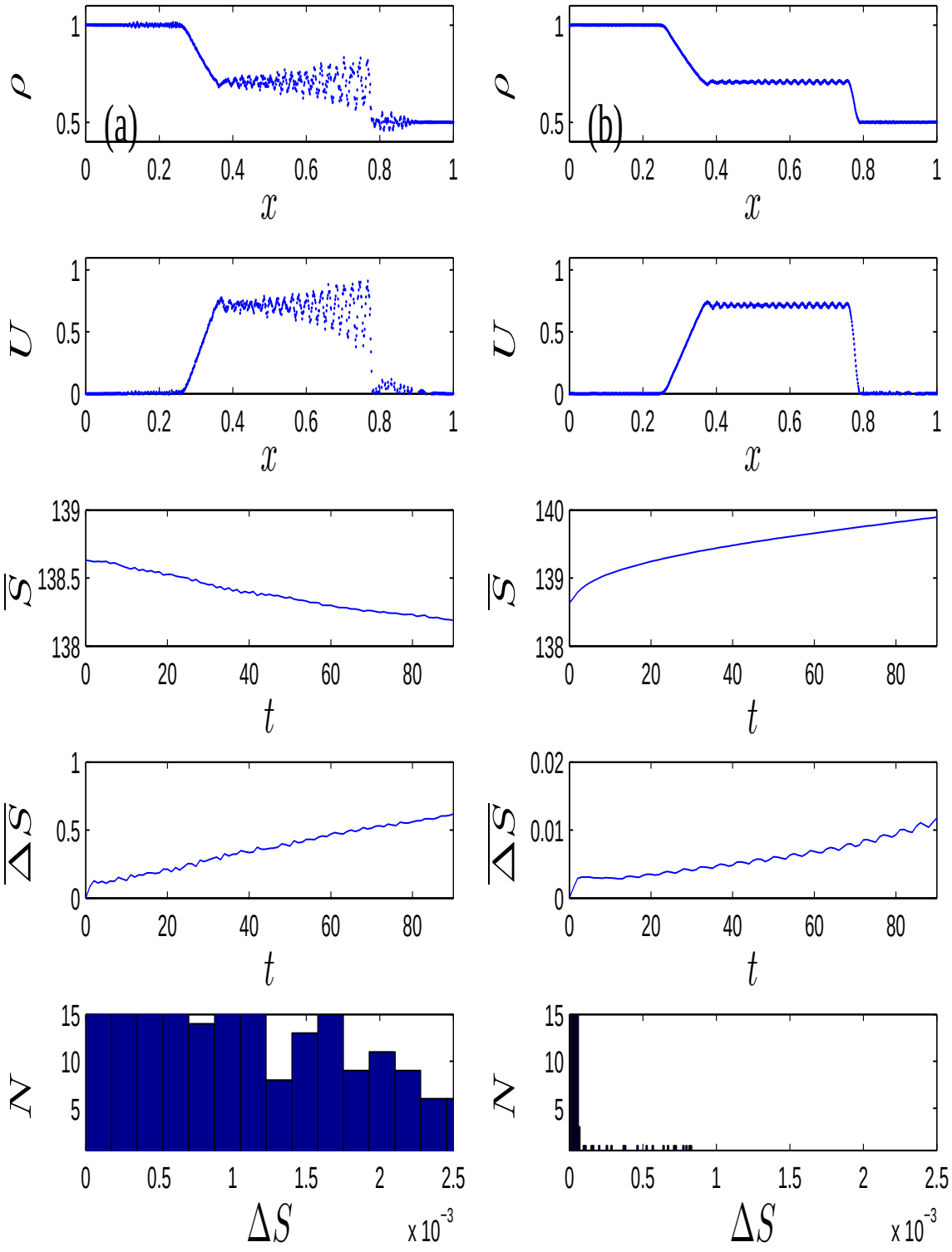

Figure 7.19: velocity set $\{-5, -2, 0, 2, 5\}$, (a) LBGK with no limiter vs (b) Smooth limiter 2 with $k_3 = 2$ and $\delta = 1.5$.

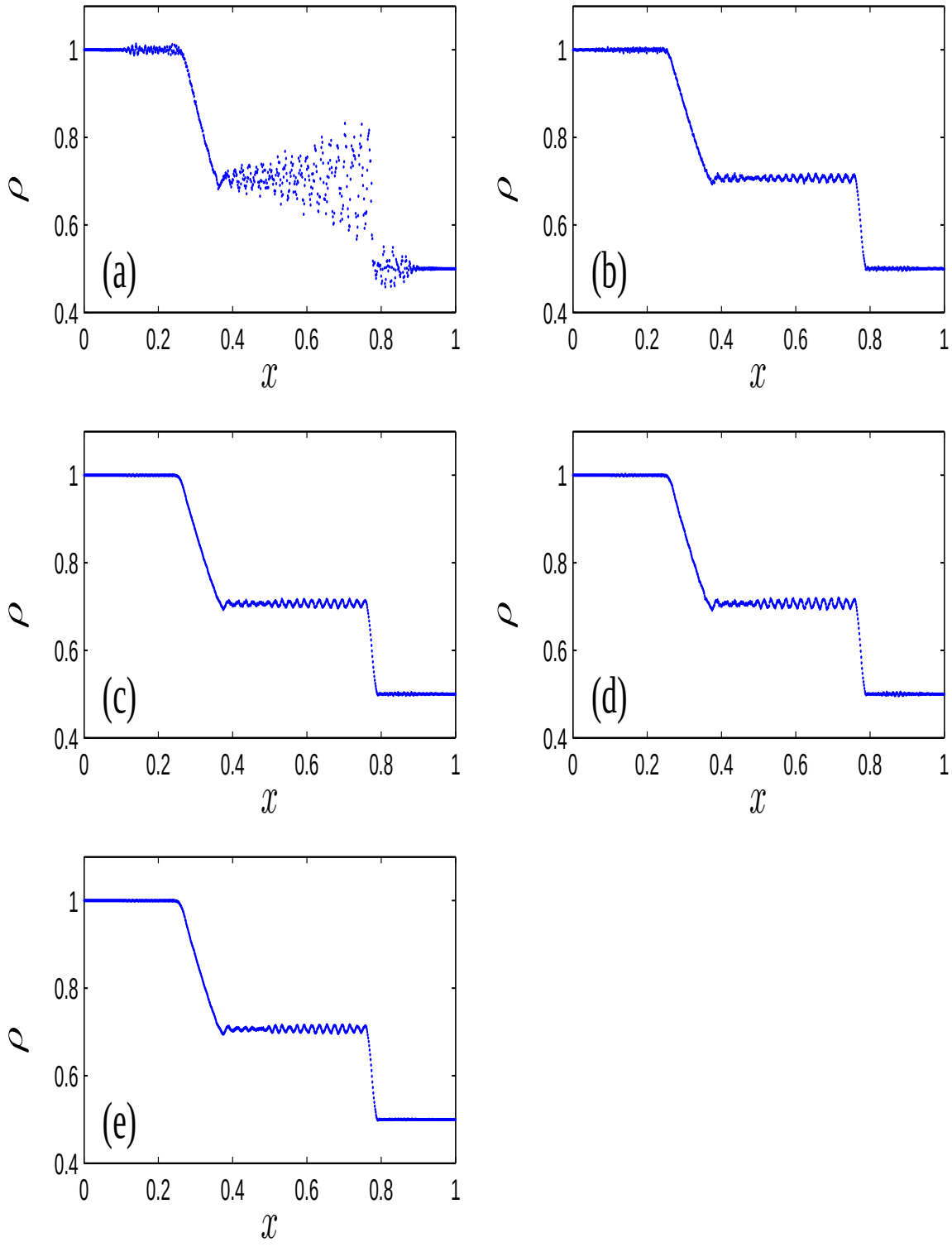

Figure 7.20: velocity set $\{-5,-2,0,2,5\}$, (a) LBGK with no limiter, and Smooth limiter 2 with (b) $k_3 = 1.0, \delta = 1.0$,(c) $k_3 = 2.0, \delta = 1.5$ (d) $k_3 = 2.0, \delta = 2.0$, and (e) $k_3 = 3.0, \delta = 2.0$.

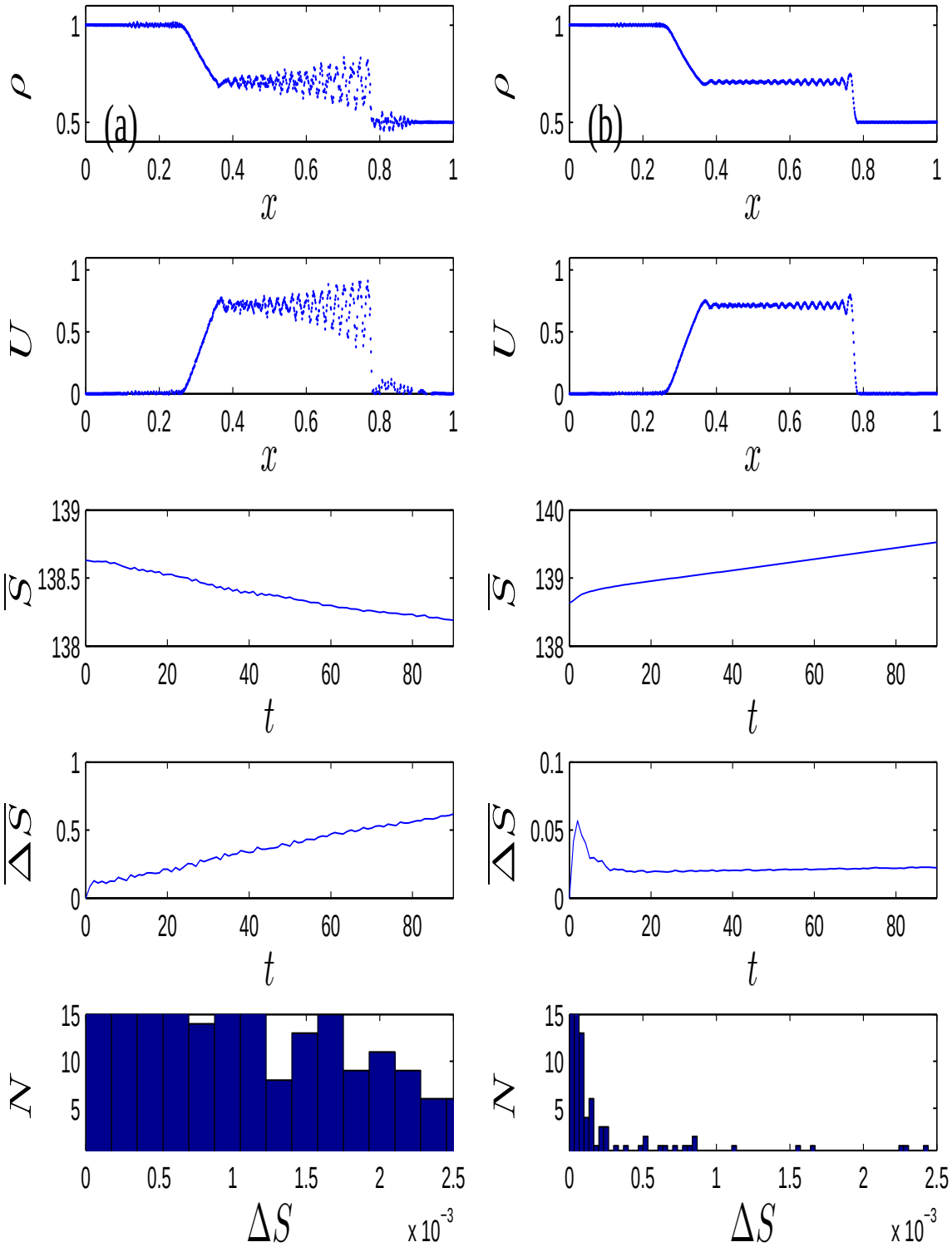

Figure 7.21: velocity set $\{-5, -2, 0, 2, 5\}$, (a) LBGK vs (b) Median limiter with $m_1 = 11$ and $\delta = 10^{-4}$.

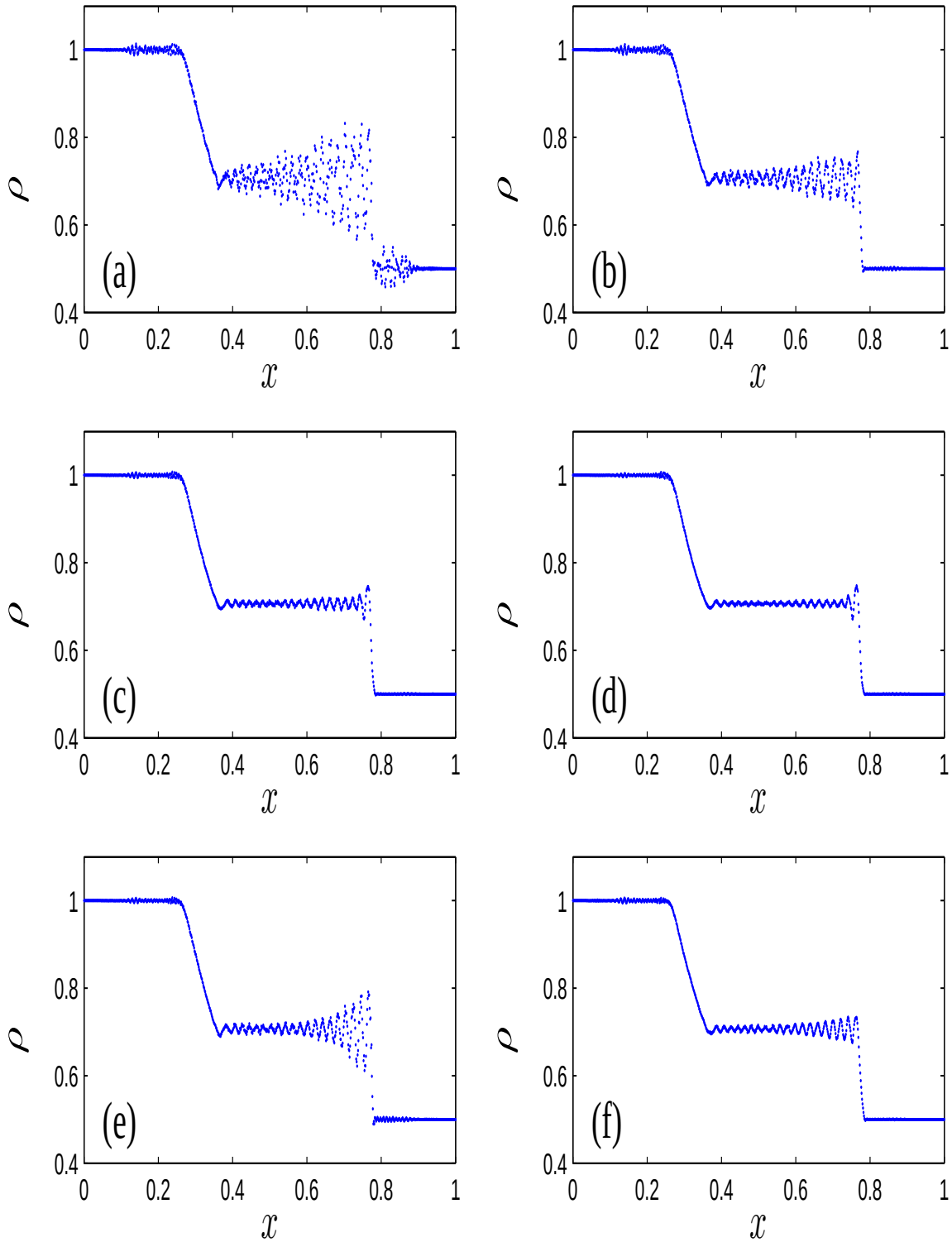

Figure 7.22: velocity set $\{-5, -2, 0, 2, 5\}$, (a) LBGK with no limiter, and Median limiter with (b) $m_1 = 11, \delta = 10^{-3}$, (c) $m_1 = 11, \delta = 10^{-4}$, (d) $m_1 = 11, \delta = 10^{-5}$, (f) $m_1 = 5, \delta = 10^{-4}$, and (e) $m_1 = 21, \delta = 10^{-4}$.

7.6.5 Maximum Median Limiter

velocity set $\{-5,-2,0,2,5\}$ LBGK compares with maximum median filter				
parameters	average ΔS	average U	Mach	Reynolds
none	7.7357×10^{-4}	7.1514×10^{-1}	3.4811×10^{-1}	5.7211×10^{11}
$\delta = 10^{-3}, m_2 = 11$	1.5030×10^{-4}	7.1269×10^{-1}	3.4692×10^{-1}	5.7016×10^{11}
$\delta = 10^{-4}, m_2 = 11$	7.6178×10^{-5}	7.1334×10^{-1}	3.4724×10^{-1}	5.7067×10^{11}
$\delta = 10^{-5}, m_2 = 11$	6.5442×10^{-5}	7.1385×10^{-1}	3.4748×10^{-1}	5.7108×10^{11}
$\delta = 10^{-4}, m_2 = 5$	1.6759×10^{-4}	7.1385×10^{-1}	3.4748×10^{-1}	5.7108×10^{11}
$\delta = 10^{-4}, m_2 = 21$	3.8228×10^{-5}	7.1333×10^{-1}	3.4723×10^{-1}	5.7066×10^{11}

7.6.6 Mean Limiter

velocity set $\{-5,-2,0,2,5\}$ LBGK compares with mean filter				
parameters	average ΔS	average U	Mach	Reynolds
none	7.7357×10^{-4}	7.1514×10^{-1}	3.4811×10^{-1}	5.7211×10^{11}
$\delta = 10^{-2}, k_4 = 1$	4.9693×10^{-4}	7.1277×10^{-1}	3.4696×10^{-1}	5.7022×10^{11}
$\delta = 10^{-3}, k_4 = 1$	6.9997×10^{-5}	7.1323×10^{-1}	3.4718×10^{-1}	5.7059×10^{11}
$\delta = 10^{-4}, k_4 = 1$	1.8258×10^{-5}	7.1406×10^{-1}	3.4759×10^{-1}	5.7125×10^{11}
$\delta = 10^{-5}, k_4 = 1$	1.5120×10^{-5}	7.1440×10^{-1}	3.4775×10^{-1}	5.7152×10^{11}
$\delta = 10^{-3}, k_4 = 1.5$	6.7438×10^{-5}	7.1376×10^{-1}	3.4744×10^{-1}	5.7101×10^{11}

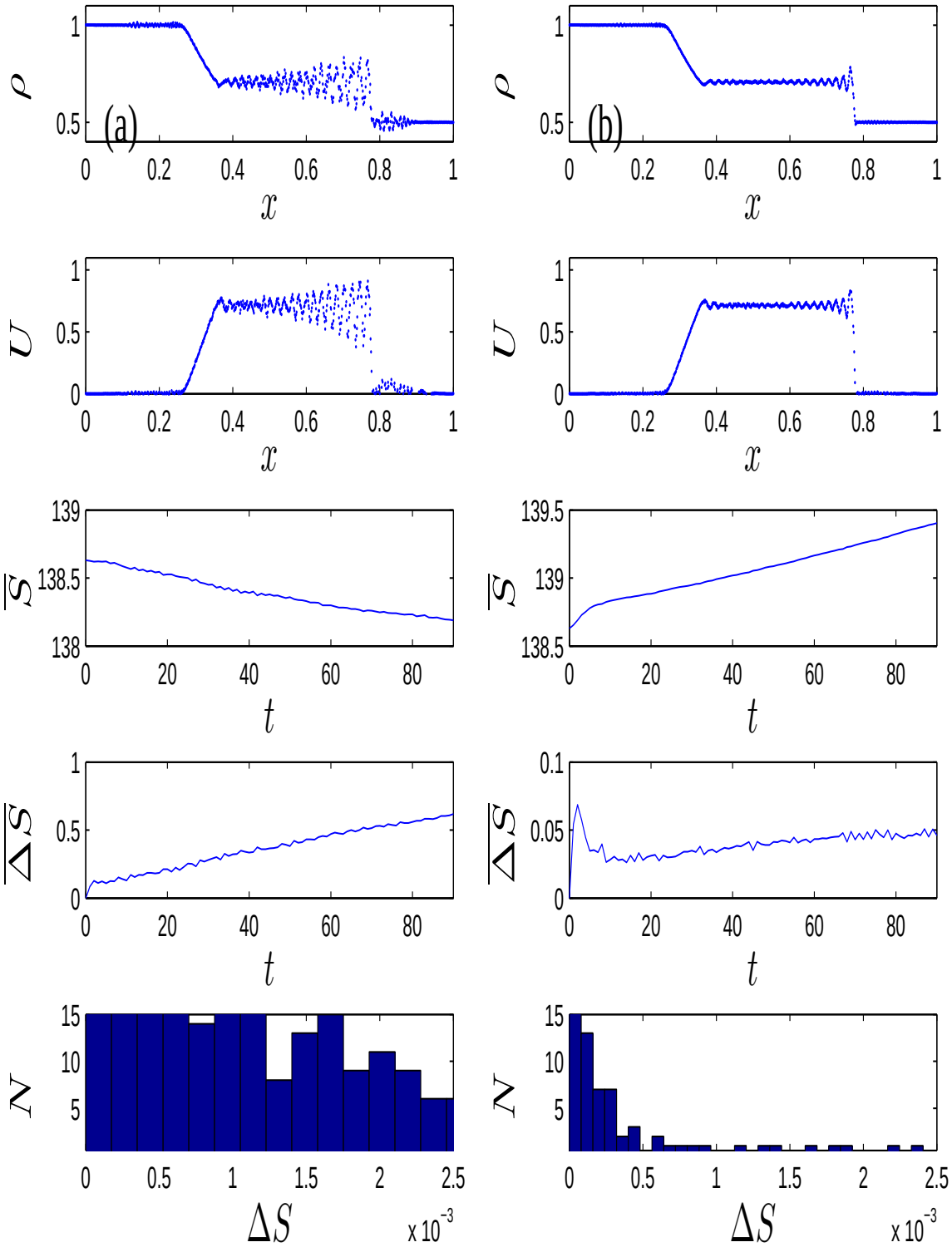

Figure 7.23: velocity set $\{-5,-2,0,2,5\}$, (a) LBGK vs (b) maximum median limiter with $m_2 = 11$ and $\delta = 10^{-4}$.

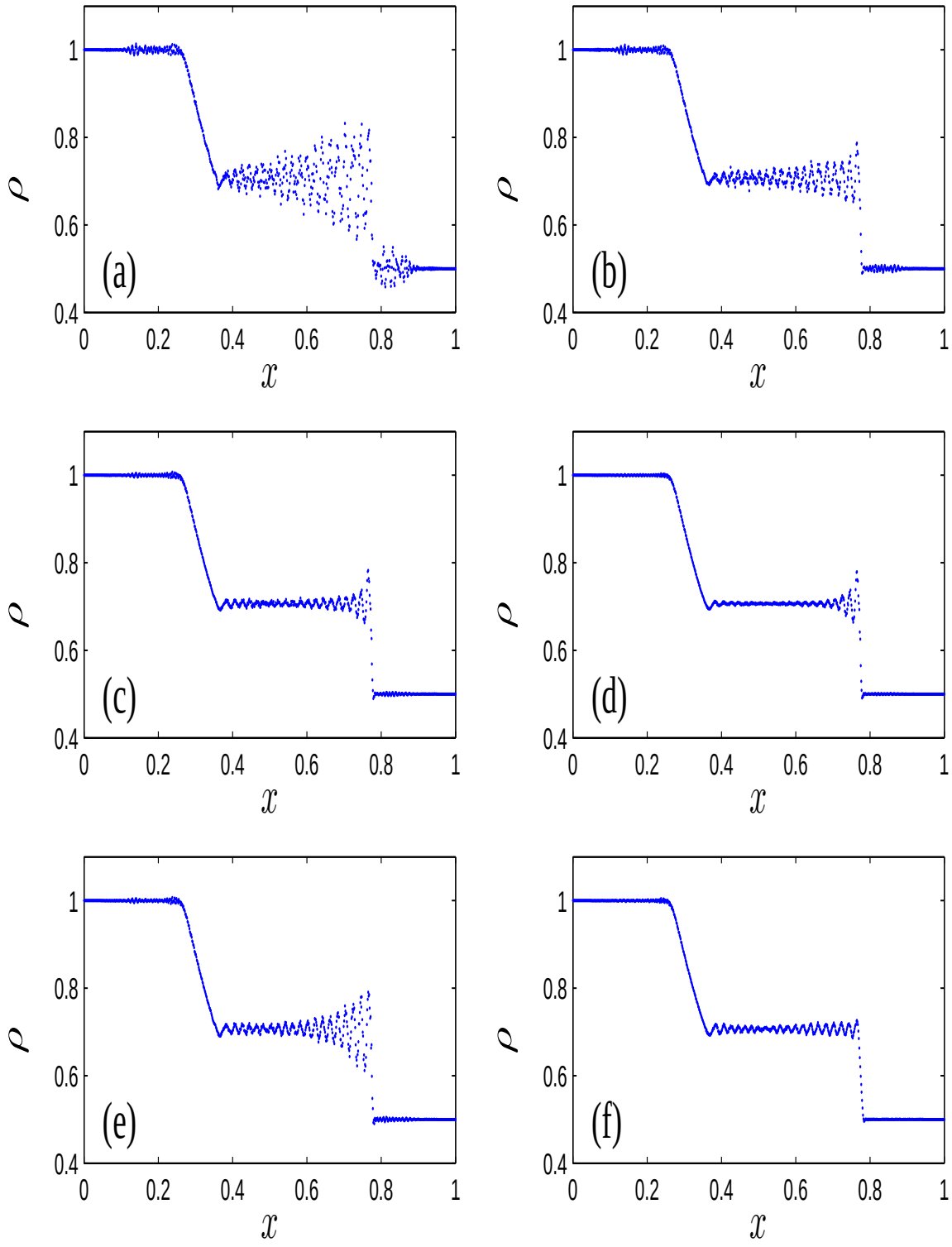

Figure 7.24: velocity set $\{-5,-2,0,2,5\}$, (a) LBGK with no limiter, and maximum median limiter with (b) $m_2 = 11, \delta = 10^{-3}$, (c) $m_2 = 11, \delta = 10^{-4}$, (d) $m_2 = 11, \delta = 10^{-5}$, (f) $m_2 = 5, \delta = 10^{-4}$, and (e) $m_2 = 21, \delta = 10^{-4}$.

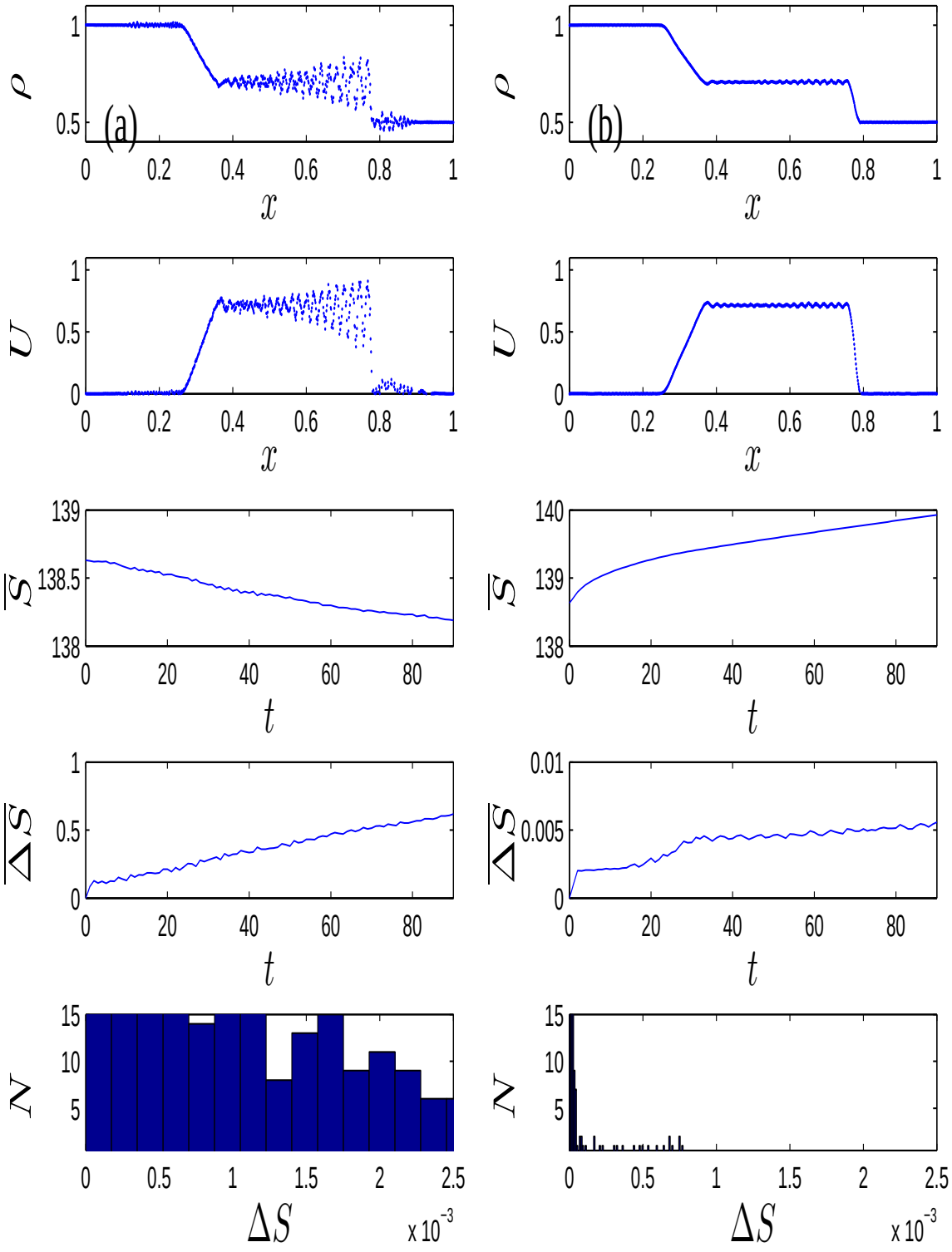

Figure 7.25: velocity set $\{-5, -2, 0, 2, 5\}$, (a) LBGK vs (b) mean limiter with $k_4 = 1$ and $\delta = 10^{-4}$.

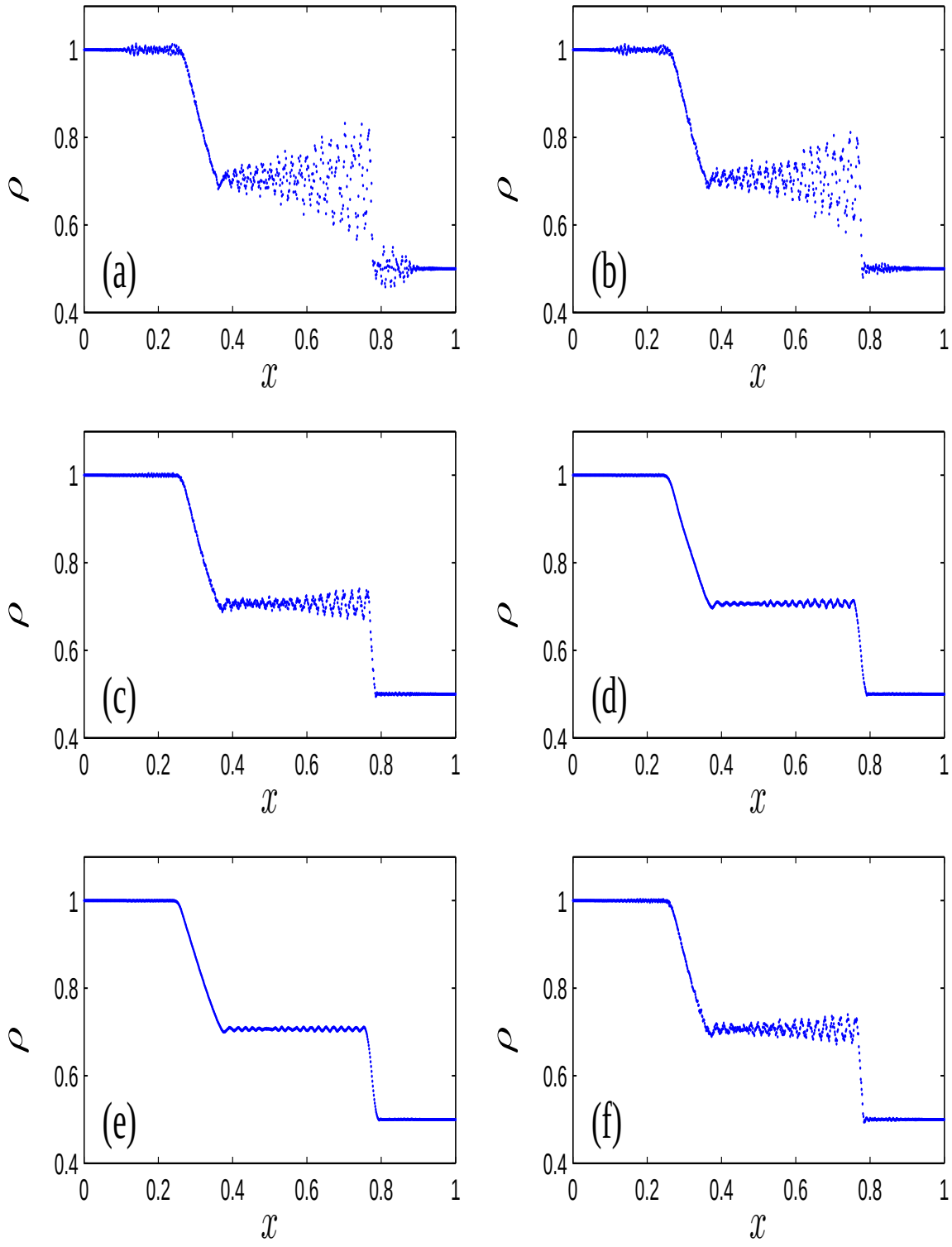

Figure 7.26: velocity set $\{-5, -2, 0, 2, 5\}$, (a) LBGK with no limiter, and mean limiter with (b) $k_4 = 1, \delta = 10^{-2}$, (c) $k_4 = 1, \delta = 10^{-3}$, (d) $k_4 = 1, \delta = 10^{-4}$, (e) $k_4 = 1, \delta = 10^{-5}$, and (f) $k_4 = 1.5, \delta = 10^{-3}$.

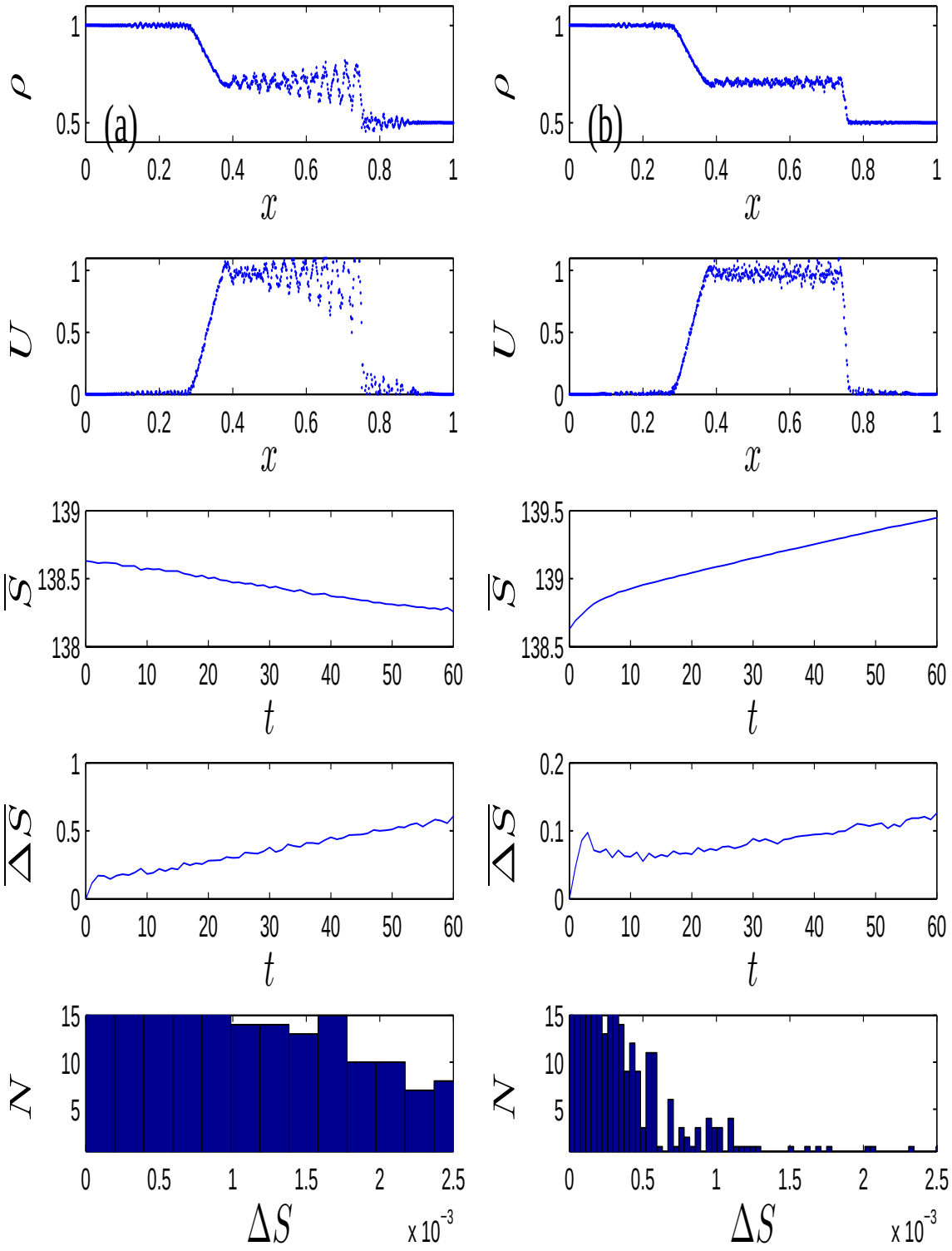

Figure 7.27: velocity set $\{-7,-3,0,3,7\}$, (a) LBGK vs (b)Ehrenfests' with $k_1 = 5$ and $\delta = 10^{-4}$.

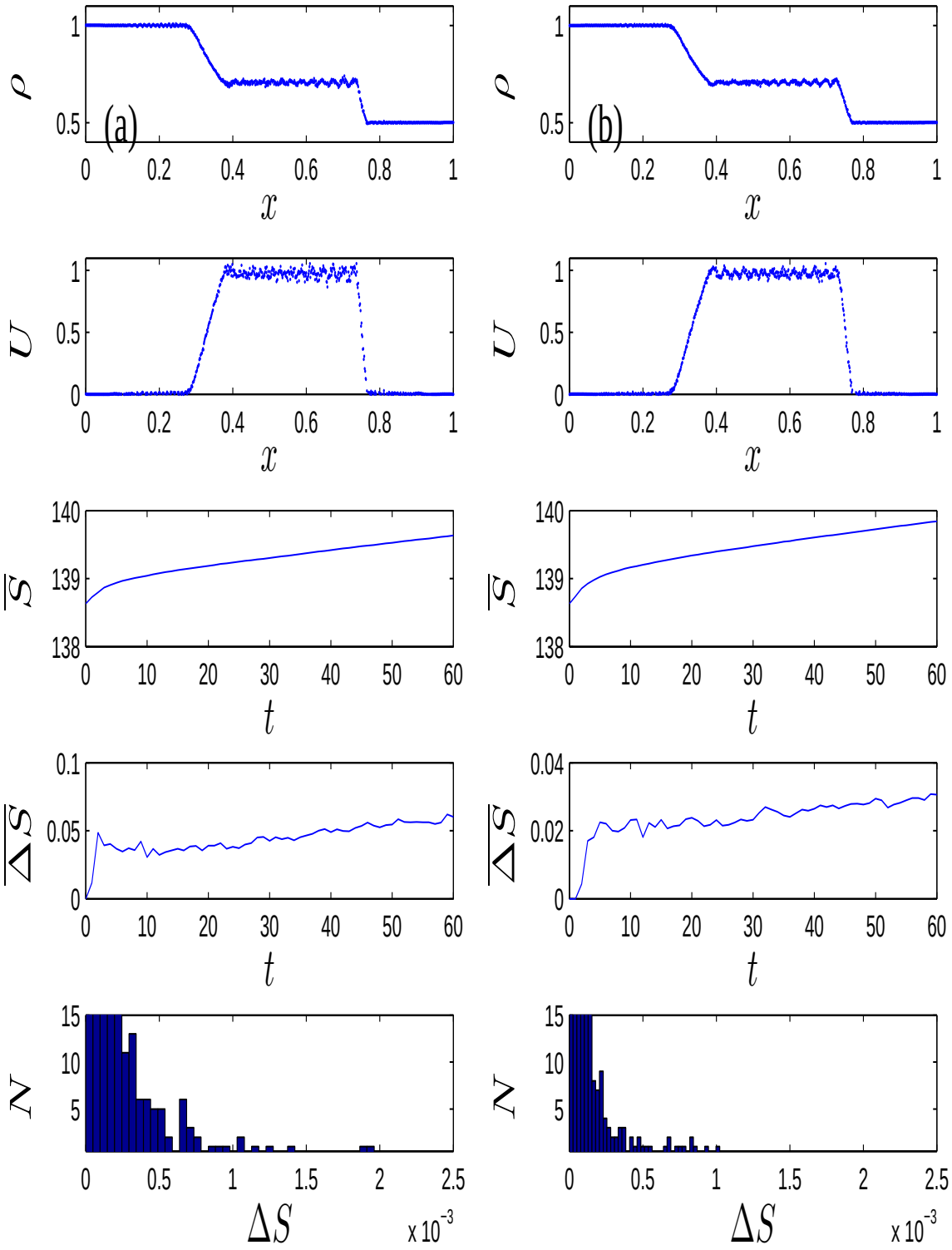

Figure 7.28: velocity set $\{-7, -3, 0, 3, 7\}$, Ehrenfests' with $\delta = 10^{-4}$, (a) $k_1 = 10$ and (b) $k_1 = 19$.

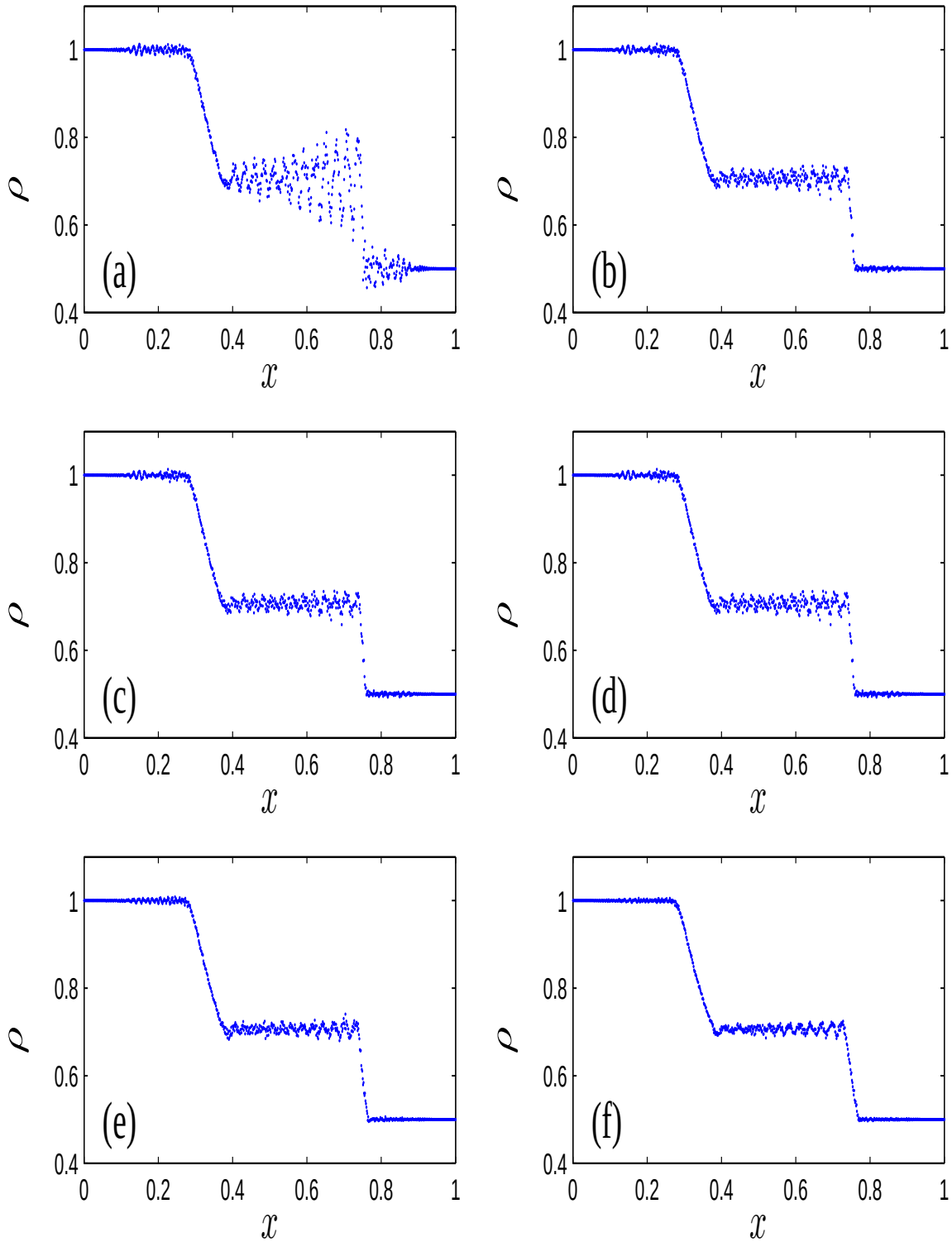

Figure 7.29: velocity set $\{-7,-3,0,3,7\}$, (a) LBGK with no limiter, and Ehrenfests' with (b) $k_1 = 5, \delta = 10^{-3}$, (c) $k_1 = 5, \delta = 10^{-4}$, (d) $k_1 = 5, \delta = 10^{-5}$, (e) $k_1 = 10, \delta = 10^{-5}$, and (f) $k_1 = 19, \delta = 10^{-5}$.

7.7 Velocity Set $\{-7, -3, 0, 3, 7\}$

7.7.1 Ehrenfests' Regularisation

velocity set $\{-7, -3, 0, 3, 7\}$ LBGK compares with Ehrenfests' limiter				
parameters	average ΔS	average U	Mach	Reynolds
none	7.6042×10^{-4}	9.7176×10^{-1}	3.4664×10^{-1}	7.7741×10^{11}
$\delta = 10^{-3}, k_1 = 5$	1.7489×10^{-4}	9.7029×10^{-1}	3.4611×10^{-1}	7.7623×10^{11}
$\delta = 10^{-4}, k_1 = 5$	1.7489×10^{-4}	9.7029×10^{-1}	3.4611×10^{-1}	7.7623×10^{11}
$\delta = 10^{-5}, k_1 = 5$	1.7489×10^{-4}	9.7029×10^{-1}	3.4611×10^{-1}	7.7623×10^{11}
$\delta = 10^{-5}, k_1 = 10$	9.0613×10^{-5}	9.7373×10^{-1}	3.4734×10^{-1}	7.7899×10^{11}
$\delta = 10^{-5}, k_1 = 19$	5.3942×10^{-5}	9.7469×10^{-1}	3.4768×10^{-1}	7.7975×10^{11}

7.7.2 Smooth Limiter 1

velocity set $\{-7, -3, 0, 3, 7\}$ LBGK compares with smooth limiter 1				
parameters	average ΔS	average U	Mach	Reynolds
none	7.6042×10^{-4}	9.7176×10^{-1}	3.4664×10^{-1}	7.7741×10^{11}
$\delta = 10^{-2}, k_2 = 0.5$	3.1860×10^{-4}	9.7223×10^{-1}	3.4680×10^{-1}	7.7779×10^{11}
$\delta = 5.5 \times 10^{-2}, k_2 = 0.5$	6.1610×10^{-5}	9.7436×10^{-1}	3.4756×10^{-1}	7.7949×10^{11}
$\delta = 10^{-1}, k_2 = 0.5$	3.6085×10^{-5}	9.7424×10^{-1}	3.4752×10^{-1}	7.7940×10^{11}
$\delta = 10^{-2}, k_2 = 1$	8.3530×10^{-5}	9.7265×10^{-1}	3.4695×10^{-1}	7.7812×10^{11}
$\delta = 2 \times 10^{-2}, k_2 = 1$	4.0028×10^{-5}	9.7422×10^{-1}	3.4751×10^{-1}	7.7937×10^{11}
$\delta = 10^{-1}, k_2 = 1$	2.2998×10^{-6}	9.7416×10^{-1}	3.4749×10^{-1}	7.7933×10^{11}

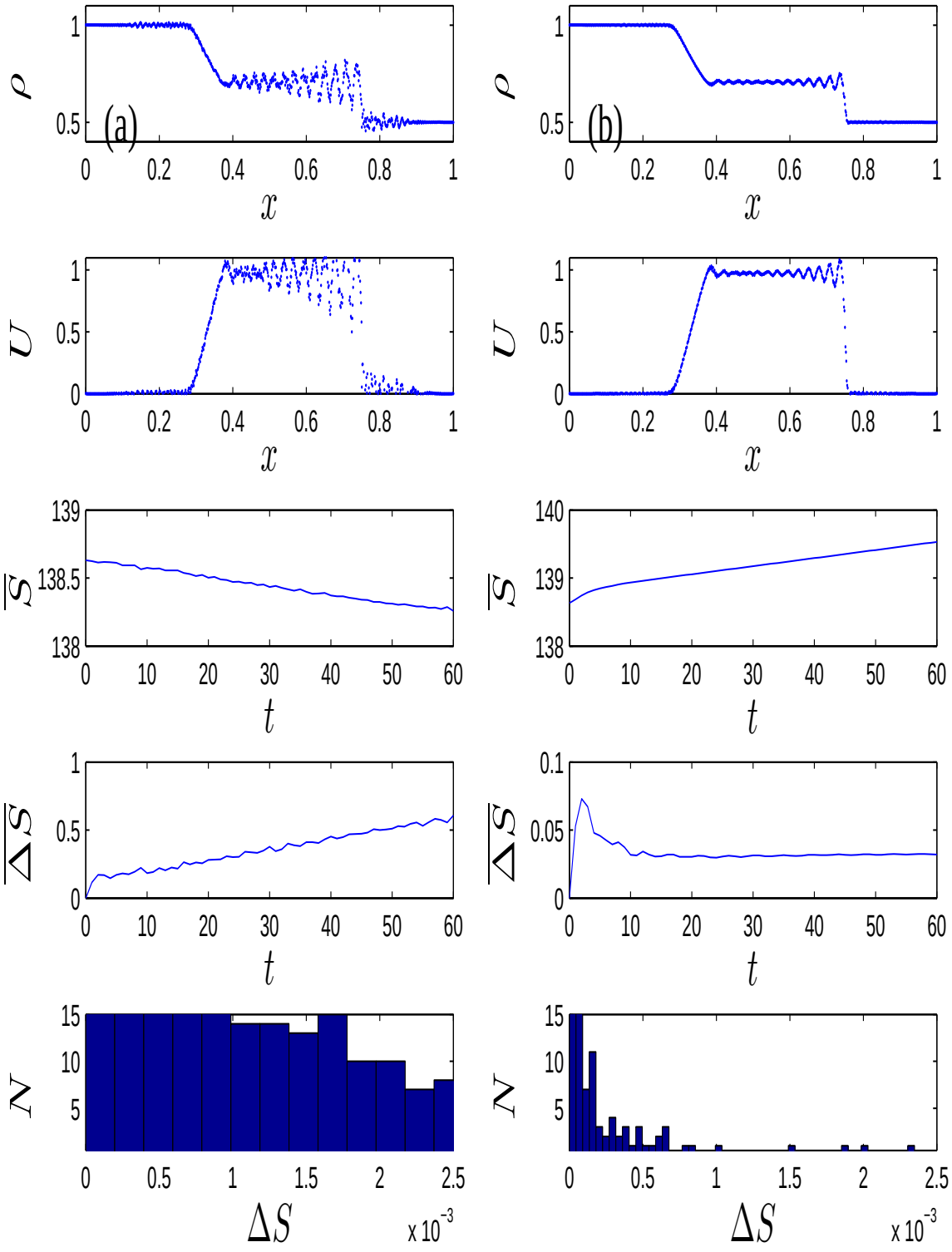

Figure 7.30: velocity set $\{-7,-3,0,3,7\}$,(a) LBGK vs (b) Smooth limiter 1 with $k_2 = 0.5$ and $\delta = 5.5 \times 10^{-2}$.

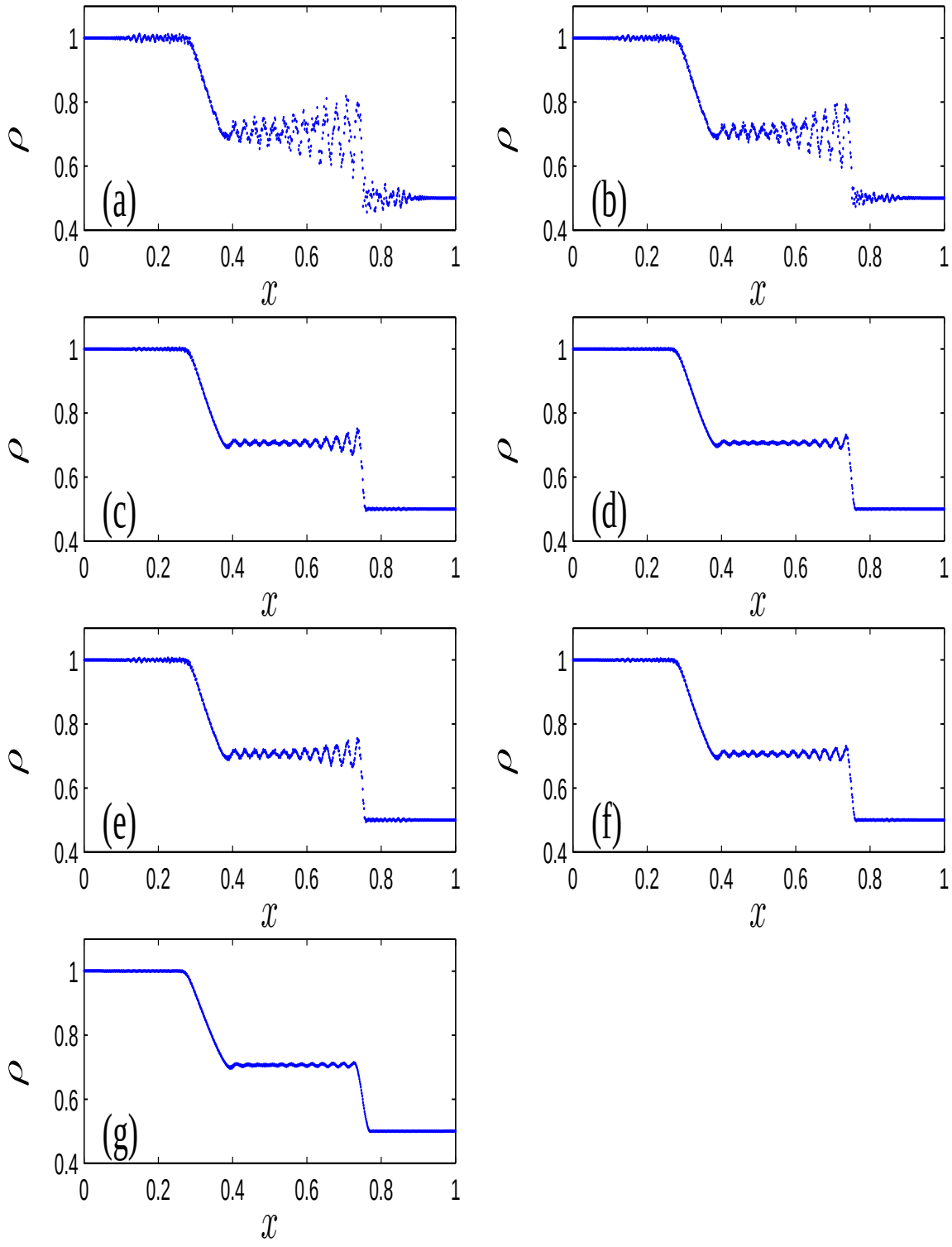

Figure 7.31: velocity set $\{-7,-3,0,3,7\}$, (a) LBGK with no limiter, and Smooth limiter 1 with (b) $k_2 = 0.5, \delta = 10^{-2}$, (c) $k_2 = 0.5, \delta = 5.5 \times 10^{-2}$, (d) $k_2 = 0.5, \delta = 10^{-1}$, (e) $k_2 = 1, \delta = 10^{-2}$, (f) $k_2 = 1, \delta = 2 \times 10^{-2}$, and (g) $k_2 = 1, \delta = 10^{-1}$.

7.7.3 Smooth Limiter 2

velocity set $\{-7,-3,0,3,7\}$ LBGK compares with Smooth limiter 2				
parameters	average ΔS	average U	Mach	Reynolds
none	7.6042×10^{-4}	9.7176×10^{-1}	3.4664×10^{-1}	7.7741×10^{11}
$\delta = 1, k_3 = 1$	4.3463×10^{-5}	9.7359×10^{-1}	3.4729×10^{-1}	7.7887×10^{11}
$\delta = 1.5, k_3 = 2$	2.8319×10^{-5}	9.7468×10^{-1}	3.4768×10^{-1}	7.7974×10^{11}
$\delta = 2, k_3 = 2$	3.2335×10^{-5}	9.7383×10^{-1}	3.4737×10^{-1}	7.7906×10^{11}
$\delta = 2, k_3 = 3$	2.8555×10^{-5}	9.7352×10^{-1}	3.4726×10^{-1}	7.7882×10^{11}

7.7.4 Median Limiter

velocity set $\{-7,-3,0,3,7\}$ LBGK compares with Median filter				
parameters	average ΔS	average U	Mach	Reynolds
none	7.6042×10^{-4}	9.7176×10^{-1}	3.4664×10^{-1}	7.7741×10^{11}
$\delta = 10^{-3}, m_1 = 11$	1.5234×10^{-4}	9.7158×10^{-1}	3.4657×10^{-1}	7.7726×10^{11}
$\delta = 10^{-4}, m_1 = 11$	6.1560×10^{-5}	9.7432×10^{-1}	3.4755×10^{-1}	7.7945×10^{11}
$\delta = 10^{-5}, m_1 = 11$	5.7121×10^{-5}	9.7366×10^{-1}	3.4731×10^{-1}	7.7893×10^{11}
$\delta = 10^{-4}, m_1 = 5$	2.7783×10^{-5}	9.7022×10^{-1}	3.4609×10^{-1}	7.7619×10^{11}
$\delta = 10^{-4}, m_1 = 21$	4.5741×10^{-5}	9.7478×10^{-1}	3.4771×10^{-1}	7.7983×10^{11}

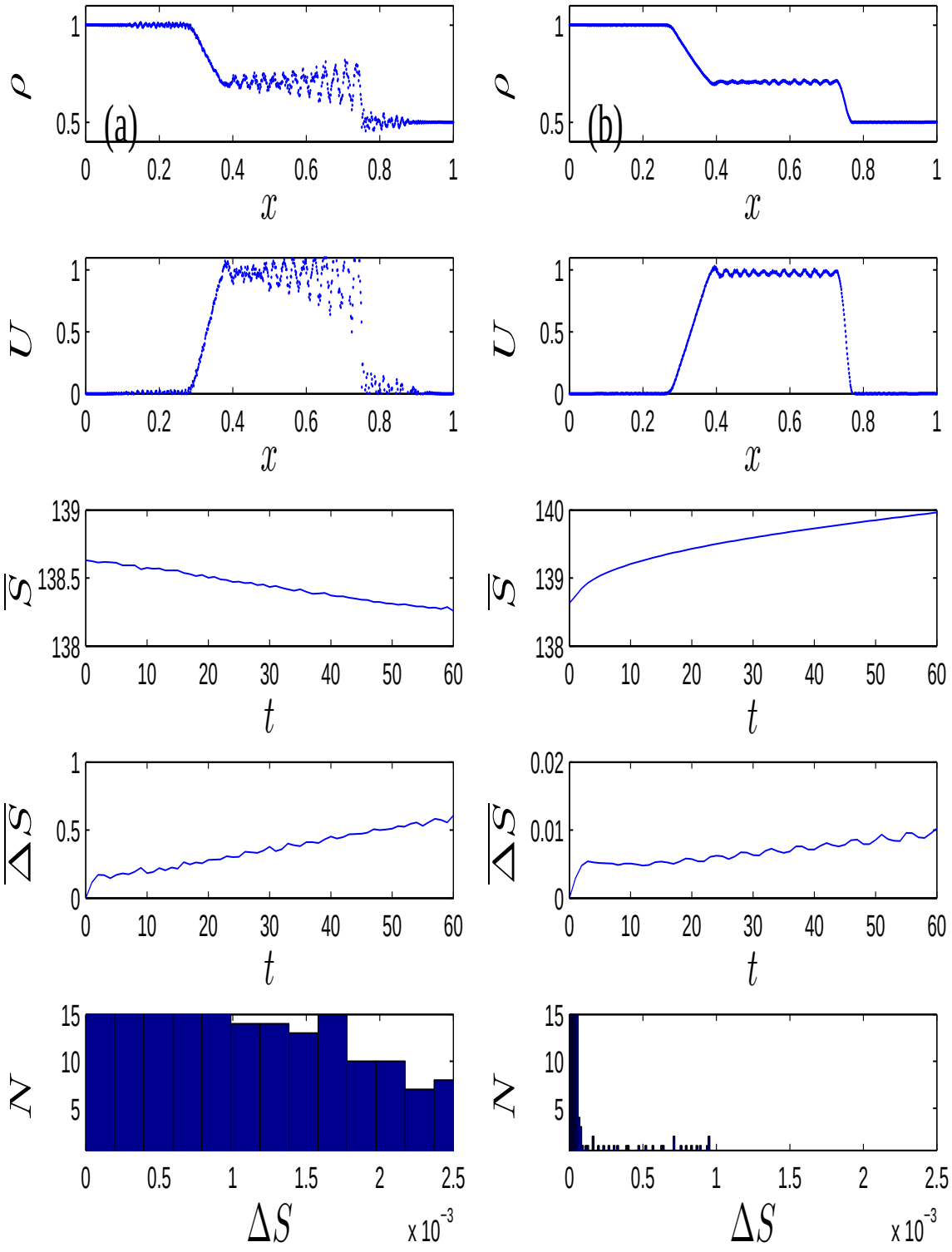

Figure 7.32: velocity set $\{-7,-3,0,3,7\}$, (a) LBGK vs (b) Smooth limiter 2 with $k_3 = 2$ and $\delta = 1.5$.

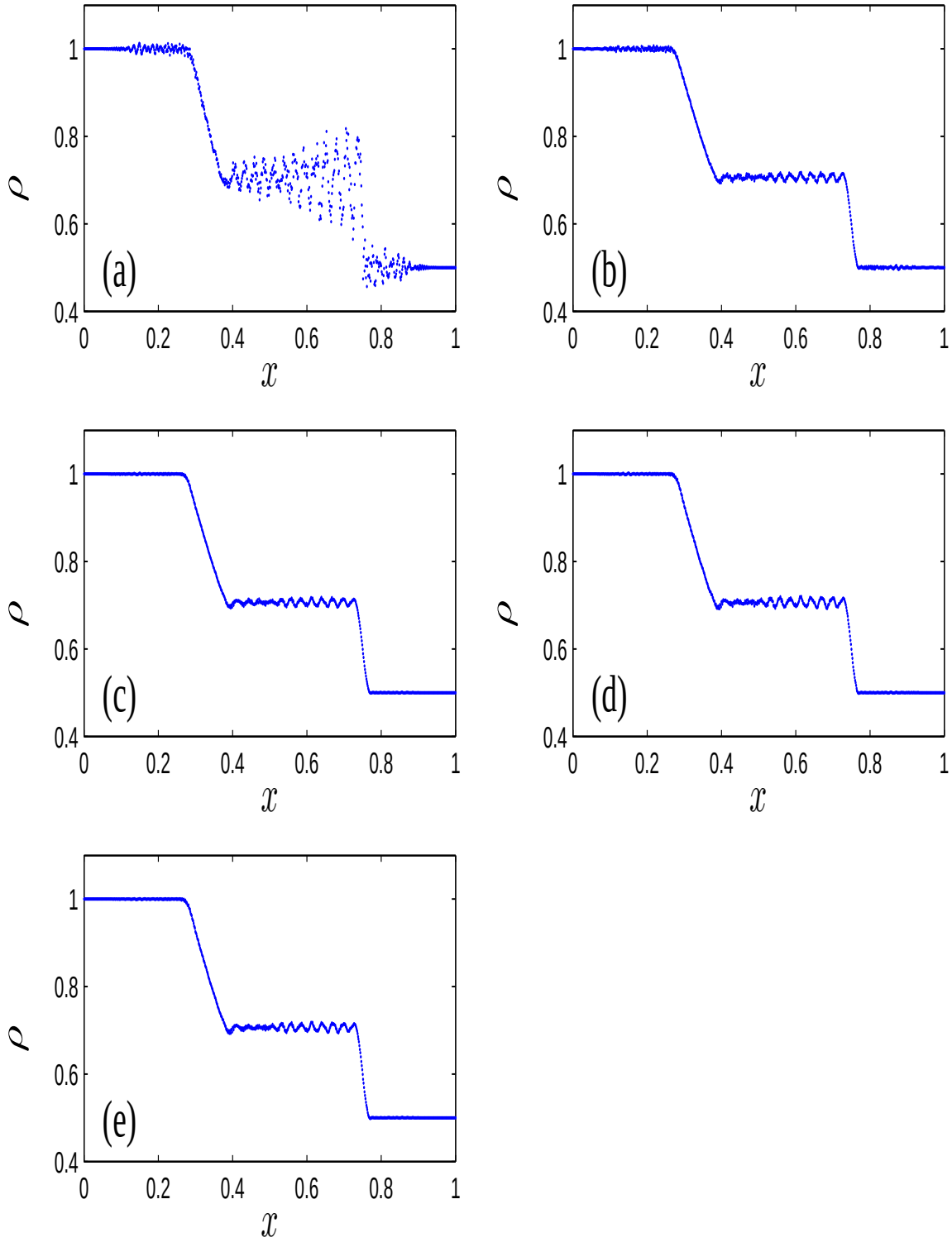

Figure 7.33: velocity set $\{-7,-3,0,3,7\}$, (a) LBGK with no limiter, and Smooth limiter 2 with (b) $k_3 = 1.0, \delta = 1.0$, (c) $k_3 = 2.0, \delta = 1.5$, (d) $k_3 = 2.0, \delta = 2.0$ (e) $k_3 = 3.0, \delta = 2.0$.

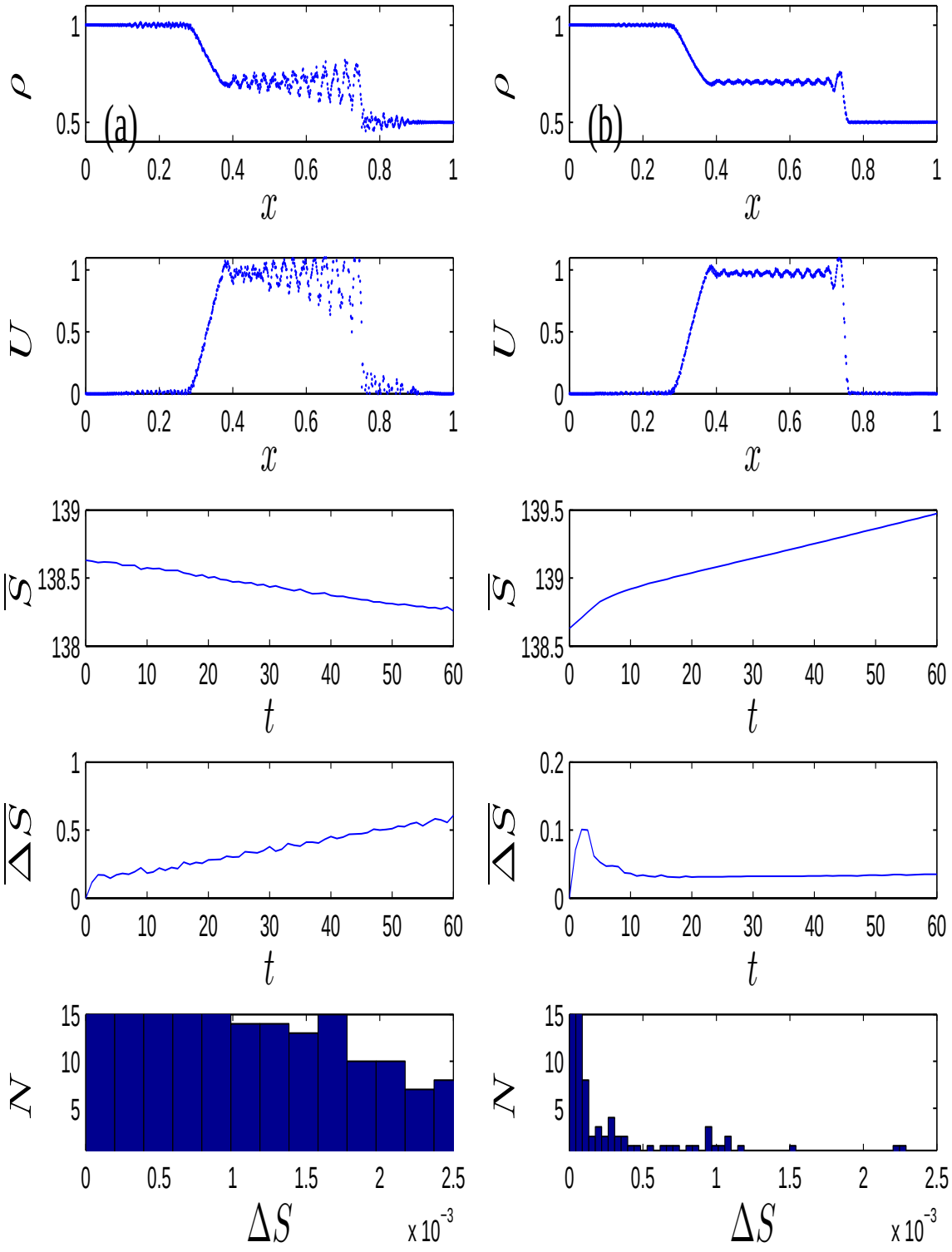

Figure 7.34: velocity set $\{-7, -3, 0, 3, 7\}$, (a) LBGK vs (b) Median limiter with $m_1 = 11$ and $\delta = 10^{-4}$.

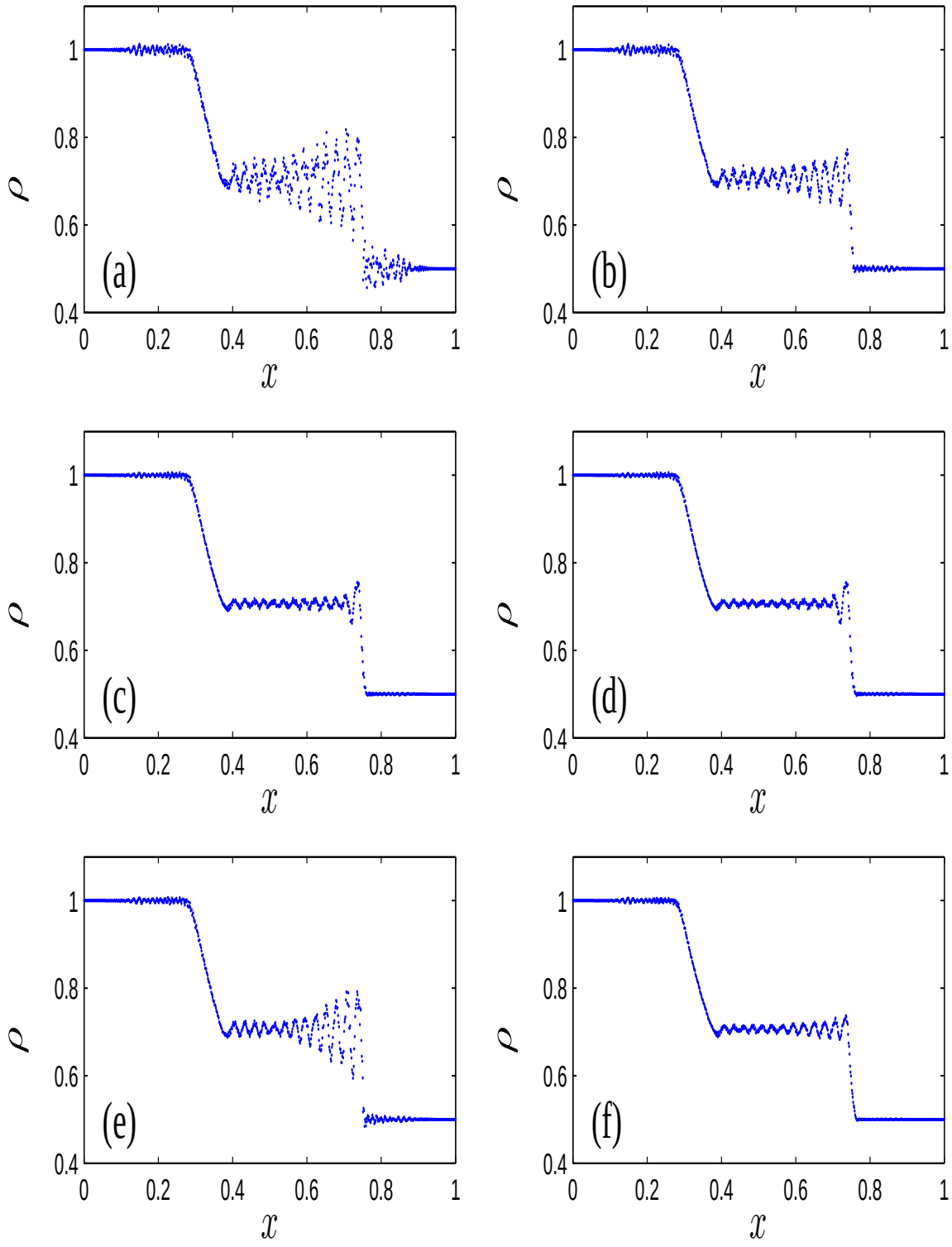

Figure 7.35: velocity set $\{-7,-3,0,3,7\}$, (a) LBGK with no limiter, and Median limiter with (b) $m_1 = 11, \delta = 10^{-3}$, (c) $m_1 = 11, \delta = 10^{-4}$, (d) $m_1 = 11, \delta = 10^{-5}$, (f) $m_1 = 5, \delta = 10^{-4}$, and (e) $m_1 = 21, \delta = 10^{-4}$.

7.7.5 Maximum Median Limiter

velocity set $\{-7,-3,0,3,7\}$ LBGK compares with maximum median filter				
parameters	average ΔS	average U	Mach	Reynolds
none	7.6042×10^{-4}	9.7176×10^{-1}	3.4664×10^{-1}	7.7741×10^{11}
$\delta = 10^{-3}, m_2 = 11$	2.2376×10^{-4}	9.7113×10^{-1}	3.4641×10^{-1}	7.7690×10^{11}
$\delta = 10^{-4}, m_2 = 11$	1.3657×10^{-4}	9.7215×10^{-1}	3.4677×10^{-1}	7.7772×10^{11}
$\delta = 10^{-5}, m_2 = 11$	1.2659×10^{-5}	9.7314×10^{-1}	3.4713×10^{-1}	7.7851×10^{11}
$\delta = 10^{-4}, m_2 = 5$	2.8124×10^{-4}	9.7065×10^{-1}	3.4624×10^{-1}	7.7652×10^{11}
$\delta = 10^{-4}, m_2 = 21$	6.3525×10^{-5}	9.7447×10^{-1}	3.4760×10^{-1}	7.7958×10^{11}

7.7.6 Mean Limiter

velocity set $\{-7,-3,0,3,7\}$ LBGK compares with mean filter				
parameters	average ΔS	average U	Mach	Reynolds
none	7.6042×10^{-4}	9.7176×10^{-1}	3.4664×10^{-1}	7.7741×10^{11}
$\delta = 10^{-2}, k_4 = 1$	5.3791×10^{-4}	9.7204×10^{-1}	3.4673×10^{-1}	7.7763×10^{11}
$\delta = 10^{-3}, k_4 = 1$	7.1116×10^{-5}	9.7265×10^{-1}	3.4695×10^{-1}	7.7812×10^{11}
$\delta = 10^{-4}, k_4 = 1$	2.4692×10^{-5}	9.7556×10^{-1}	3.4799×10^{-1}	7.8045×10^{11}
$\delta = 10^{-5}, k_4 = 1$	2.2553×10^{-5}	9.7575×10^{-1}	3.4806×10^{-1}	7.8060×10^{11}
$\delta = 10^{-3}, k_4 = 1.5$	6.8374×10^{-5}	9.7206×10^{-1}	3.4674×10^{-1}	7.7765×10^{11}

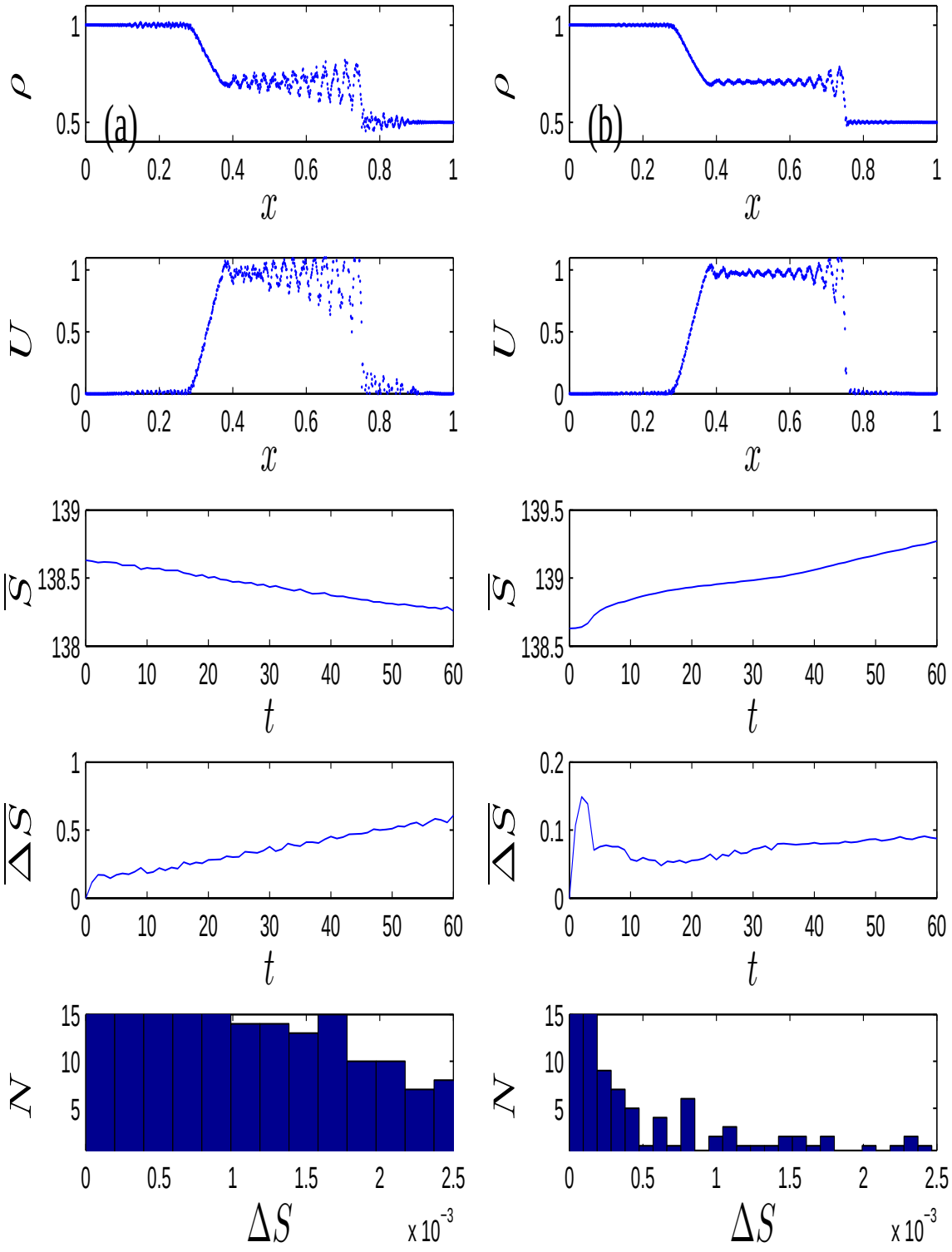

Figure 7.36: velocity set $\{-7,-3,0,3,7\}$, (a) LBGK vs (b) maximum median limiter with $m_2 = 11$ and $\delta = 10^{-4}$.

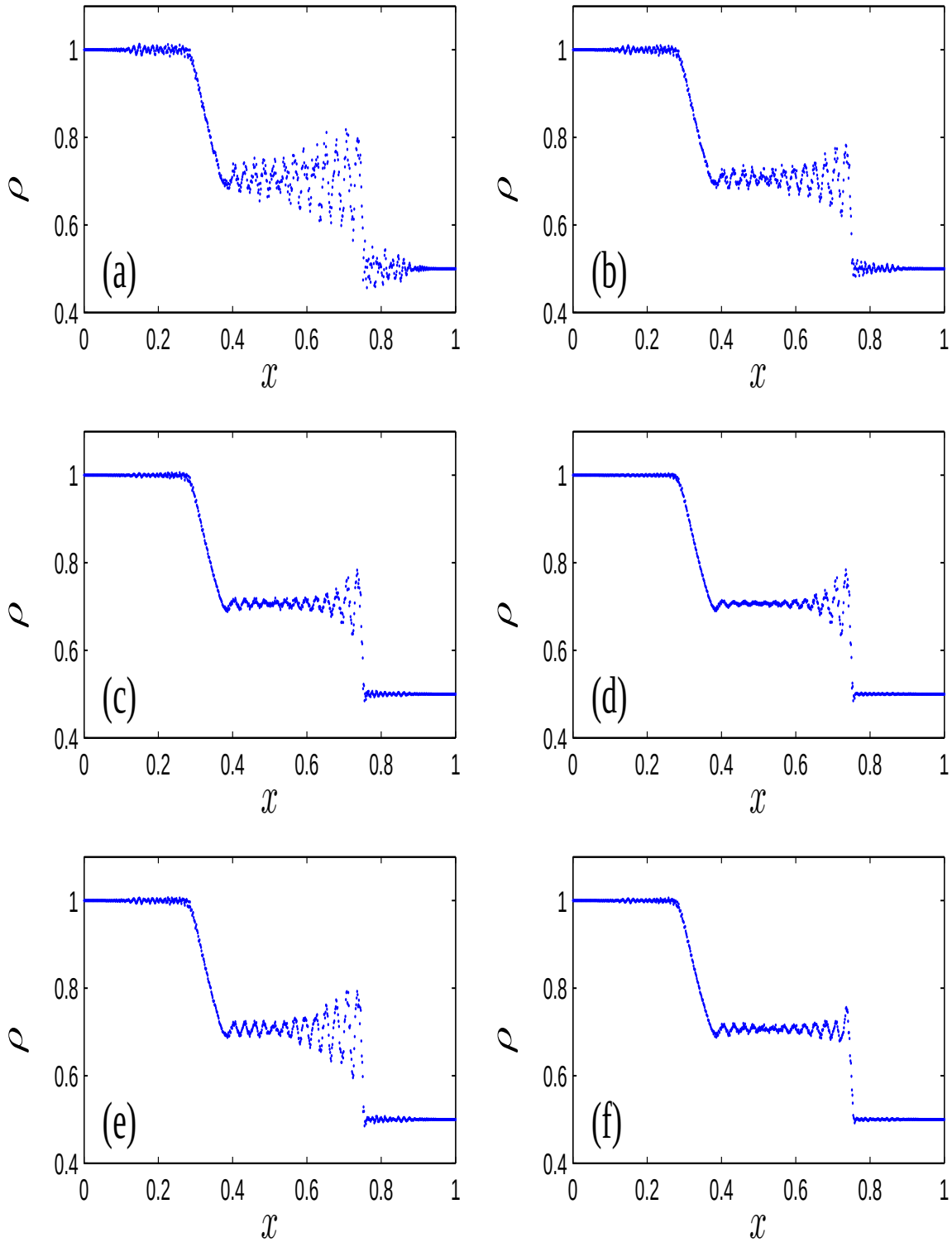

Figure 7.37: velocity set $\{-7,-3,0,3,7\}$, (a) LBGK with no limiter, and maximum median limiter with (b) $m_2 = 11, \delta = 10^{-3}$, (c) $m_2 = 11, \delta = 10^{-4}$, (d) $m_2 = 11, \delta = 10^{-5}$, (f) $m_2 = 5, \delta = 10^{-4}$, and (e) $m_2 = 21, \delta = 10^{-4}$.

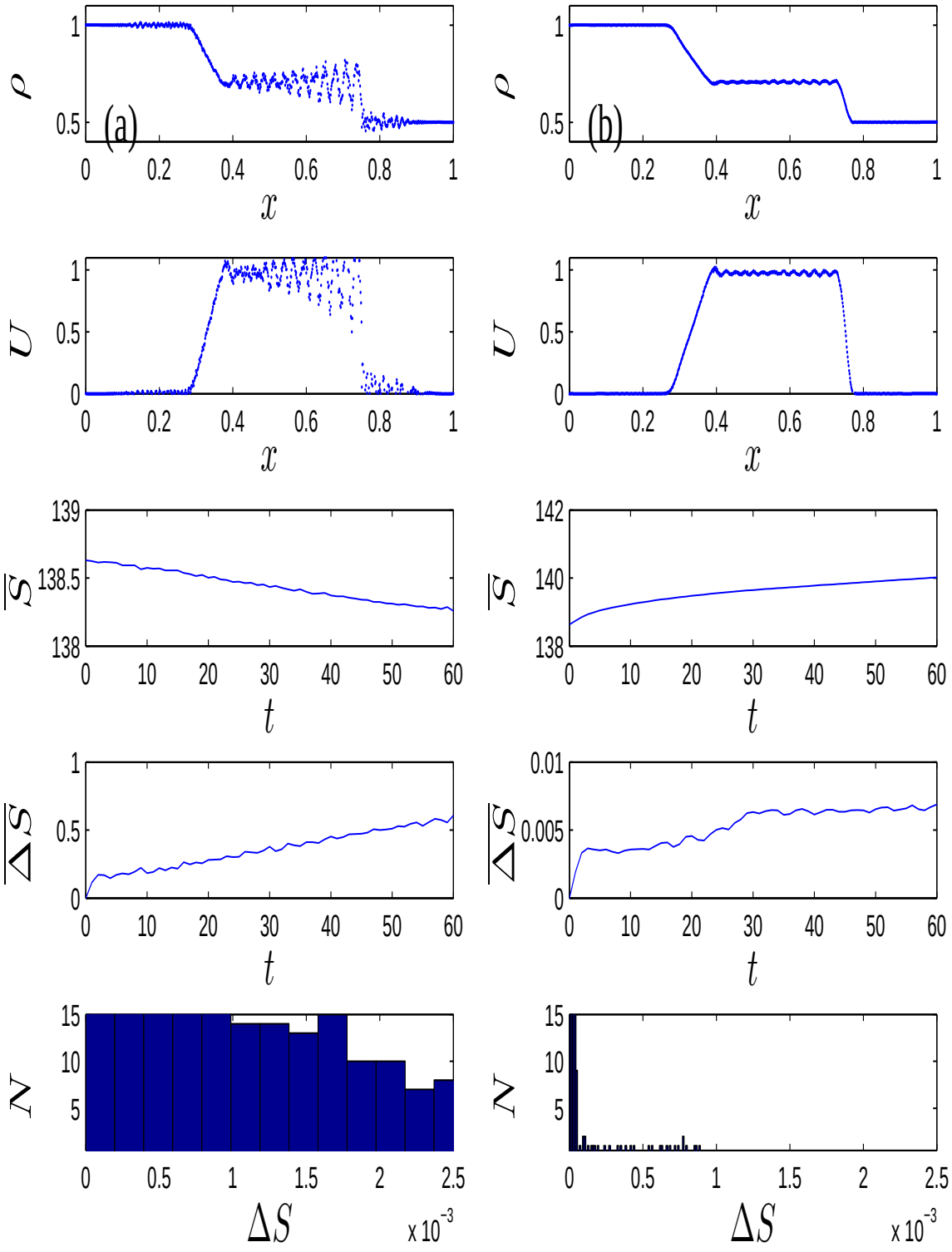

Figure 7.38: velocity set $\{-7,-3,0,3,7\}$, (a) LBGK vs (b) mean limiter with $k_4 = 1$ and $\delta = 10^{-4}$.

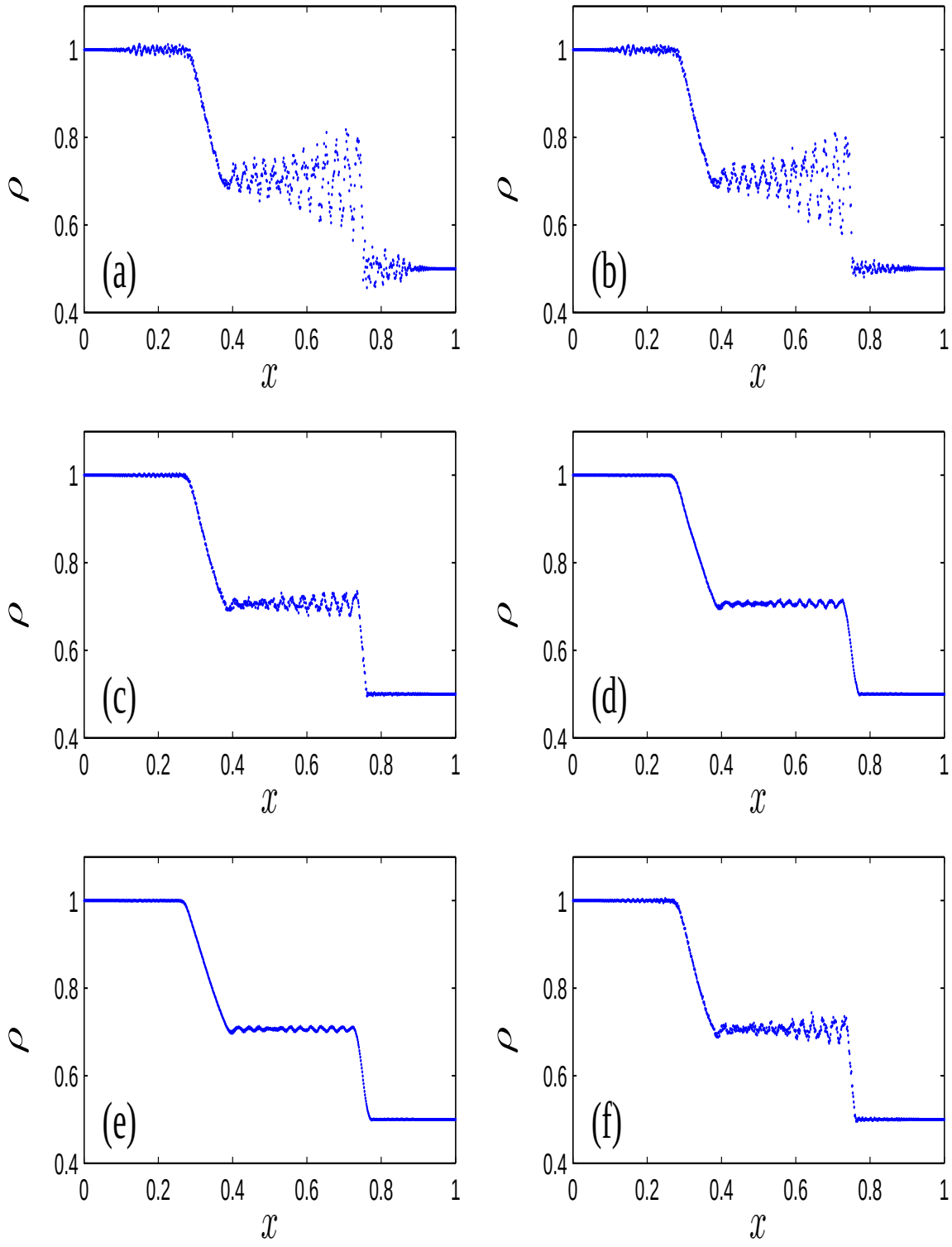

Figure 7.39: velocity set $\{-7,-3,0,3,7\}$, (a) LBGK with no limiter, and mean limiter with (b) $k_4 = 1, \delta = 10^{-2}$, (c) $k_4 = 1, \delta = 10^{-3}$, (d) $k_4 = 1, \delta = 10^{-4}$ (e) $k_4 = 1, \delta = 10^{-5}$, and (f) $k_4 = 1.5, \delta = 10^{-3}$.

Chapter 8

Conclusion and Future Work

For the problem in which the LBM suffers the stability deficiencies for high Reynolds number, in this thesis, we have provided some solutions by using nonequilibrium entropy. These nonequilibrium entropy limiters are tested in shock tube. The performance of these limiters for LBGK in comparison with LBGK only shows that they are much more effective in removing spurious oscillations in the presence of sharp gradients. In this chapter, the conclusions are drawn and some future work will be discussed.

8.1 Conclusion

Flux limiters schemes combine high resolution schemes in areas with smooth fields and first order schemes in areas with sharp gradients. In other words, flux limiters are based on the choice between spurious oscillations in high order non-monotone schemes and additional dissipation in first order schemes. The construction of all the limiters is based on:

$$f \rightarrow f^* + \phi \times (f - f^*). \tag{8.1}$$

Notice that all the limiters do not change the macroscopic variables. In the following, the conclusion is summarized into five points.

1. How can one construct the nonequilibrium entropy limiters for LBM with non-entropic quasiequilibria [44]? One of the solutions for this question is to use Kullback entropy. For the given macroscopic variables, the Kullback entropy reaches its maximum at the point $f = f^*$ for both continuous and discrete distributions. Therefore, if the quasiequilibrium f^* is nonentropic, the Kullback entropy $-S_K(f)$ is used.

2. The weights are the bridge from continuous density to discrete distribution f_i. The values of hydrodynamic normalized weights are all positive and the sum of the values of weights is equal to 1. Weights are additional variables.

3. The positive rule and Ehrenfests' regularization offer localised corrections, and they are very easy and computationally cheap. The positive rule is based on a very simple concept: when the population is negative in a collision step, the positive rule enables the negative population to go back to the positive boundary. The positive rule is enforced throughout the simulations for LBGK both with and without limiters. The positive rule and the Ehrenfests' regularization provide a gentle transformation from big nonequilibrium states to quasiequilibrium states without modifying any other distribution states. The performance of Ehrenfests' regularization with the five-velocity sets for LBGK can effectively remove the spurious oscillations.

4. The two smooth limiters filter each nonequilibrium entropy. There are a lot of options to build the function ϕ. These two limiters satisfy the first property of the monotonic condition. The behavior of these two limiters for LBGK is efficient to remove the big oscillations in both the shock and the

post shock regions for all the velocity sets.

5. The smooth median entropy limiter, the maximum median entropy filter and the mean entropy filter are all double monotonic filters. These three limiters involve the local structure. The smooth median entropy limiter is a more robust average than the mean entropy limiter, since a single non-important value in a neighborhood does not influence the selection of median value significantly. Furthermore, the median entropy filter does not wipe out the sharp fronts completely in the shock region, as we can see from the figures for all the five-velocity sets. For all these three limiters, the number of neighbors involved also can effect the oscillations for the both shock and post shock regions, especially they can remove the sharp fronts when the number of neighbors involved is big. The smooth median entropy limiter and the maximum median entropy limiter have quite similar performance apart from the sharp fronts in the shock regions.

As mentioned before, there is always a tradeoff between spurious oscillations in high order non-monotone schemes and additional dissipation in the first order schemes. This concept originally came from S.K.Godunov whom illustrated that a linear scheme for a PDE could not, at the same time, be monotone and second order accurate. Therefore, the shock and post-shock regions should not be extremely smooth, which it means that too much dissipation has brought up by the limiters. Consequently the Reynolds number decreases, i.e. the kinematic viscosity which we initially defined as a constant value 10^{-9} will change to a bigger value. When too much dissipation is brought up by the limiters, the simulation will lose accuracy. On the other hand, when a little dissipation is brought up, the spurious oscillations cannot be removed effectively. The median entropy limiter is preferred, since it works in a way such that it removes the spurious oscillations

effectively for both shock and post-shock regions and at the same time does not introduce too much dissipation.

8.2 Future Work

Although the limiters introduced here can remove the spurious oscillations effectively in 1D shock tube simulations with three-velocity sets and five-velocity sets, they still need to be tested in higher dimensions and much wider range of velocity sets. All the 6 limiters can be applied in 2D and 3D dimensions as well, for example, lid driven cavity, and square passing cylinder.

For many researchers, the simulation of low kinematic viscosity flows, i.e. high Reynolds number, is not easy to obtain stable and accurate solutions. As the Reynolds number increases, the less accurate and unstable of the simulation would be. The nonequilibrium entropy limiters provide a way to deal with high Reynolds number. The concept of constructing the nonequilibrium entropy limiters are reasonably simple, so the applications of these limiters can be widely adapted to different areas of research. There is a big range of applications can be used such as airfoil for NACA.

There are also other ways of constructing nonequilibrium entropy limiters according to ones interests for the research.

Bibliography

[1] E. F. Toro. *Riemann Solvers and Numerical Methods for Fluid Dynamics: A Practical Introduction*. Springer, 1999.

[2] P. Balachandran. *Fundamentals of Compressible Fluid Dynamics*. Prentice-Hall of India, 2006.

[3] Eitan Tadmor and WenGang Zhong. Entropy stable approximations of Navier-Stokes Equations with no artificial numerical viscosity. *Journal of Hyperbolic Differential Equations*, Volume 3, pp. 529-559, 2006.

[4] Bimalendu Narayan Roy. *Fundamentals Of Classical Statistical Thermodynamics*. Wiley, 2002.

[5] E.T. Jaynes. Gibbs vs Boltzmann Entropies. *Journal of Physics*, Vol 33, No. 5, 391-398, 1965.

[6] J.W. Gibbs. *Elementary principles in statistical mechanics*. New York.(1981) Woodbridge, CT: Ox Bow Press ISBN 0-918024-20-X.

[7] R.V.L. Hartley. Transmission of Information. *Bell System Technical Journal*, July 1928, P. 535-563.

[8] S. Kullback. *Information theory and statistics*. Wiley, New York, 1959.

[9] C.E. Shannon. A Mathematical Theory of Communication. *The Bell System Technical Journal*, Vol.27, pp.379-423,623-656, July, October, 1948.

[10] S. Kullback and R.A. Leibler. On Information and Sufficiency. *The Annals of Mathematical Statistics*, Vol. 22, No.1, pp.78-86, 1951.

[11] J.P.Burg. *Maximum entropy spectral analysis*. PhD thesis, Stanford University, 1975.

[12] F. W. Sears, G. L. Salinger. *Thermodynamics, Kinetic Theory, and Statistical Thermodynamics*. Addison-Wesley Principles of Physics Series, 1975, 0-201-06894-x.

[13] J. P. Holman. *Thermodynamics*. McGraw-Hill Book Company, 1969, ISBN:0-07-029633-2.

[14] C. H. Collie. *Kinetic theory and entropy*. Longman Group Limited, 1982, ISBN:0-582-44368-7.

[15] Dilip Kondepudi, Ilya Prigogine. *Modern Thermodynamics*. 1952, ISBN:0-471-97394-7.

[16] N. Cressie and T. Read. Multinomial Goodness of Fit Tests. *Journal of the Royal Statisitical Society*, Series B 46, 440-464, 1984.

[17] E. Vivies and A.Planes. Is Tsallis thermodynamics nonextensive? *Phys. Rev. Lett*, 88, No 2, 2002.

[18] Alexander N. Gorban and Iliya V. Karlin and Hans Christian Ottinger, The additive generalization of the Boltzmann entropy. *Phys. RevE.*, 67.067104

[19] J. S. Dugdale. *Entropy and its physical meaning*. Taylor and Francis LTD, 1996.

[20] Bimalendu N. Roy. *Fundamentals of classical and statistical thermodynamics*, Wiley, 2002.

[21] Robert D. Zucker and Oscar Biblarz. *Fundamentals of gas dynamics*. J.Wiley, 2002.

[22] S. M. Yahya. *Fundamentals Of Compressible Flow*. New Age International Ltd, third edition, 2003.

[23] John David Anderson. *Modern compressible flow: with historical perspective* . McGraw-Hill, 3rd Edition, ISBN 0-07-242443-5, 2004.

[24] B. Chopard, P. Luthi and A. Masselot. Cellular Automata and Lattice Boltzmann Techniques: An Approach to Model and Simulate Complex Systems. University of Geneva, Switzerland.

[25] Dieter A.Wolf-Gladrow. *Lattice-gas cellular automata and lattice Boltzmann models: an introduction*, Springer, 2000, ISBN 3-540-66973-6.

[26] Li-Shi Luo, Lattice-Gas Automata and Lattice Boltzmann Equations for Two-Dimensional Hydrodynamics, PhD theis, Georgia Institute of Technology, April 1993.

[27] Daniele L.Marchisio and Rodney O.Fox. *Multiphase reacting flows: Modelling and Simulation*. Springer Wien New York, 2007.

[28] Daniel H.Rothman and Stiphane Zaleski. *Lattice-Gas Cellular Automata: Simple Models of Complex Hydrodynamics*. Combridge University Press, 1997.

[29] Sauro Succi. *The Lattice Boltzmann Equation for Fluid Dynamics and Beyond*. Oxford university press, Clarendon, 2001.

[30] Yong Shi, T. S. Zhao, and Z. L. Guo. Thermal Lattice Bhatnagar-Gross-Krook model for flows with viscous heat dissipation in the incompressible limit. *Phys. Rev. E* 70, 066310, 2004.

[31] P. L. Bhatnagar, E. P. Gross and M. Krook. A model for collision processes in Gases. 1. Small amplitude processes in charged and neutral one-component systems. *Phys. Rev.* Volume 94, Number 3, May 1, 1954.

[32] J.P.Boris and D.L.Book. Flux-Corrected Transport: I. SHASTA, a fluid transport algorithm that works. *Journal of Computational Physics, 11, 38-69(1973).*

[33] J.P.Boris and D.L.Book. Flux-Corrected Transport: 2. SHASTA, Generalization of the method. *Journal of Computational Physics* 18, 248, 1975.

[34] J.P.Boris and D.L.Book, Flux-Corrected Transport: 3. SHASTA, minimal error FCT algorithms, *Journal of Computational Physics*, 20, 397, 1976.

[35] Steven T. Zalesak. Fully multidimensional Flux-Corrected Transport algorithms for fluids. *Journal of Computational Physics*, 31:335-362, 1979.

[36] Steven T. Zalesak. Very high order and pseudospectral Flux-Corrected Transport(FCT) algorithms for consrvation laws. In R. Vichnevetsky and R.S.Stepleman, editors, *Advances in computer methods for partial differential equations*, pages 126-134, 1981.

[37] D.Kuzmin, R.Lohner and S.Turek. *Flux-Corrected Transport.* Springer, 2005.

[38] Shyam S. Chikatamarla and Illiya V. Karlin, Entropy and Galilean Invariance of Lattice Boltzmann Theories. *Physical Review Letters*, PRL 97, 190601, 2006.

[39] Guy R. McNamara, and Gianluigi Zanetti. Use of the Boltzmann Equation to Simulate Lattice-Gas Automata. *Physical Review Letters*, Volume 61, Number 20, 1988.

[40] A. N. Gorban. Basic Types of Coarse-Graining. In A. N. Gorban, N. Kazantzis, I. G. Kevrekidis, H.C. Ottinger, and C. Theodoropoulos, editors, *Model Reduction and Coarse-Graining Approaches for Multiscale Phenomena*, pages 117-176. Springer, Berlin-Heidelberg-New York, 2006.

[41] S. Ansumali and I. V. Karlin. Kinetic boundary conditions in the lattice Boltzmann method. *Phys. Rev. E*, 66(2):026311, 2002.

[42] R. A. Brownlee, A. N. Gorban and J. Levesley. Stabilisation of the lattice Boltzmann method using the Ehrenfests' coarse-graining idea. *Phys. Rev. E*, 74:037703, 2006.

[43] R. A. Brownlee, A. N. Gorban and J. Levesley. Stable simulation of fluid flow with high Reynolds number using Ehrenfests' steps. *Numer. Algorithms*, 45(1-4):389-408, 2007.

[44] R. A. Brownlee, A. N. Gorban and J. Levesley. Nonequilibrium entropy limiters in lattice Boltzmann methods. *Physica A*, 387 (2008) 385-406.

[45] R. A. Brownlee, A. N. Gorban and J. Levesley. Stability and stabilisation of the lattice Boltzmann method. *Phys. Rev.*. E75(2007), 036711.

[46] R. A. Brownlee, A. N. Gorban and J. Levesley. Stabilisation of the lattice Boltzmann method Magic steps and salvation operations. *Phys. Rev. E 75, 036711*, 2007.

[47] Iliya V. Karlin, Santosh Ansumali, Christos E. Frouzakis and Shyam Sunder Chikatamarla, Elements of the lattice Boltzmann method I: Linear advection equation. *Commun. Comput. Phy*, 1(2006),616-655.

[48] Iliya V. Karlin, Santosh Ansumali, Christos E. Frouzakis and Shyam Sunder Chikatamarla, Elements of the lattice Boltzmann method 2: Kinetics and hydrodynamics in one dimension. *Commun. Comput. Phy*, 2(2007),196-238.

[49] S. Ansumali and I. V. Karlin, Stabilization of the Lattice Boltzmann method by the H theorem: A numerical test, *Phys. Rev.*, E62(6) 7999-8003, 2000.

[50] J.W. Tukey. *Exploratory data analysis*. Addison-Wesley. Reading, Mass. 1974.

[51] W. K. Pratt. *Digital image processing*. John Wiley and Sons, INc. New York, 1978.

[52] Peter D.Lax, *On dispersive difference shemes*. New York University; Courant institute of Mahtematical Science, New York, NY 10012, USA

[53] Y.Li, R. Shock, R.Zhang and H.Chen. Numerical study of flow past an impulsively started cylinder by the lattice Boltzmann method. *J. Fluid Mech.*, 519:273-00, 2004.

[54] F. Tosi, S. Ubertini, S.Succi, H.Chen and I.V. Karlin. Numerical stability of entropic versus positivity-enforcing lattice Boltzmann schemes. *Math. Comput. Simulation*, 72:227-231, 2006.

[55] B. Van Leer. Towards the ultimate conservative difference scheme 3. Upstream-centered finite-difference schemes for ideal compressible flow. *J. Comp. Phys*, 23(1977), 263-275.

[56] L. V. Karlin, A. N. Gorban, S. Succi and V. Boffi. Maximum entropy principle for lattice kinetic equations. *Phys. Rev. Lett*, 81:6-9, 1998.

[57] P. K. Sweby. High resolution schemes using flux-limiters for hyperbolic conservation laws. *SIAM J. Num. Anal.*, 21(1984), 995-1011.

[58] P. L. Roe. Characteristic-based schemes for the Euler equations. *Ann. Rev. Fluid Mech.*, 18(1986), 337-365.

[59] R.Benzi, S.Succi, and M.Vergassola. The lattice Boltzmann-equation theory and applications. *Physics Reports*, 222(3):145-197, 1992.

[60] S. Chen and G. D. Doolean. Lattice Boltzmann method for fluid flows. *Annu. Rev. Fluid. Mech.*, 30:329-364, 1998.

[61] F. Higuera, S. Succi, and R. Benzi. Lattice Gas dynamics with enhanced collisions. *Europhys. Lett.*, 9:345-349, 1989.

[62] M. W. Frank. *Fluid Mechanics*. Third edition, McGraw-Hill Inc., 1994.

[63] D. J. Acheson. *Elementary Fluid Dynamics*. Oxford University Press, 1990

[64] Y. B. Zeldovich. Proof of the Uniqueness of the Solution of the Equations of the Law of Mass Action, In: Selected Works of Yakov Borisovich Zeldovich, Vol. 1, Princeton University Press, Princeton, 1996.

[65] A. Gorban, B. Kaganovich, S. Filippov, A. Keiko, V. Shamansky and I. Shirkalin. *Thermodynamic Equilibria and Extrema: Analysis of Attainability Regions and Partial Equilibrium*. Springer, Berlin, Herdelberg, New York, 2006.

[66] A. N. Gorban. Equilibrium encircling. Equations of chemical kinetics and their thermodynamic analysis, Nauka, Novosibirsk, 1984.

[67] H. Qian. Relative entropy: free energy associated with equilibrium fluctuations and nonequilibrium deviations. *Phys. Rev. E*, 63(2001), 042103.

[68] I. V. Karlin, A. N. Gorban, S. Succi and V. Boffi. Maximum entropy principle for lattice kinetic equations. *Phys. Rev. Lett.*, 81:6-9, 1998.

[69] I. V. Karlin, A. Ferrante, and H. C. Ottinger. Perfect entropy functions of the lattice Boltzmann method. *Europhys. Lette.*, 47:182-188, 1999.

[70] A. N. Gorban, I. V. Karlin, and H. C. Ottinger, and L. L. Tatainova. Ehrenfest's argument extended to a formalism of nonquilibrium thermodynamics. *Phys. Rev. E.*, 62:066124, 2001.

[71] T.N.Phillips and G.W.Roberts. Lattice Boltzmann models for non-Newtonian flows. *Journal of Applied Mathematics*, 2011, 76, 790-816.

[72] S. Ansumali, and I. V. Karlin. Kinetic boundary conditions in the lattice Boltzmann method. *Phys. Rev. E66*, 026311, 2002.

[73] S. Ansumali, I. V. Karlin, and H. C. Ottinger. Minimum entropic kinetic models for hydrodynamics. *Europhys. Let.*, 63(6): 798-804, 2003.

[74] B. M. Boghosian, J. Yepez, P. V. Coveney, and A. J. Wager. Entropic lattice Boltzmann methods. *Phil. Trans. Roy. Soc.* A, 362:1691-1702, 2004.

[75] Alexander N. Gorban, Iliya V. Karlin. Family of additive entropy functions out of thermodynamics limit. *Physical Review E 67*, 016104, 2003.

[76] Cedric Villani. H-Theorem and beyond: Boltzmann's entropy in today's mathematics. *http://math.univ-lyon1.fr/ villani/Cedrif/P11.Boltzmann.pdf*, 2006.

[77] David J. Packwood, Jeremy Levesley, and Alexander N. Gorban. Time step expansions and the invariant manifold approach to lattice Boltzmann models. *Coping with Complexity: Model Reduction and Data Analysis*, page 169-205.

[78] R. A. Brownlee, J. Levesley, D. Packwood and A. N. Gorban. Add-ons for Lattice Boltzmann Methods: Regularization, Filtering and Limiters. *arxiv:1110.0270*, 2011.

[79] Tahir Saeed Khan. Stabilizing Lattice Boltzmann Simulation of Flows Past Bluff Bodies by Introduction of Ehrenfests' Limiters. *PhD Thesis*. University of Leicester, 2011.

[80] L. S. Luo, W. Liao, X. Chen, Y. Peng, and W. Zhang. Numerics of the lattice Boltzmann method: Effects of collision models on the lattice Boltzmann simulations. *Phys Rev E*, 2011, 83:056710.

[81] A.N.Gorban, P.A.Gorban and G.Judge. Entropy: The Markov Ordering Approach. *Entropy*. 2010, 12(5):1145-1193.